PUERTO RICO COASTAL STUDY

DRAFT INTEGRATED FEASIBILITY REPORT AND ENVIRONMENTAL ASSESSMENT

APPENDIX A
Engineering

November 2020

US Army Corps of Engineers
Jacksonville District

TABLE OF CONTENTS

LIST OF FIGURES

LIST OF TABLES

1.0 PROJECT BACKGROUND

When the first oceans were formed on this planet in the ancient past, long before the dawn of history, a never-ending struggle between the land and the sea began. The conflict, once started, has gone on and continues with unabated vigor today. Thus, the need for shore protection projects began when man entered the narrow strip of land bordering these bodies of waters, intending to remain there and participate in the battle of the land against the sea. This battle persists in the island nation of Puerto Rico, where 66.7% of the total 3.6 million people live in coastal areas around the island (NOAA, 2020a).

Coastal storm damages contribute to public safety hazards via coastal inundation, shoreline erosion, and large waves. Major storm events like Hurricanes (TC; also known as a tropical cyclone) Irma and Maria in September 2017 and Extratropical Cyclone (ET; also known as northeasters or nor'easters) Riley in March 2018 recently impacted Puerto Rico's infrastructure and Puerto Rican lives, yielding a state of emergency. Roughly five months after the two, billion-dollar events (Irma and Maria) drastically affected Puerto Rico, the Bipartisan Budget Act of 2018 (BBA 2018) was signed into law (Public Law 115-123). Approximately one year (yr) after these events, the BBA 2018 authorized the United States (US) Army Corps of Engineers (USACE) to conduct the Puerto Rico Coastal Storm Risk Management Study (Puerto Rico Coastal Study or PRCS) in three yrs at a cost of $3 million (full-Federal expense). The PRCS, studied by the Jacksonville District (SAJ), is intended to determine Federal interest over a 50-yr analysis period to address coastal storm risks and protect the people and infrastructure along the north and west coasts of Puerto Rico.

1.1 Study Location and Objective

The Commonwealth of Puerto Rico is an island that lies in the northeast Caribbean Sea. BBA 2018 authorized an island-wide federal interest analysis, but the imposed time and funding constraints required this study to focus on the most vulnerable coastal areas prone to inundation, wave, and erosion damages. The nonfederal sponsor for this study, the Puerto Rico Department of Environmental and Natural Resources (DNER), provided local input to focus the study team on the areas of greatest importance (see main report for additional information on early screening efforts). Following initial screening, the study focused on two coastal municipalities: San Juan and Rincón (Figure A - 1).

Puerto Rico's most populated municipality, San Juan, is located on the island's northern coast, bordering the Atlantic Ocean. The study area in the capital city includes the 6.7 mile (mi) coastal stretch from Boca de Cangrejos (eastern-most point) to El Boquerón (western-most point) that comprises Carolina, Isla Verde, Ocean Park, and Condado (Figure A - 2). Rincón is situated on the northwest coast, borders the Mona Passage, and is primarily known for its surfing, fishing, and marine preserves (the famous Tres Palmas Marine Preserve is immediately north of the Rincón study area). Figure A - 3 shows the Rincón study area, which spans 2.3 mi from the Rincón Marina at Punta Ensenada (northern-most point) to Córcega (southern-most point). The objective of this study is to assess potential storm damage susceptibility and associated alternative solutions to reduce economic and social impacts from inundation, wave, and erosion damages at these two locations.

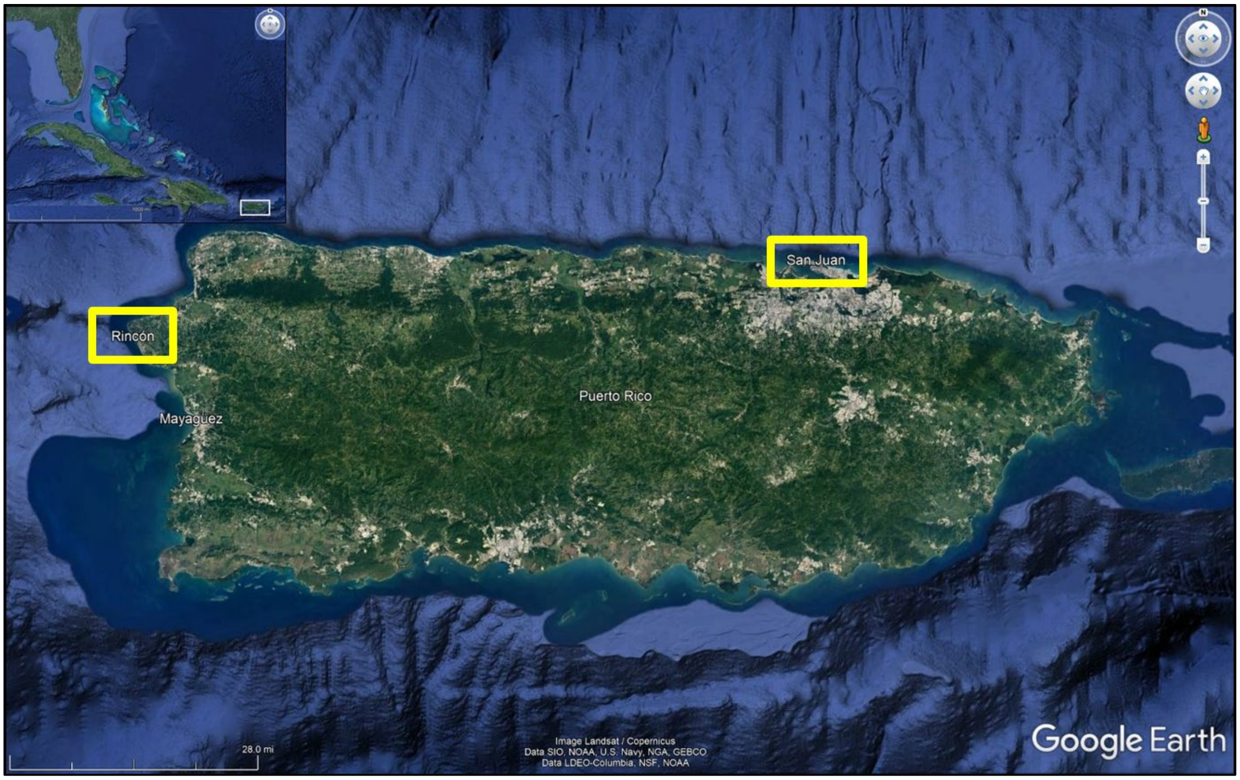

Figure A - 1. Study Area Regional Map

Figure A - 2. PRCS's San Juan Study Area

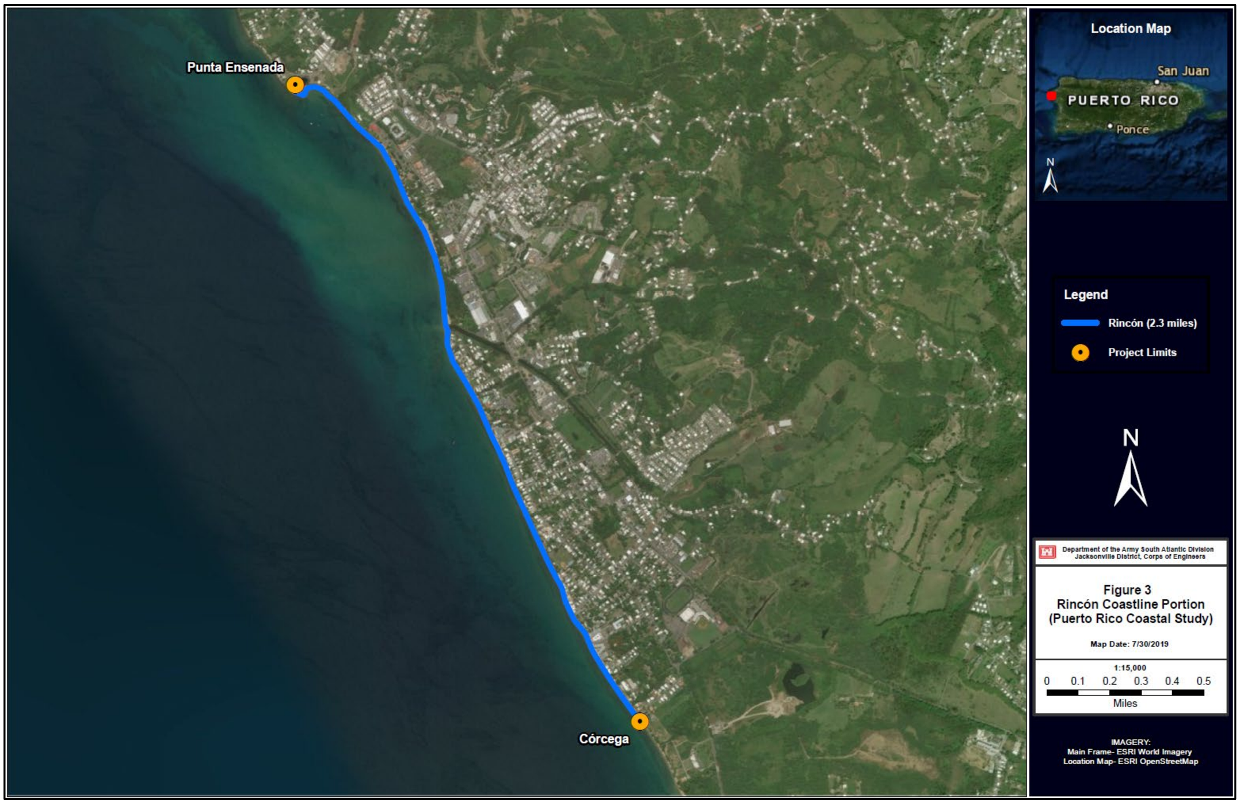

Figure A - 3. PRCS's Rincón Study Area

1.2 Existing Coastal Conditions

1.2.1 San Juan Conditions

The observations presented here are in order from east to west for the San Juan area, where existing condition photos relate to the stations shown in the first figure of each "pocket" beach section (pocket beaches for this discussion are areas delineated east to west by rocky headland points and/or inlet features). The photos within the figures shown in this section were taken in June 2019. Generally wider beaches and fewer structures are present in the eastern portion of San Juan (Carolina) with smaller beaches and an increase in hard structures to the west (especially in Condado). An offshore and relatively shallow fringing reef is present in front of these four pocket beaches and is an important aspect of the San Juan hydrodynamic environment (discussed later in this appendix). The shallow depth of the reef initiates wave breaking and dissipates wave energy propagating toward the coastline (this can be seen even during mild days like in Figure A - 2). The point features segregating each pocket beach largely contain little to no dry beach with nearshore hardbottom and protective rock structures (revetments, seawalls, breakwaters, etc.). The central portion of each pocket beach mostly contains dry sand, minimal and intermittent dunes, and little to no dune vegetation.

1.2.1.1 <u>Carolina</u>

The Carolina pocket beach contains the least amount of hard structures for any beach in San Juan from Boca de Cangrejos to El Boquerón. The easternmost 0.5 mi contains essentially no beach, where a rock revetment protects the main road in the area, PR 187. Sparse structures east of station C3 in Figure 4 consist of public parking lots, a beach club villa, and a public park that do not feature flood protection seaward of their slab foundations. The dry beach in this area is up to 200 feet (ft) wide and contains a mildly sloping beach that appeared slightly deflated in June 2019, as shown in Figure A - 5 and Figure A - 6. The only portion of beach within Carolina that contains dunes or protective upland vegetation is directly landward of station C3 and only about 650 ft long (Figure A - 8).

Carolina's upland structures are generally west of station C3 (aerial shown in Figure A - 4), where the coastline conditions are relatively consistent between stations C3 and C6: the dry beach largely mimics conditions to the east with a mildly sloping and slightly deflated beach berm, sparse and intermittent dunes, virtually no upland vegetation, and no hard coastal inundation protection (such as seawalls or revetments; Figure A - 8). Nearshore hardbottom, diminishing beach width, and prominent hard structures largely represented the western portion of Carolina from C6 to C9 (Figure A - 9). Roads with storm drain culverts terminating on the beach berm near C9 present focal points for coastal storm inundation (Figure A - 10), and seawalls in this area may lead to erosive wave reflection during large storm events (Figure A - 11). If nourishment is considered in future coastal storm risk management (CSRM) efforts in the western portion of Carolina, storm drain runoff from culverts in the seawalls would likely present major erosion problems within any future dune or beach berm construction.

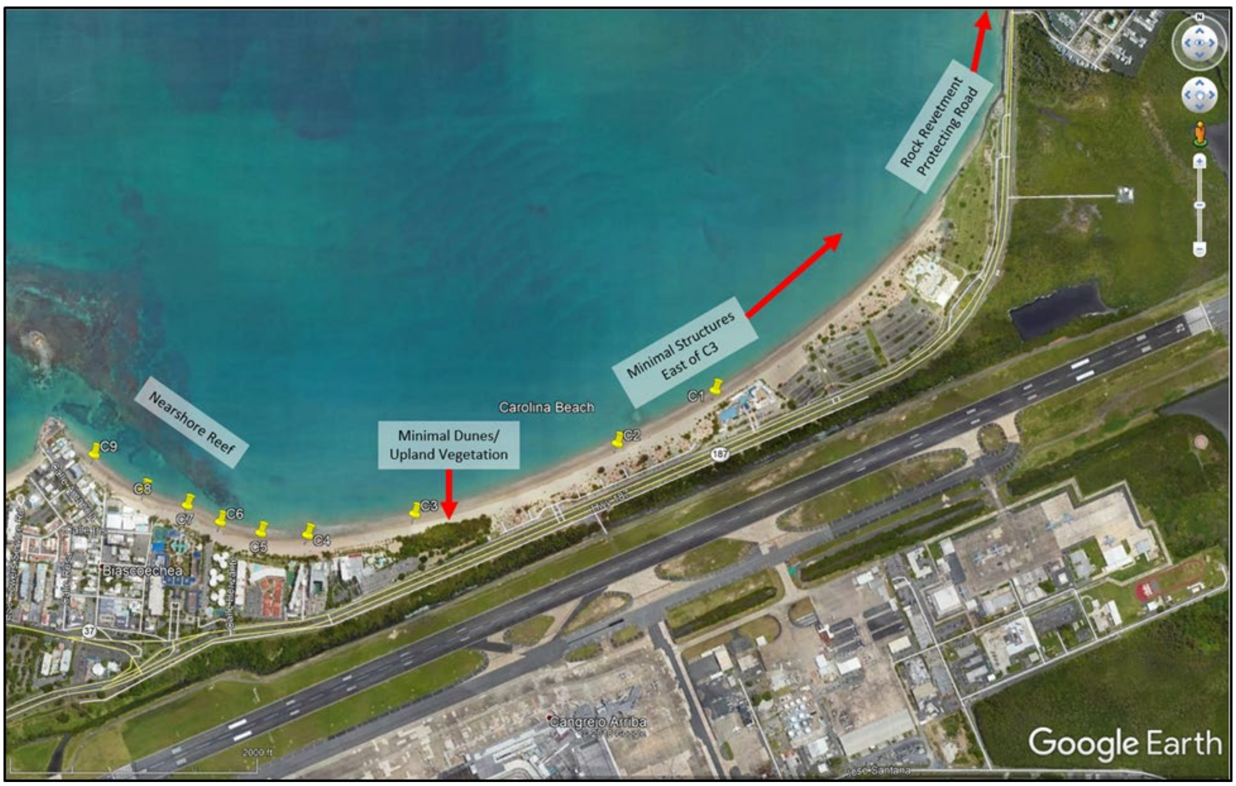

Figure A - 4. Carolina Areas of Interest

Figure A - 5. Existing Beach near C1 in Carolina, Facing East

Figure A - 6. Wide and Sloped Beach Berm near C3 in Carolina, Facing West

Figure A - 7. Narrow, Low-Lying Dune near C3 in Carolina, Facing South

Figure A - 8. Generally Similar Beach Conditions C3-C6; Photos near C5, Facing West

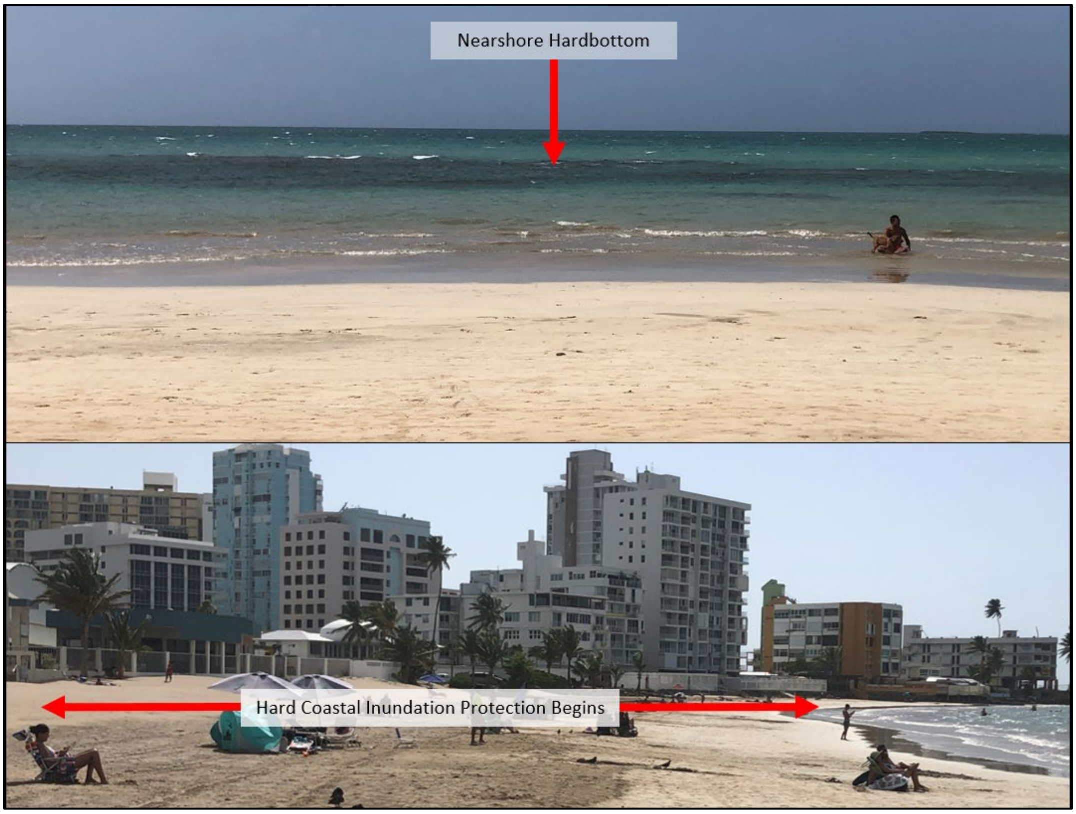

Figure A - 9. Coastline Features near C7, Facing North (Top) and Facing West (Bottom)

Figure A - 10. Inundation Focal Points near C8 (Top) and C9 (Bottom), Facing West

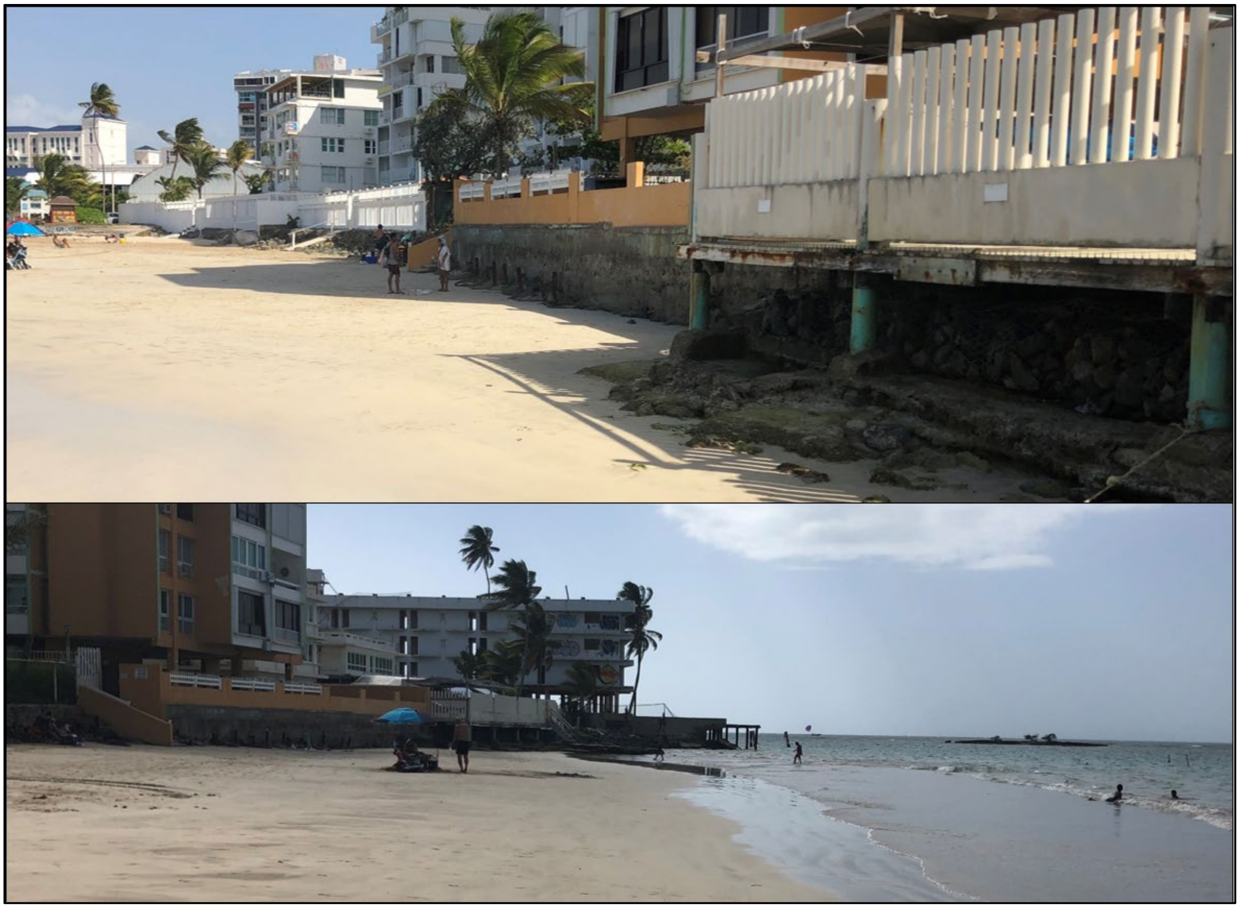

Figure A - 11. Western Carolina Sea Walls near C9 Facing South (Top) and North (Bottom)

1.2.1.2 Isla Verde

Punta El Medio, which segregates Carolina to the east and Isla Verde to the west (Figure A - 12), contains similar coastline conditions on either side. Seawalls and rock revetment around the point experience daily coastal water encroachment. A dry, mildly-sloping beach generally widens from Punta El Medio traversing west in Isla Verde to stations IV3/IV4 (the widest portion of dry beach in Isla Verde). Coastal infrastructure in this section are largely unprotected by artificial CSRM features or natural dunes (Figure A - 13 and Figure A - 14). Consistent conditions from IV3 west to IV6 include a wide dry beach berm, low-lying structure and road elevations, and little to no upland inundation protection features (dunes, vegetation, hard structures, etc.), as shown in Figure A - 15. The dry beach narrows from IV6/IV7 to IV12, and upland structure protection largely increases in that area (Figure A - 16). IV6 to IV10 contains intermittent dunes and sparse upland vegetation, but coastal construction appears to trend seaward near IV9/IV10 and terminates in the center of the natural dune line (exposed seawall shown near IV10 in Figure A - 17). The diminishing beach width to the west of this area is likely compounded by structures built too close to the coast.

The shoreline from IV12 to IV14 consists of a 700-ft-long detached rock breakwater with three small rock groins in the nearshore zone, large seawalls, and small rock riprap protecting upland coastal structures. Wave energy and current circulation patterns appear to impact these structures during large events, as a portion of seawall is undermined, and riprap rock is displaced near IV13 (Figure A - 18). West-northwest of IV14 is likely the most critically exposed portion of Isla Verde. According to locals, coastal high-rise development between IV14 and IV15 terminated in the early stages of construction, and the area was abandoned. A small seawall protects the coastline between IV14 and IV15 but is actively overtopped during low-energy, wind-driven waves. Overtopping and wave reflection from the seawall may actively promote erosion on either side of the seawall. Rock riprap generally protects the coastline west-northwest of IV15 in western Isla Verde.

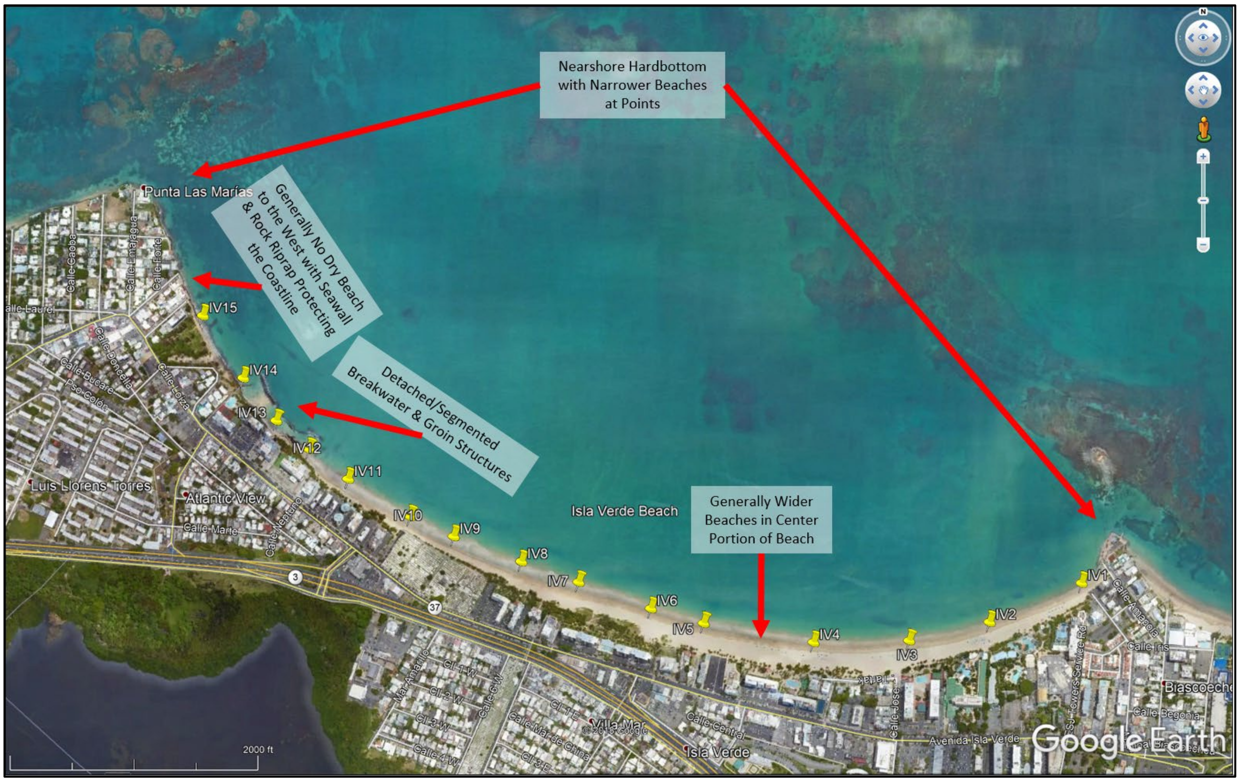

Figure A - 12. Isla Verde Areas of Interest

Figure A - 13. Western Punta El Medio in Isla Verde near IV1 (Top) and IV3 (Bottom), Facing East

Figure A - 14. Existing Coastal Conditions near IV3/IV4 (Top is Facing West and Bottom is Facing South)

Figure A - 15. Decreasing Beach Widths and Increasing Flood Protection near IV6/IV7, Facing West

Figure A - 16. Upland Seawall near IV10, Facing East

Figure A - 17. Seawalls near IV13, Facing West

Figure A - 18. Breakwater and Groins from IV12 to IV14, Facing Northwest (Left) to Southeast (Right)

1.2.1.3 Ocean Park

Like Carolina and Isla Verde, the eastern and western beach extents in Ocean Park contain little to no dry beach with prevalent nearshore hardbottom and a wider central beach expanse. Punta Las Marías is the point that segments Isla Verde to the east and Ocean Park to the West. It resembles Punta El Medio by largely containing seawalls and rock riprap protecting upland structures from inundation, erosion, and wave attack.

Nearshore hardbottom is exposed at low tide east of station OP5, and a narrow, mildly sloping beach berm (with no dune or upland vegetation) adjoins hard coastal structures in small sections between OP1 and OP5 (Figure A - 20). The seawalls in this area are relatively large, but storm drain culverts exist within the seawalls that could act as focal points for flood waters during costal storms. Like the culverts in seawalls and under roads in Carolina, these features could pose major dune and/or berm erosion problems if nourishment is constructed in this area. The coastline between OP5 and OP7 is somewhat unique to Ocean Park, as it contains the only stretch that is not developed with homes or condominiums. This area is historically known for extensive coastal inundation since storm surge and wave attack can focus on this unprotected stretch of coast. Hard structures to the east and west may allow coastal water energy to follow the path of least resistance at Dr. José Celso Barbosa Park as it propagates landward. Energetic conditions have eroded fronting beaches (at OP5 and OP7), and the berm crest is set back at the center of the park (just west of OP6). At the time of inspection (June 2019), erosive coastal forcing formed a large scarp near OP5/OP6, exposed nearshore hardbottom, and undermined the eastern edge of the seawall protecting western Calle Park Blvd. A mixture of riprap and concrete placed at the northwestern corner of the road's seawall is likely an emergency measure to protect upland public property. Additionally, sheet pile seawall remnants are buried in the beach berm near OP7. Figure A - 21 shows the concaved beach with structures on either side of the park expanse.

Contrary to the aerial shown in Figure A - 19, the shoreline from OP7 to OP8 is extremely eroded, and ocean waters regularly encroach the seawalls protecting upland structures (Figure A - 22). The beach width increases from OP8 to its widest point in Ocean Park near OP11. Sparse dunes with upland vegetation are present between OP10 and OP11. However, this feature likely wouldn't impede flood waters during a storm event, as water could traverse through dune gaps and impact upland structures. Figure A - 23 shows the features from OP8 to OP11.

The beach width generally decreases from OP11 to OP16. Lack of dunes and upland vegetation and two storm drain runoff culverts that terminate in the berm near OP12 and OP14 all accentuate flood risk potential in this area (Figure A - 24). The narrowing beach berm at the western end of Ocean Park Beach near Punta Piedrita (the point at the western end of Ocean Park) is synonymous with the other beaches' extremes – nearshore hardbottom is exposed and ocean waters regularly encroach upland structures. Further, the relatively small seawall protecting condos at Punta Piedrita failed and concrete debris is scattered in the nearshore zone.

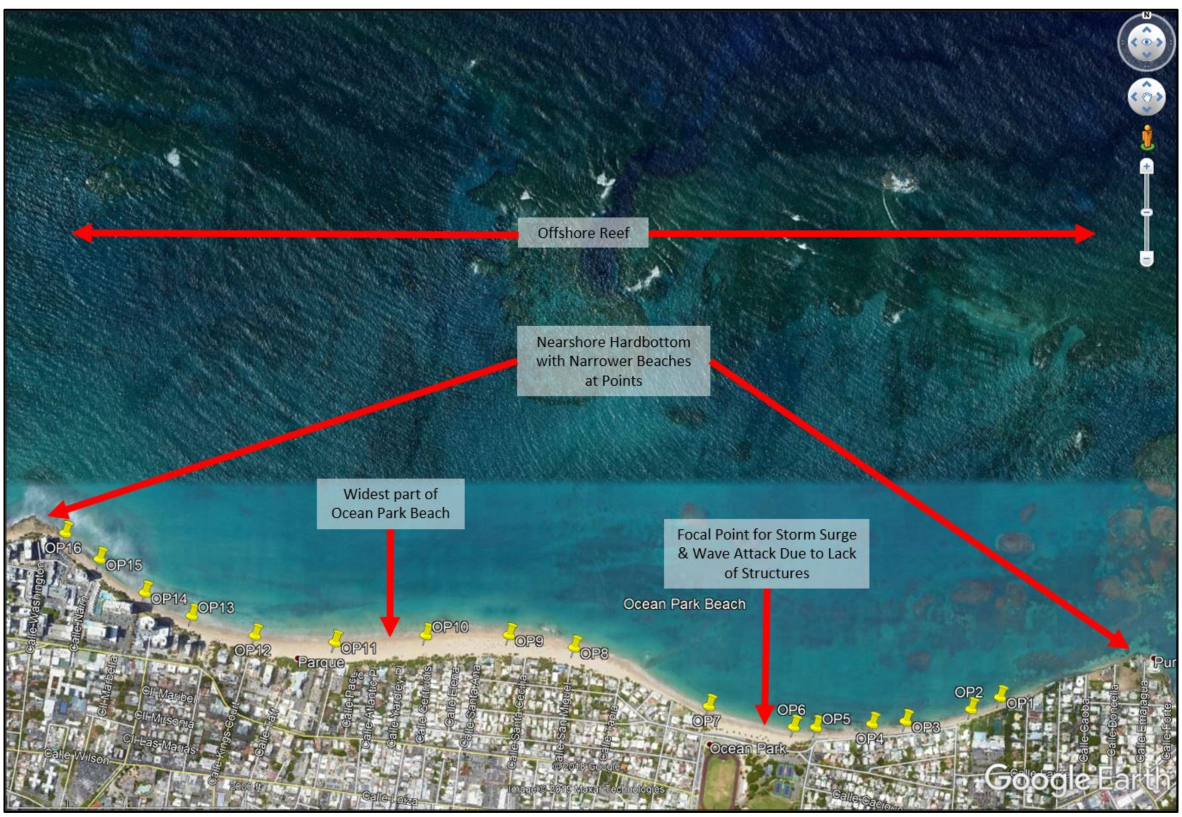

Figure A - 19. Ocean Park Beach Areas of Interest

Figure A - 20. Eastern Ocean Park Beach near OP1 (Top) and OP5 (Bottom), Facing East

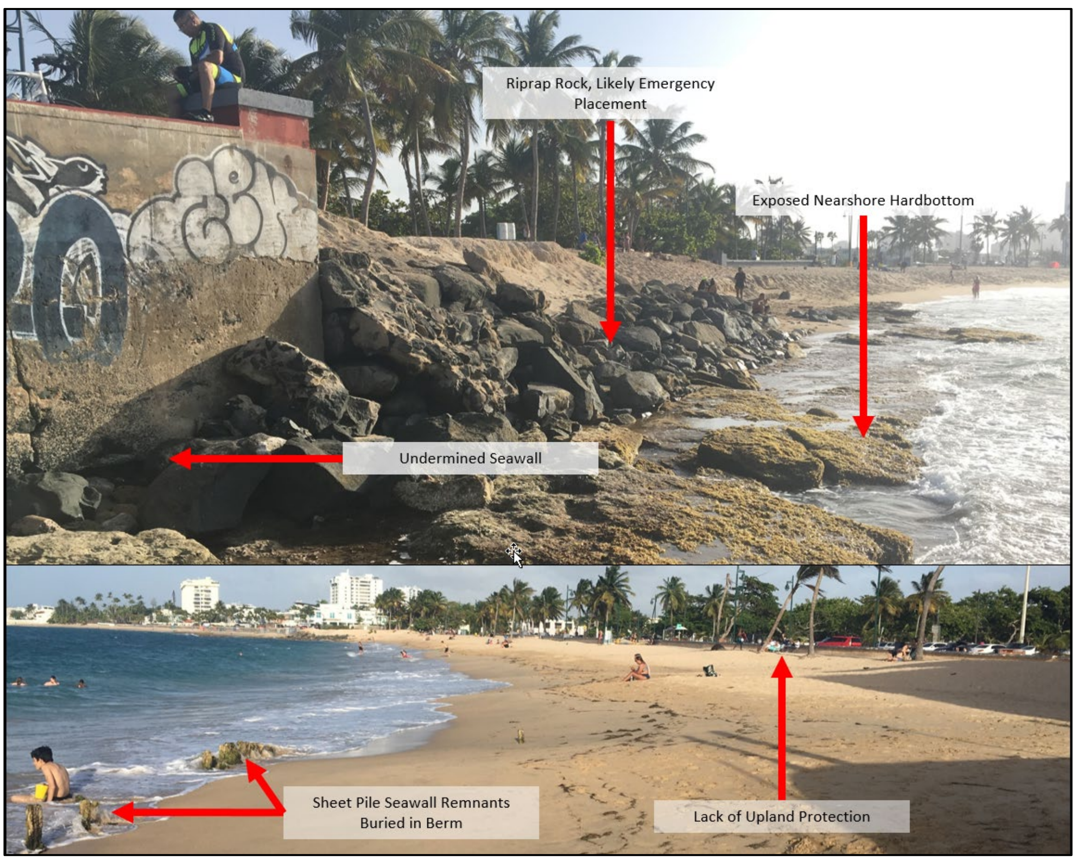

Figure A - 21. Ocean Park near OP5 (Top, Facing West) and OP7 (Bottom, Facing East)

Figure A - 22. Ocean Water Encroachment and Undermined Seawalls Just West of Ocean Park

Figure A - 23. Widening Beach Traversing West from OP8 to OP11

Figure A - 24. Western Ocean Park Beach from OP12 to OP16

1.2.1.4 Condado

Condado contains the smallest area of dry beach out of the four San Juan beaches detailed in this report (as indicated in Figure A - 25). The eastern 0.5 mi from Punta Piedrita (near station CO1) west to the inclined groin at La Ventana al Mar (CO8-CO9) encompasses nearly all the dry beach in this expanse, where the widest part of the beach is centered around a small, porous groin at CO5. The western 0.5 mi from the angled groin to El Boquerón contain virtually no dry beach and waves regularly break directly on exposed nearshore reef, seawalls, and rock revetments.

The beach berm width generally increases from CO1 to CO5, where virtually no dry beach exists east of CO4. Exposed nearshore hardbottom adjoined large condominium seawalls, and two road runoff culverts drain rainwater from roads to the ocean in this portion of beach (Figure A - 26 and Figure A - 27). Conversely, structures between CO4 and CO7 largely contain first floor elevations in line with the flat beach berm crest without soft or hard shoreline protection (Figure A - 28 and Figure A - 29). The shoreline from CO7 to CO9 is protected by a large, inclined groin. The roughly 500-ft-long, 50-ft-wide groin consists of large rock riprap surrounding a recreational concrete cap walkway. Damaged railings shown in Figure A - 30 are likely a result of recent major storm impacts.

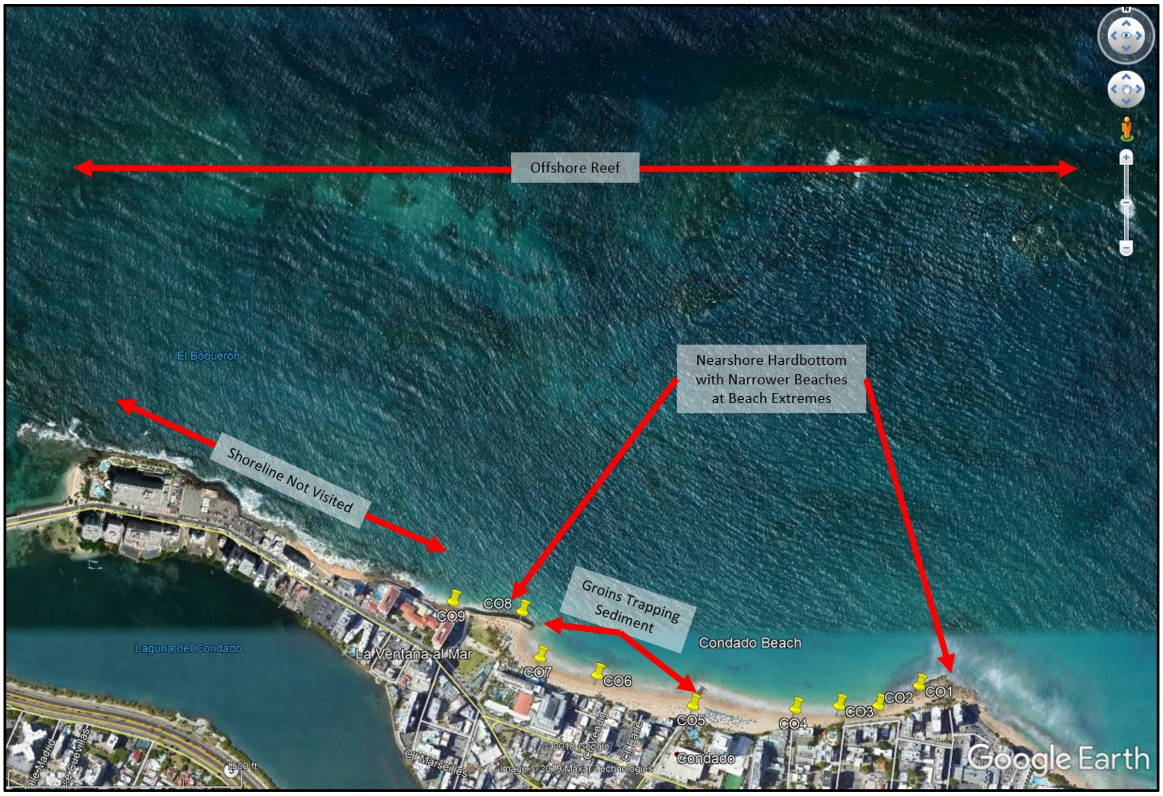

Figure A - 25. Condado Beach Areas of Interest

Figure A - 26. Eastern Condado Beach from CO1 to CO4

Figure A - 27. Eastern Condado Beach at CO5

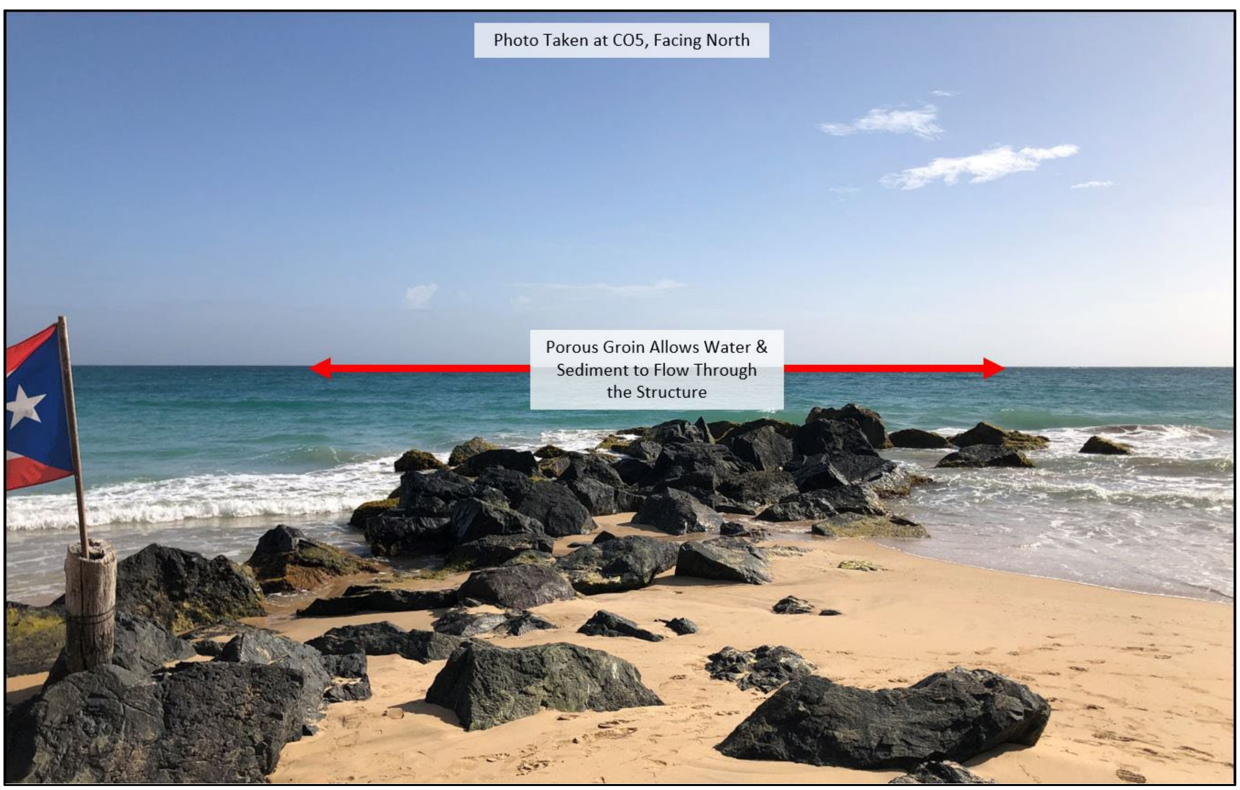

Figure A - 28. Groin Feature at CO5

Figure A - 29. Eastern Condado Beach from CO6 to CO7

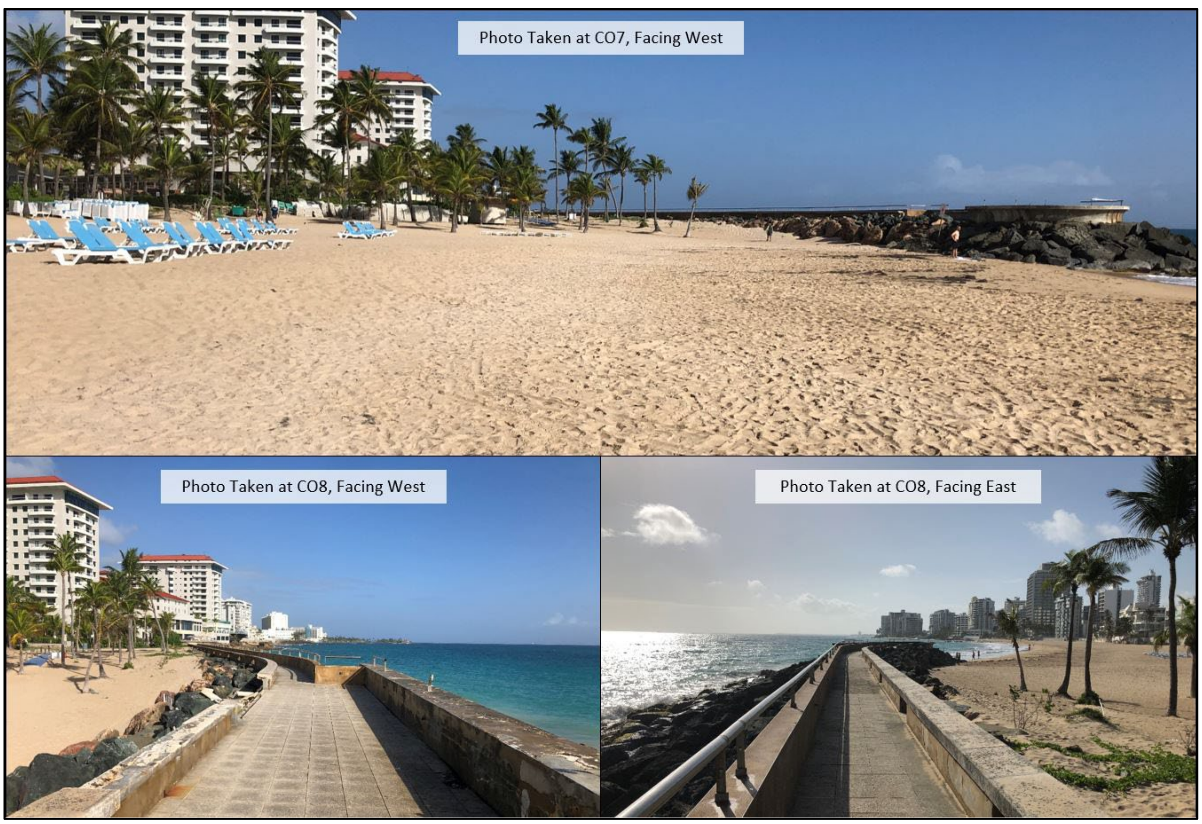

Figure A - 30. Eastern Condado Beach from CO7 to CO8

1.2.2 Rincón Conditions

The observations presented here are in order from north to south for the Rincón study area. The shoreline from the Rincón Marina to Córcega generally contains wider beaches and elevated berm crests to the north and narrower beaches with abandoned homes, some physically in the water, to the south. Intermittently exposed hardbottom to the north and prevalent submerged hardbottom to the south typically characterizes the nearshore zone. The upland region is typically defined by minimal dunes and/or dune vegetation with some seawalls and relatively small revetments protecting homes and hotels. Some small canals that drain upland freshwater to the Mona Passage are noted from the marina to the central portion of the study area coastline.

1.2.2.1 <u>Rincón "A"</u>

For this report, Rincón is split into two sections: Rincón A to the north and Rincón B to the south, delineated by the mouth of Quebrada Los Ramos that drains into the Mona Passage, as shown in Figure A - 31. The northern stretch of coast from station R1 to R5 contains less coastal structures than the southern shoreline. R1 to R2 consists of a rock groin at the Rincón Marina to the north, narrow, mildly-sloping beach berms and nearshore hardbottom throughout, minimal upland structures, and a small canal draining freshwater to the Mona Passage (Figure A - 32 and Figure A - 33). The shoreline from R2 to R4 contains intermittent sections of no dry beach between nearshore/exposed hardbottom and upland structures, likely resulting from construction too close to the coast (Figure A - 34). However, the dry beach berm trended wider south of R3, as coastal construction is set back from the shoreline (Figure A - 35). The beach is widest from R4 to Quebrada Los Ramos (Figure A - 36), where a small scarp has formed, likely from canal flushing during rainfall and/or wave runup during storm events.

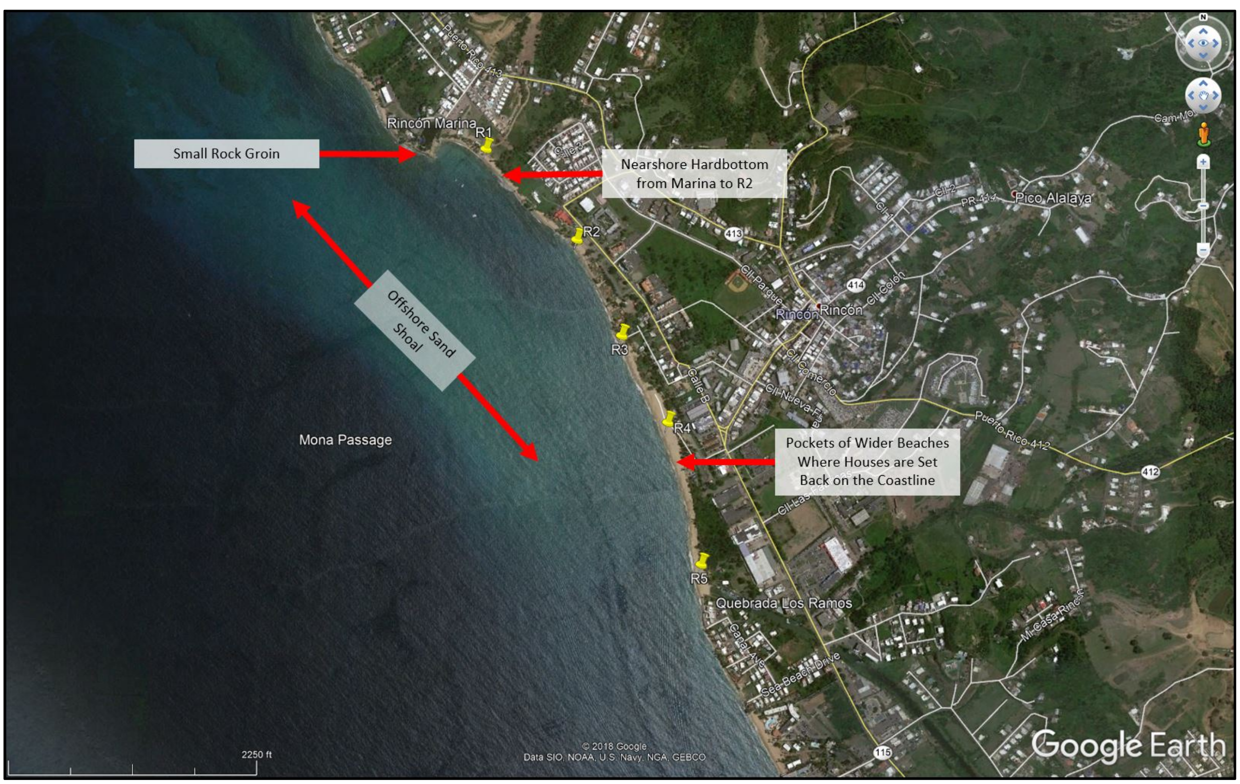

Figure A - 31. Rincón "A" Areas of Interest

Figure A - 32. Coastal Features North of R1

Figure A - 33. Coastal Features from R1 to R2

Figure A - 34. Failed Seawall and Nearshore Hardbottom near R2

Figure A - 35. Wider Beaches from R3 to R4

Figure A - 36. Widest Part of Rincón between R4 and R5, North of Quebrada Los Ramos

1.2.2.2 Rincón "B"

The southern portion of the Rincón study area (Rincón "B") spans from Quebrada Los Ramos to Córcega and generally consists of coastline with minimal to no dry beach. Like the area north of Quebrada Los Ramos, homes and hotels may have been built too close to the coastline in Rincón B. Pockets of dry beach only exist where structures are set back from the shoreline. Visible nearshore hardbottom begins just north of station R9 and was largely exposed after TC Maria and ET Riley in fall 2017 to spring 2018 (local communication and Google Earth Imagery analyses). Structures to the south (especially in Córcega) are regularly encroached by coastal waters and are either undermined with completely failed foundations or protected by emergency riprap placement. Seawalls and revetment in front of homes and hotels make up many of these structures, and some homes in Córcega appear abandoned. Figure A - 38 through Figure A - 42 depict the area south of Quebrada Los Ramos as described herein.

Figure A - 37. Rincón "B" Areas of Interest

Figure A - 38. Rock Revetment and Debris in front of Small Seawalls near R6/R7

Figure A - 39. Active Water Encroachment to Seaward-Most Structures near R8/R9

Figure A - 40. Visible Nearshore Hardbottom near R9

Figure A - 41. Small Beaches Exist Where Structures Are Set Back from the Coast near R10

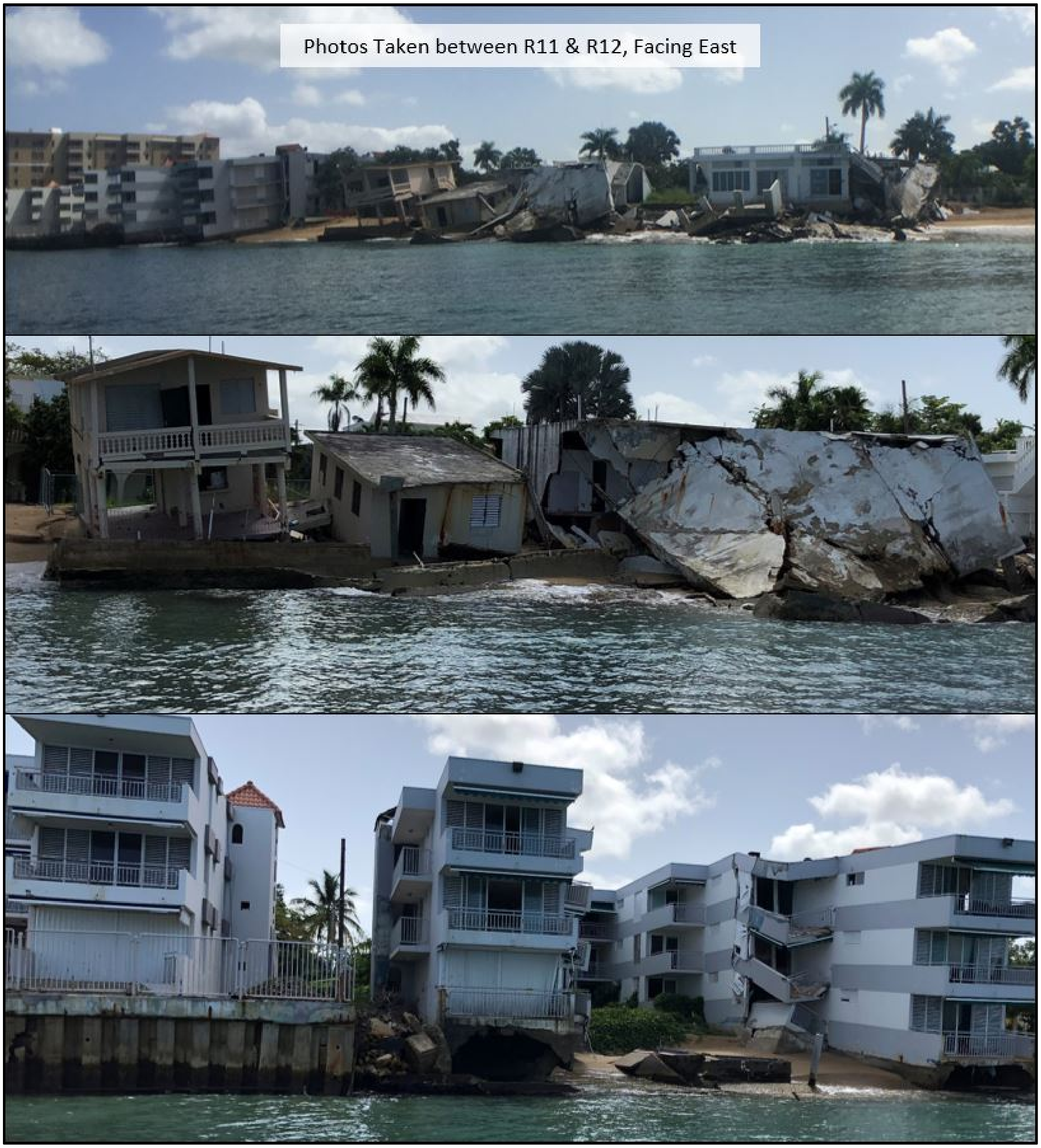

Figure A - 42. Destroyed Homes and Active Water Encroachment in Stella and Córcega

2.0 COASTAL HAZARDS IN PUERTO RICO

Natural coastal hazards can be broken down into two categories: short- and long-term processes. Understanding how to quantify and efficiently mitigate the threat posed by coastal hazards is vital to the resilience of coastal communities. Short-term coastal events reside on a temporal scale of days, hours, or sometimes even minutes. These events include TC and ET systems, tides (high tide amplitudes), wind, and waves. Accurately quantifying possible flood and erosion thresholds due to these constituents can be accomplished by different computational modeling suites (Bredesen, 2015). Long-term processes act over a period of months, yrs, decades, or longer. Relative sea level change (SLC) is the primary long-term process considered in this study. Short- and long-term events, and more notably the hazards that result from these events in Puerto Rico, is the focus of this appendix.

2.1 Short-Term Coastal Processes

The most destructive coastal hazard within Puerto Rico is a TC. Warm, moist ocean waters evaporate in tropical latitudes, condensing to form clouds (USGS, 2014b). Warm air continues to rise, causing atmospheric pressure to drop due to less air mass at the ocean's surface. The pressure differential and energy transfer from the condensation results in cooler air temperatures that blow from high to low pressure, creating a circular "eye" of the newly formed storm system. The cooler air subsides slowly within the eye-wall region before rising again. This process forms winds that rotate counterclockwise (ccw) in the northern hemisphere due to the earth's rotation on its axis. The storm intensifies, using the latent heat from warm tropical waters as an energy source (Bredesen, 2015). Two of the most notable TC events in Puerto Rico in the last century include TC Hugo (1989) and TC Maria (2017). These events battered the island with intense winds, heavy rain, large waves, and relatively large storm surge (more on Maria's "relatively large" storm surge in Puerto Rico later in this report).

Atmospheric variations in the northern hemisphere's winter months can cause ET's, which are coastal cyclonic storms that rotate ccw in a low-pressure system around a central low-pressure extreme that are generally in higher latitudes than TCs (Bredesen, 2015). Depending on the nature of the event, ET's can impact extensive spans of Puerto Rican coastline with days of large, long-period waves, while spinning thousands of mi away (no direct wind and rain impact). It is important to note that while this study focuses on CSRM efforts, there are two coastal storms components that are not considered are direct wind impacts and rainfall.

2.1.1 Astronomical Tides

Astronomical tides generally fluctuate because of the gravitational influences of the moon, sun, and the earth. Tides are generally well understood and relatively easy to predict from established astronomical tidal constituents. The National Oceanic and Atmospheric Administration (NOAA) regularly publishes tide tables for selected locations along coastlines around the world. These tables provide times of high and low tides, as well as predicted tidal amplitudes that aid in coastal study's modeling and design efforts.

2.1.1.1 San Juan Tides

Tides in San Juan, Puerto Rico are mainly affected by mixed, semidiurnal tidal fluctuations of the Atlantic Ocean with two high and two low tides that occur at different elevations per tidal day. This study used tide phases and amplitudes for hydrodynamic and economic life-cycle modeling in San Juan that were acquired from the NOAA tide station 9755371 (San Juan, La Puntilla) in the San Juan Bay, as shown in Figure A - 43. The NOAA gauge presently contains astronomical tide data that dates to November 1977.

Tidal datums for the San Juan study area are referenced to the Puerto Rico Vertical Datum of 2002 (PRVD02) from the tidal epoch period of 1983 – 2001, are based on a discontinuous, 17-yr analysis period, and have a mean tidal range of 1.11 ft (Table A - 1). The PRVD02 vertical datum is the official vertical datum of Puerto Rico and will be used as the referenced datum for water level criteria in most of this report.

It is important to note that PRVD02 was created via a geodetic leveling network, and the relation between a stationary point (a benchmark) and the Mean Sea Level (MSL) datum at that benchmark (NOAA, 2012b). Therefore, MSL is a datum related to average local water levels around a tide station (may change by location), but PRVD02 is an island-wide, stationary geodetic datum as a part of NOAA's overall National Spatial Reference System (NOAA, 2012b). The San Juan NOAA tide station 9755371 hosts the benchmark used in this effort; thus, PRVD02 and MSL should always be equal in San Juan, Puerto Rico. Some figures represented in this report may reference MSL instead of PRVD02 for this reason.

Figure A - 43. NOAA Tide Stations with Long-Term Records in the Vicinity of San Juan, Puerto Rico

Table A - 1. San Juan Tidal Datums (NOAA Station 9755371)

Location: 18° 27.6' N, 66° 7.0' W Analysis Periods: Jan. 1983 - Dec. 1987, Jan. 1990 - Dec. 2001	
Datum	**Elevation (ft-PRVD02)**
Mean Higher-High Water (MHHW)	0.81
Mean High Water (MHW)	0.55
Puerto Rico Vertical Datum of 2002 (PRVD02)	0.00
Mean Sea Level (MSL)	0.00
Mean Low Water (MLW)	-0.56
Mean Lower-Low Water (MLLW)	-0.77

2.1.1.2 Rincón Tides

Water levels in the Rincón study area are mainly affected by wind and semi-diurnal tidal fluctuations of the Mona Passage connecting the Atlantic Ocean and Caribbean Sea basins. Tidal datums in the Rincón study area vicinity were gathered using NOAA's Mayagüez, Puerto Rico Station 9759394 shown in Figure A - 44. Table A - 2 shows the elevations from that gauge, which are referred to PRVD02 from the tidal epoch period of 1983 – 2001, are based on a 10-month analysis period ranging from May 2015 – February 2016, and have a mean tidal range of 1.05 ft. These elevations were used in this study's Rincón modeling and alternative design activities. It is important to note that while the San Juan study area contains the same datum elevations for MSL and PRVD02, Rincón's local water levels average slightly lower than the static PRVD02 elevation. Thus, MSL and PRVD02 are not interchangeable in this location.

Figure A - 44. NOAA Tide Stations with Long-Term Records in the Vicinity of Rincón, Puerto Rico

Table A - 2. Rincón Tidal Datums (NOAA Station 9759394)

Location: 18° 13.1' N, 67° 9.7' W Analysis Period: May 2015 - Feb. 2016	
Datum	**Elevation (ft-PRVD02)**
Mean Higher-High Water (MHHW)	0.73
Mean High Water (MHW)	0.52
Puerto Rico Vertical Datum of 2002 (PRVD02)	0.00
Mean Sea Level (MSL)	-0.02
Mean Low Water (MLW)	-0.53
Mean Lower-Low Water (MLLW)	-0.66

2.1.2 Direct and Indirect Wind Forcing

The earth and its atmosphere are a continually changing dynamic system. Earth's air, for instance, is constantly driven by the globe's rotation on its axis, its revolution around the sun, and the transfer of energy from the sun (Tarbuck and Lutgens, 2006). Solar energy heats the earth unevenly due to the planet's motions. This non-uniform energy distribution induces constantly shifting circulation patterns, which manifest themselves in the form of winds (Bredesen, 2015). The energy transfer process continues into the earth's surface, where sporadic heating from the sun assists the macro-scale water movements creating ocean currents. Wind transfers energy into the water's surface due to friction and pressure gradients, building waves and inducing surface currents. These forces, whether large or small, continually shape earth's evolving surface features (Bredesen, 2015). This evolution may be most noticeable along coastlines, where land, air, and water merge (Tarbuck and Lutgens, 2006).

There are two aspects of wind forcing that may be considered in CSRM studies: direct wind forcing and indirect wind forcing. Direct wind forcing is wind load on a structure, whereas indirect wind forcing is energy applied from waves, surge, and currents that result from the transfer of wind energy to water via shear stress. While both are important, only the latter is considered in this study. Thus, direct wind damage to coastal structures is not considered in the overall CSRM measures discussed herein.

2.1.2.1 General Puerto Rico Wind Climate

The Commonwealth of Puerto Rico lies within the tropical trade wind zone, resulting in moderate winds from a prevailing easterly direction all yr long. Increased north-northeast winds during fall, winter, and spring seasons primarily occur from ET cyclones in the mid- to northern-Atlantic Basin. Extreme conditions from tropical systems generally impact the island in the summer and fall months. Wind data around the island are available from sources such as the USACE Wave Information Study (WIS) Program and NOAA's various platforms for coastal and climatological data.

The WIS is a wind and wave hindcast database for various stations located along the U.S. Atlantic, Gulf of Mexico, and Caribbean coastlines. Available data include six stations around the island that contain hindcast time series of wind speed, wind direction, wave height, wave period, and wave direction in 1-hour intervals for the 35-yr period of 1980 – 2014 (Figure A - 45). NOAA's Integrated Ocean Observing System (IOOS) produces and compiles high-quality coastal, ocean, and lake data across 11 regions spanning the US Pacific, Atlantic, Great Lakes, and Caribbean coasts. Compiled data from sources such as satellites, ocean buoys, and pressure gauges are displayed in an integrated view for each region. The Caribbean Integrated Coastal Ocean Observing System (CARICOOS) Website is a data portal for the IOOS Caribbean Region developed for Puerto Rico and the Virgin Islands that brings together coastal ocean data including wind, waves, tides, and ocean currents. Notable CARICOOS data around Puerto Rico include the National Data Buoy Center's (NDBC) stations near San Juan and Rincón (Figure A - 46). Notably, Oceanweather, Inc. (OWI) hindcast and operational wind data were obtained around Puerto Rico to assist with forcing the models that were used in this study. A detailed explanation of those data is further described in Section 3.2 of this report.

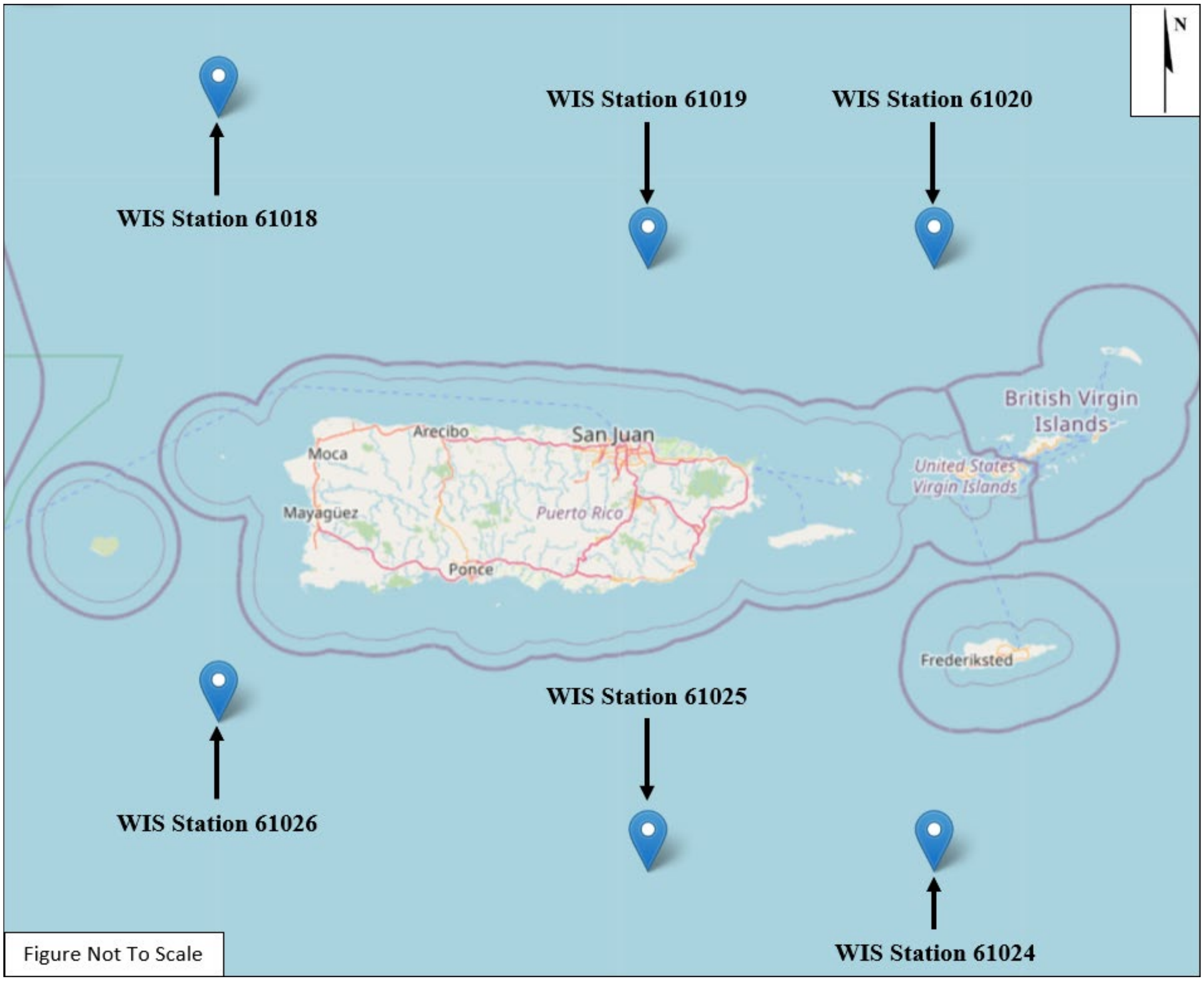

Figure A - 45. WIS Stations around Puerto Rico

Figure A - 46. CARICOOS Stations around Puerto Rico

2.1.2.2 San Juan Wind Forcing

While the NDBC Station just off the San Juan coastline (18° 28.4' N, 66° 5.9' W) contains wind data from 2010-2020, WIS Station 61019 (approximately 37 mi north of San Juan at 19° 0.0' N, 66° 0.0' W) is the closest station to the San Juan study area with somewhat of a long-term record (35 yrs vs 11 yrs). Both stations are shown in Figure A - 47, and both stations were used to assess the general wind climate in San Juan. Table A - 3 and Figure A - 48 show that the prevailing wind direction is from the east. Approximately 94.0% of the WIS wind records from 1980 to 2014 were from the northeast (NE) to southeast (SE) quadrants. Average wind speeds during this time top out around 16.4 miles per hour (mph) from the east-NE quadrant. These data show the prevalence of tropical trade winds in San Juan but don't fully detail wind impacts in the area. Tropical wind forcing is much less frequent but much more intense. In the matter of hours, TC wind fields can batter San Juan with wind gusts over 150 mph (i.e. TC Irma and TC Maria in 2017).

Figure A - 47. NDBC and WIS Stations near San Juan, Puerto Rico

Table A - 3. General San Juan Wind Climate by Direction and Speed

Wind Direction (from)	WIS Station 61019 (1980-2014)	
	Percent Occurrence (%)	Average Wind Speed (mph)
N	1.7	13.0
NE	13.8	16.4
E	66.6	15.9
SE	13.6	12.2
S	2.5	10.8
SW	0.8	10.2
W	0.5	10.6
NW	0.6	11.5

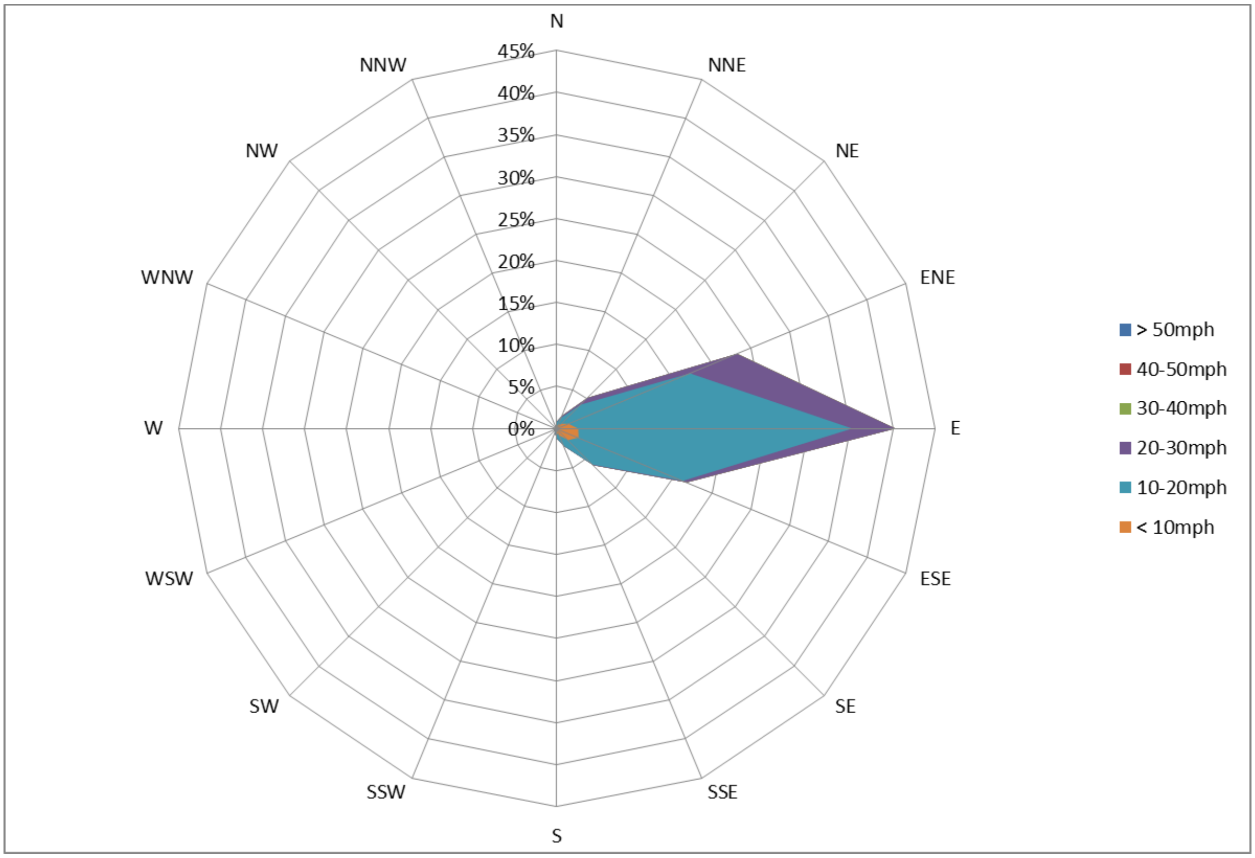

Figure A - 48. General San Juan Wind Climate by Direction and Speed

2.1.2.3 <u>Rincón Wind Forcing</u>

The three wind stations closest to the Rincón study area are WIS 61018, WIS 61026, and NDBC PTRP4 (Figure A - 49). WIS Station 61018 (19° 30.0' N, 67° 30.0' W) lies roughly 81.0 mi NNW of the Rincón study area in the Atlantic Ocean, and WIS Station 61026 (17° 30.0' N, 67° 30.0' W) lies approximately 60.0 mi SSW of Rincón in the Caribbean Sea. While these two stations contain 35 yrs of hindcast wind data, they are too far from the project site to be considered within the local wind regime. However, NDBC PTRP4 is an inland wind gauge that includes an 8-yr period of record from 2012 to 2019 and is located 1.7 mi NE of the Rincón study area at 18° 22.0' N, 67° 15.1' W. Table A - 4 and Figure A - 51 show that the prevailing winds (like San Juan) are from the eastern quadrant, where 79.2% of the wind records come from the NE to SE directions. Tropical systems (as previously mentioned) impact the area on a less frequent basis; thus, extreme wind conditions aren't represented in the average wind data shown below, and TC winds can exceed 150 mph (i.e. TC Maria) and devastate the area of Rincón.

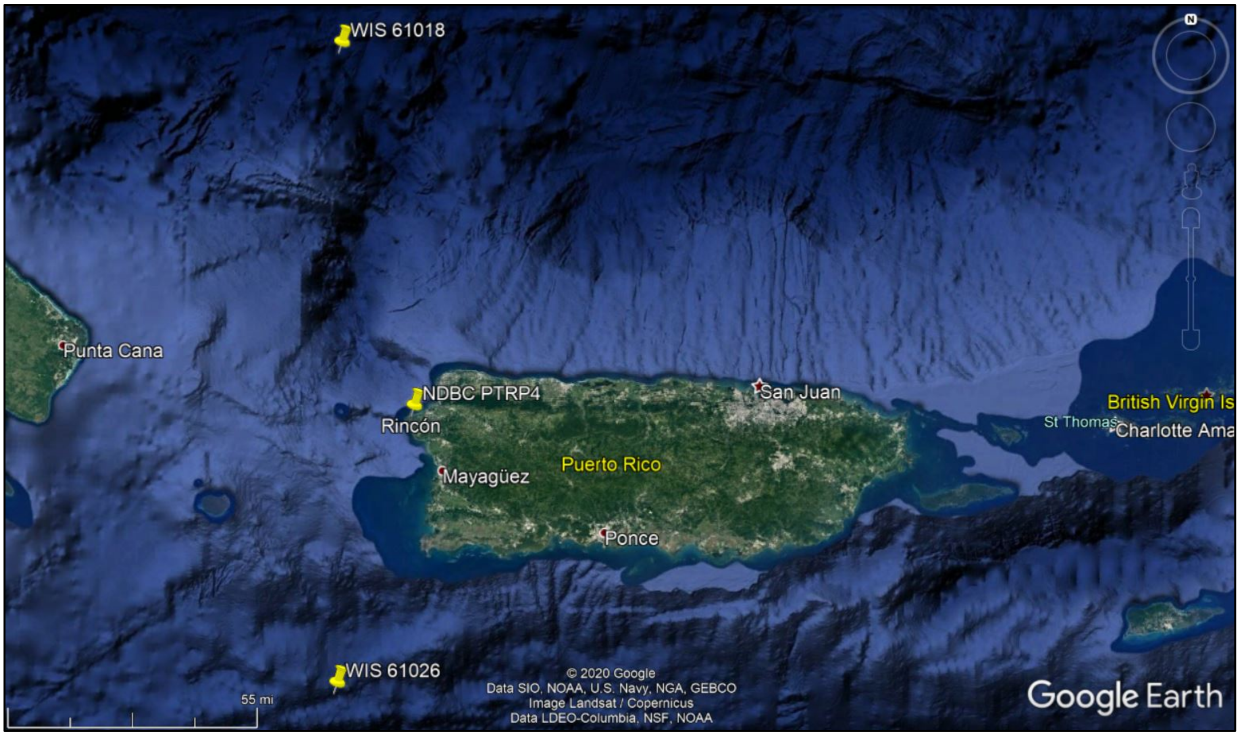

Figure A - 49. NDBC and WIS Stations near Rincón, Puerto Rico

Table A - 4. General Rincón Wind Climate by Direction and Speed

Wind Direction (from)	NDBC Station PTRP4 (2012-2019)	
	Percent Occurrence (%)	Average Wind Speed (mph)
N	7.7	7.5
NE	21.5	7.5
E	44.6	5.4
SE	13.1	4.0
S	4.4	5.2
SW	2.0	4.3
W	2.3	3.0
NW	4.4	3.6

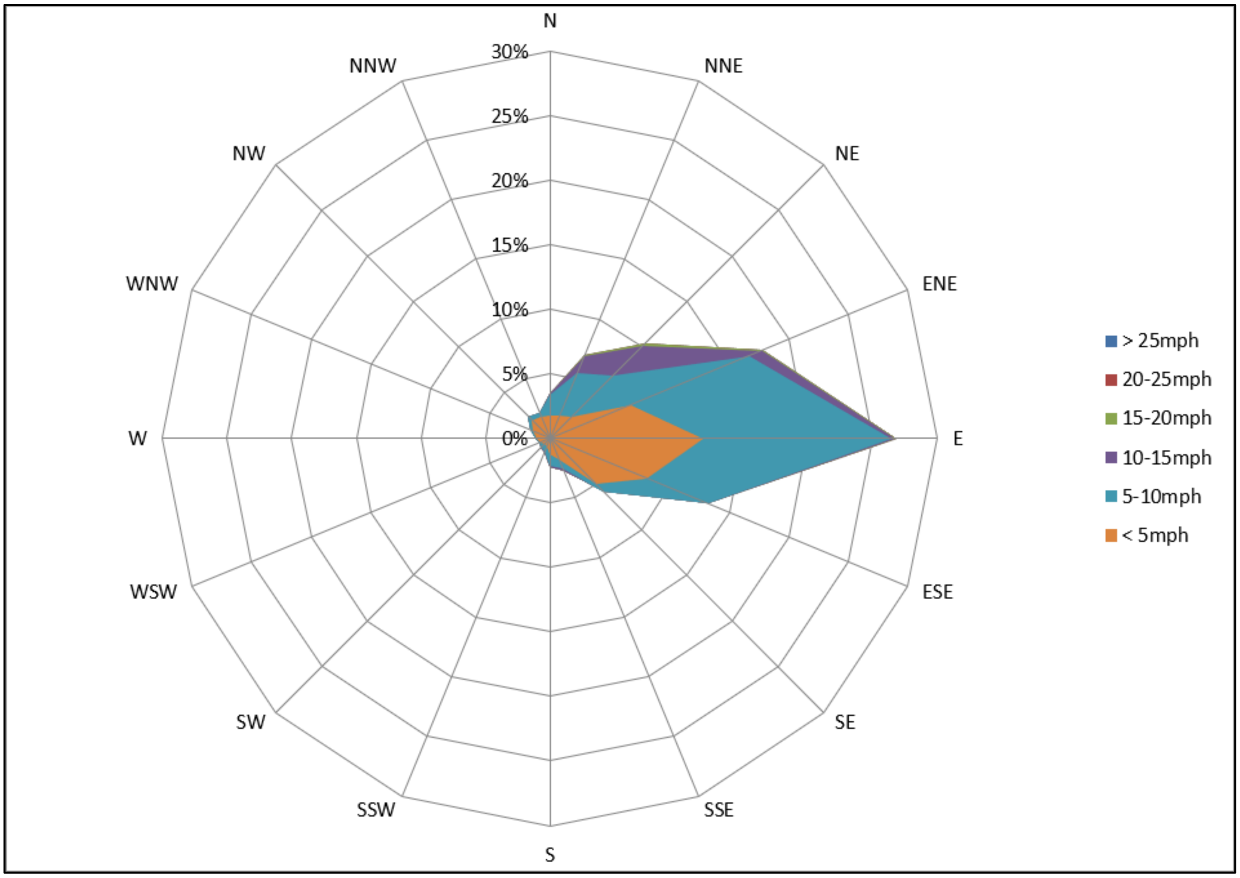

Figure A - 50. General Rincón Wind Climate by Direction and Speed

2.1.3 General Puerto Rico Wave Climate

Although individual wave events are considered short-term processes, coastlines nearly always endure the presence of waves due to the vastness of ocean surface area and the non-stop movement of the earth's atmosphere. Waves can be generated from thousands of miles away or immediately adjacent to a shoreline's location. Wind that imparts energy to the ocean's surface far from a project site can drive a wave train over a long fetch, generally resulting in higher periods and wave heights. Local, small-fetch wind-waves can yield high-frequency wave attack problems to local coastline infrastructure; and while waves are generated close to and far from a project site, they are usually the prime drivers for coastline damages. This section discusses the general wave climate in San Juan and Rincón, but the specific wave characteristics used in modeling efforts are discussed in more detail in Section 3.2.

Wave data around the island and near the two focus areas of San Juan and Rincon were obtained from similar gauges or hindcast databases as detailed in the general wind climate section (Section 2.1.2). Six WIS stations around the island contain wave height, wave period, and wave direction data in 1-hour intervals for the 35-yr period of record (1980-2014), as shown in Figure A - 45. NOAA's CARICOOS data portal compiles notable wave data stations around Puerto Rico, including the NDBC stations near San Juan and Rincon (Figure A - 46). Notably, OWI hindcast and operational wave data were obtained around Puerto Rico to assist with forcing the models that were used in this study. A detailed explanation of those data is further described in Section 3.2 of this report.

2.1.3.1 San Juan Wave Forcing

The wave stations that are closest to the San Juan study area are the same gauges as detailed in Section 2.1.2.2 and Shown in Figure A - 47 (WIS Station 61019 and NDBC Station 41053). WIS Station 61019 provides 35 yrs of offshore, deep-water wave characteristics from 1980-2014 and NDBC Station 41053 lies just off the San Juan coastline in shallower water. These data provide good indication of incoming waves that affect the coastal areas of San Juan, which is predominantly exposed to short-period, local wind-waves with periodic exposure to longer-period storm swells. Periodic damage to upland development is partially attributable to large storm waves produced primarily by ET's during the late fall, winter, and early spring months and tropical disturbances during the summer and early fall months. Storm passage (ETs and TCs) is frequent for the study area; even without landfall, a storm system passing within several hundred miles may cause an increase in waves that can affect the area.

Table A - 5 summarizes the percentage of occurrence and average wave height of the WIS waves by direction. Average wave heights range from 5.9 ft to 9.6 ft, indicating a moderate wave climate throughout the yr. Wave directions are generally from the east and northeast quadrants. This is displayed in the wave rose presented in Figure A - 51. A seasonal breakdown of wave heights show that higher wave heights are more frequent in the late fall, winter, and early spring months (November through March) and tend to originate from the northeast and east quadrant (Table A - 6). These larger wave heights can be attributed to the ET's that drive large waves towards the study area. Late spring, summer, and early fall waves (April through October), are smaller and originate predominantly from the east.

Table A - 5. San Juan's Average Wave Height by Direction

Wave Direction (from)	WIS Station #61019 (1980-2014)	
	Percentage Occurrence (%)	Average Wave Height (ft)
N	5.73	7.0
NE	30.12	6.5
E	63.74	6.2
SE	0.20	5.9
S	0.03	8.9
SW	0.01	9.6
W	0.01	6.4
NW	0.16	7.8

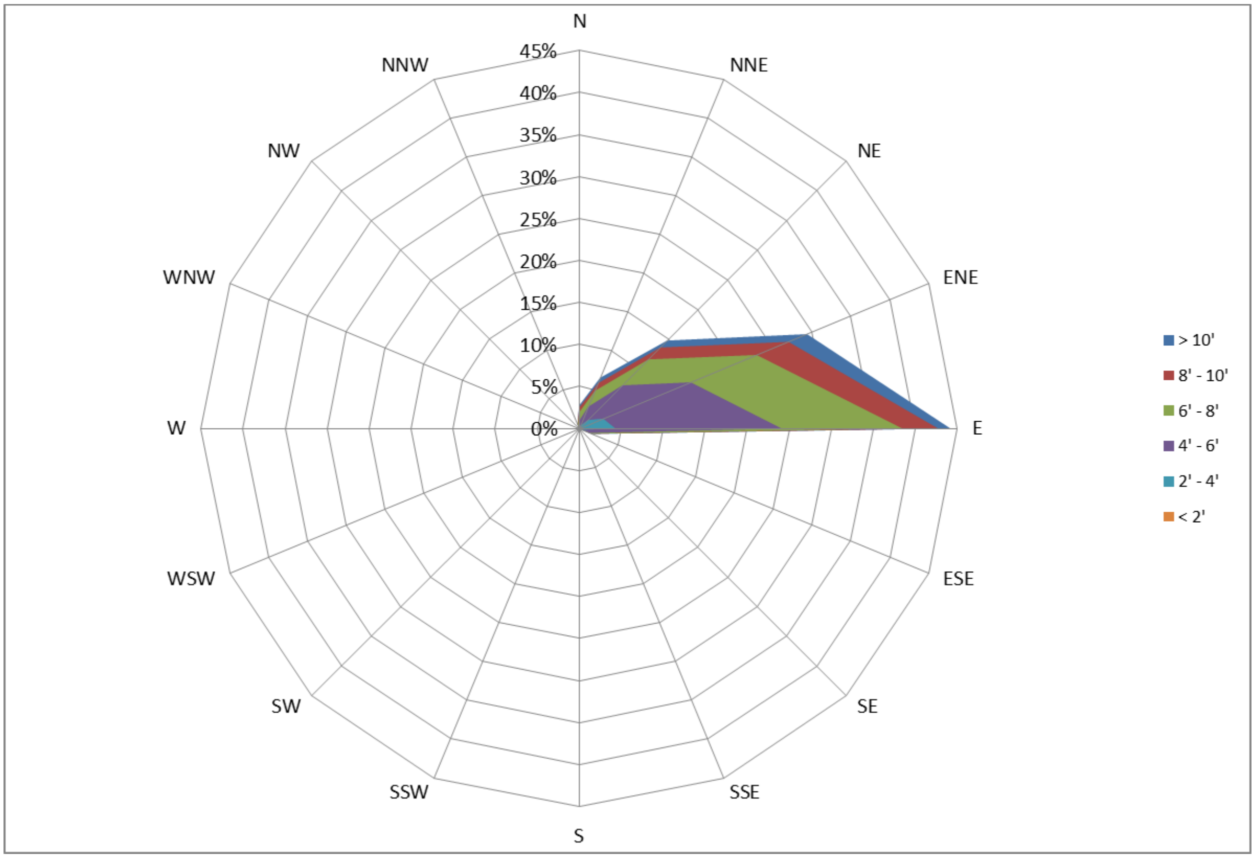

Figure A - 51. San Juan Wave Rose (WIS Station 61019)

Table A - 6. San Juan's Seasonal Wave Conditions

Month	WIS Station #61019 (1980-2014)	
	Average Wave Height (ft)	Predominant Direction (from)
January	7.8	E
February	7.5	E
March	6.8	E
April	6.0	E
May	5.3	E
June	5.4	E
July	6.1	E
August	5.6	E
September	5.4	E
October	5.6	NE
November	7.0	NE
December	7.7	NE

Table A - 7 provides a seasonal breakdown of percent occurrence by wave period. From this table, it can be seen that long period, storm-generated swells are common throughout the yr. The late fall, winter, and spring months (November to April) have slightly larger periods indicating the influence of ET's throughout the months of November through April. The highlighted values show the dominant wave period for each month. None of the dominant periods are less than 8.0 seconds.

Table A - 7. San Juan's General Wave Period Percent Occurrence (WIS Station 61019)

Wave Period (Sec)	Percent Occurrence by Wave Period Band											
	Jan	Feb	Mar	Apr	May	Jun	Jul	Aug	Sep	Oct	Nov	Dec
< 4.0	0.0	0.0	0.0	0.0	0.0	0.0	0.0	0.0	0.0	0.0	0.0	0.0
4.0 - 4.9	0.2	0.0	0.0	0.0	0.0	0.1	0.0	0.2	0.0	0.0	0.0	0.0
5.0 - 5.9	0.2	0.0	0.2	0.3	0.3	0.5	0.2	0.6	0.3	0.3	0.1	0.1
6.0 - 6.9	0.6	1.0	0.8	2.1	2.6	2.9	2.1	6.2	5.6	5.1	1.5	0.8
7.0 - 7.9	2.7	2.5	5.4	7.0	10.3	11.5	14.3	21.1	17.9	12.3	6.7	6.2
8.0 - 8.9	13.4	13.6	16.6	23.6	35.2	44.5	45.4	43.0	30.3	29.4	23.1	14.9
9.0 - 9.9	32.2	31.5	28.9	32.0	32.8	35.8	35.2	21.1	20.0	23.2	28.3	29.1
10.0 - 10.9	28.8	26.4	21.3	14.8	9.7	3.5	2.5	3.5	11.1	10.9	17.3	19.9
11.0 - 11.9	12.2	13.0	10.0	8.3	5.2	0.7	0.1	2.1	6.1	8.7	10.5	12.9
> 12.0	9.9	12.1	16.8	12.0	4.0	0.6	0.2	2.3	8.6	10.2	12.5	16.1

2.1.3.2 Rincón Wave Forcing

General wave information for the Rincon study area were obtained from the NDBC Gauge 41115 (2011-2019). Records show that average wave heights range from 1.9 ft to 4.1 ft. Wave directions are predominantly from the NNE (90.94% of the records). A seasonal breakdown of wave heights show that higher wave heights are more frequent in winter to spring months (November through March), which can be attributed to the ET storms that drive large waves towards the study area. The Rincón wave data are displayed in Table A - 8 through Table A - 10 and Figure A - 52.

Table A - 8. Rincon's Average Wave Height by Direction

Wave Direction (from)	NDBC Gauge 41115 (2011-2019)	
	Percentage Occurrence (%)	Average Wave Height (ft)
N	76.11	3.3
NE	14.83	2.6
E	0.05	2.0
SE	0.03	2.0
S	0.44	2.3
SW	2.20	2.1
W	1.76	2.0
NW	4.59	2.9

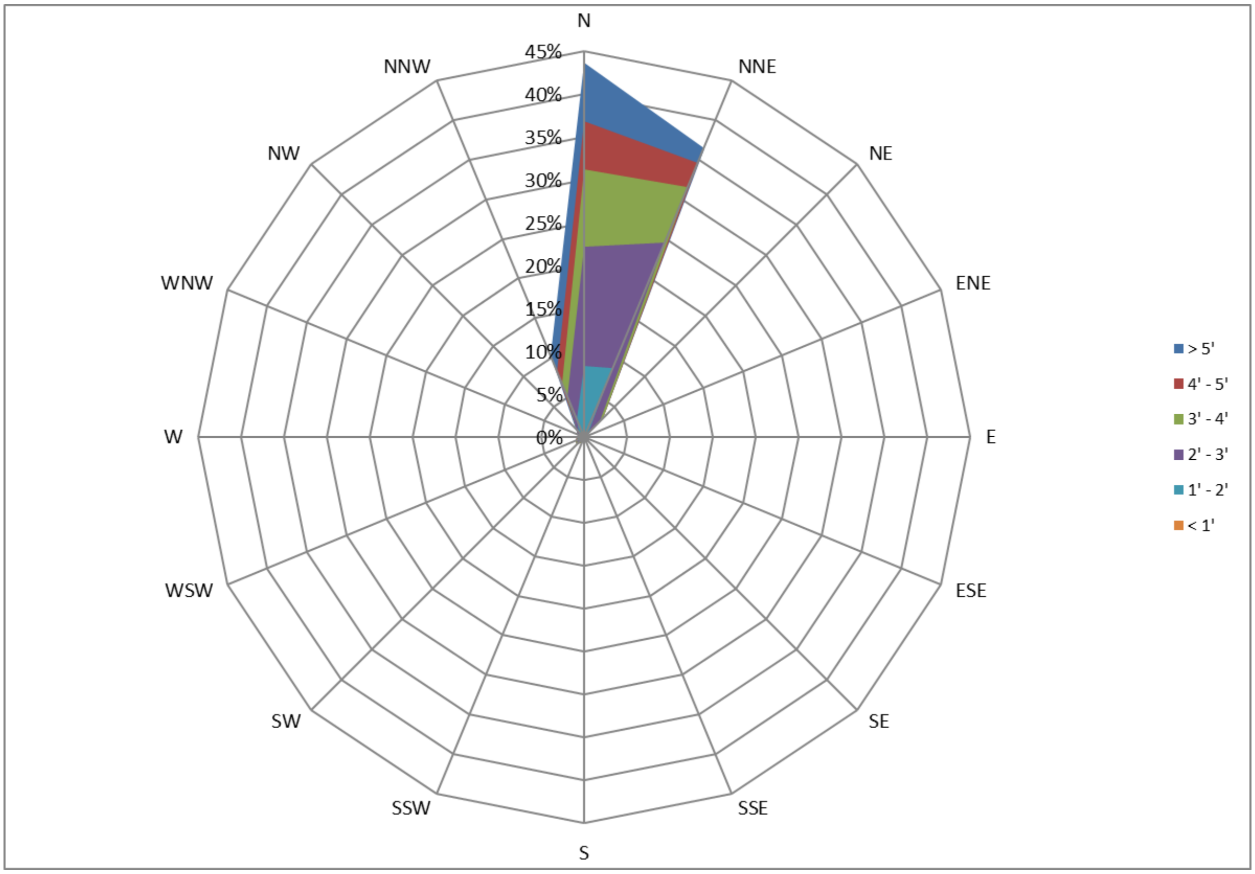

Figure A - 52. Rincon Wave Rose (NDBC Gauge 41115)

Table A - 9. Rincon's Seasonal Wave Conditions

Month	NDBC Gauge 41115 (2011-2019)	
	Average Wave Height (ft)	Predominant Direction (from)
January	3.9	N
February	4.0	N
March	4.1	N
April	3.2	N
May	2.5	N
June	1.9	N
July	2.1	N
August	2.1	N
September	2.7	N
October	2.1	N
November	4.0	N
December	4.0	N

Table A - 10. Rincon's General Wave Period Percent Occurrence (NDBC Gauge 41115)

Wave Period (Sec)	Percent Occurrence by Wave Period Band											
	Jan	Feb	Mar	Apr	May	Jun	Jul	Aug	Sep	Oct	Nov	Dec
< 4.0	0.3	0.4	0.4	1.6	1.7	5.9	7.6	6.5	3.0	0.4	0.1	0.4
4.0 - 4.9	0.2	1.1	0.4	1.2	2.2	4.6	8.9	7.6	3.3	0.8	0.1	0.3
5.0 - 5.9	2.1	3.1	1.9	3.0	11.4	15.6	30.2	32.1	10.6	5.3	2.3	2.7
6.0 - 6.9	6.2	6.6	7.0	8.1	15.8	21.9	29.3	23.3	8.7	5.1	3.5	5.7
7.0 - 7.9	12.0	9.9	9.3	13.4	14.4	15.4	13.7	9.9	9.8	8.6	7.6	7.6
8.0 - 8.9	8.6	6.8	7.6	11.7	6.6	5.8	2.9	2.6	8.8	8.5	10.7	6.6
9.0 - 9.9	22.4	20.4	24.1	21.2	15.8	10.9	3.7	6.9	18.9	21.5	31.2	33.4
10.0 - 10.9	11.5	10.6	11.3	8.3	8.1	3.9	1.3	3.2	8.3	11.5	11.2	11.6
11.0 - 11.9	19.7	16.8	16.6	11.4	12.5	8.1	1.3	5.5	16.1	19.8	14.4	13.9
> 12.0	17.0	24.5	21.5	20.1	11.5	7.9	1.1	2.4	12.5	18.7	18.9	17.8

2.2 Long-Term Coastal Processes

The two predominant long-term coastal processes considered in this study are SLC and decadal (or longer) shoreline evolution. SLC forms a backdrop for coastline evolution and is directly correlated to long-term geological and climatological processes such as land subsidence and global temperature change (Bredesen, 2015). Advancing or retreating shorelines not only play an important role in the performance of manmade coastal structures, but they can also influence natural coastline features (Dean and Dalrymple, 2002). To gain a better understanding of MSL change, historic records of water surface elevations are gathered from gauges in the study areas and projected over the lifetime of a proposed project.

2.2.1 Sea Level Change

SLC is the net long-term change in MSL due to local vertical land movement (VLM), global ice melting, and ocean water thermal expansion primarily from rising global air temperatures. Areas like Puerto Rico are experiencing a net long-term rise in MSL. Elevated mean water levels generally yield larger wave heights, more wave runup, and more overtopping, which can accelerate shoreline structure degradation. A more robust design may be required in locations that are especially sensitive to a rising water level for these reasons.

USACE Engineer Pamphlet (EP) 1100-2-1 (USACE, 2019a) and Engineer Regulation (ER) 1100-2-8162 (USACE, 2019b) provides the framework for SLC assessment in all USACE civil work projects. These guidance documents aid planning studies like the PRCS by outlining the National Research Council's (NRC) 1987 assessment of SLC (among other considerations), which advises feasibility studies consider the high probability of a net increase in global MSL. The NRC recommended three scenarios that project future SLR to the yr 2100: a low prediction of 0.50 meters (m; 1.64 ft), an intermediate estimate of 1.00 m (3.28 ft), and a high prediction of 1.50 m (4.92 ft; USACE, 2019a). This detailed assessment resulted in the NRC's formula that considered the time-varying form of eustatic SLR. USACE (2019a) updated the 1987 projections using the current tidal epoch (1983-2001) and included the most accurate global MSL change at that time to give the following equation:

$$E(t_i) = 0.0017(t_2 - t_1) + b(t_2^2 - t_1^2) \qquad \text{(Equation 1)}$$

where $E(t_i)$ is the relative SLR projected from the median tidal epoch yr (1992) to a future planning date in meters (m); 0.0017 is the USACE global MSL change in meters per yr (m/yr); t_1 is the time between the construction date and 1992 in yrs; t_2 is the time between a future planning date and 1992 in yrs; and b is a constant that varies by NRC SLC scenario in meters per yr (m/yr): 2.71×10^{-5} m/yr for the NRC I curve, 7.00×10^{-5} m/yr for the NRC II curve, and 1.13×10^{-4} m/yr for the NRC III curve. Of note, the preceding equation does not consider local VLM; thus, VLM is added to (or subtracted from) each curve if applicable.

The equation above needs ending dates to project SLC into the future. USACE (2019a and 2019b) suggest a project's life can be considered 50 yrs long for a given planning study. However, a 100-yr planning horizon should also be considered given the fact that USACE projects can extend past the 50-yr economic life cycle which the study analyses project justification. Three dates are important when projecting SLC for a given study area under this guidance: (1) the project "base" yr, which is the yr that the project's construction is assumed to be completed; (2) the end of the economic period of analysis, which is 50 yrs following construction completion; and (3) the project's adaptation horizon, which is 100 yrs following construction completion to adapt to climatological changes. The base yr for this study is 2028, the 50-yr economic period of analysis for this study is 2077, and the 100-yr adaptation horizon for this study is 2127.

2.2.1.1 Sea Level Change Tools

The USACE has developed two web-based SLC tools to enhance risk-based decision confidence: A Sea Level Change Curve Calculator and the Sea Level Tracker. Both tools provide a consistent and repeatable method to visualize coastal water levels due to varying sea levels, allow the user to compare SLC curves, and support simple exploration of how SLC has or will intersect with local elevation thresholds related to infrastructure (i.e. roads, power generating facilities, dunes, and buildings). Taken together, decision-makers can align various SLC scenarios with existing and planned engineering efforts, estimating when and how the sea level may impact critical infrastructure and planned development activities (USACE, 2018).

Extreme water levels (EWL) incorporated into the Sea Level Change Curve Calculator are based on statistical probabilities using recorded historic monthly extreme water level values. NOAA Technical Report National Ocean Service (NOS) CO-OPS 067 – "Extreme Water Levels of the United States 1893-2010" describes the methods and data used in the calculation of the exceedance probability levels using a generalized extreme value (GEV) statistical function (NOAA, 2013). The USACE method uses the same NOAA recorded monthly extreme values in a percentile statistical function, and both methods use data recorded and validated by NOAA. The extreme values at the gauge can be significantly different from what may occur at the study site due to differences in site characteristics and complex interactions of physical forces that vary between locations. It is important to note that the level of confidence in the exceedance probability decreases with longer return periods.

The USACE Sea Level Tracker (USACE, 2018) tool provides historic sea level trends from selected gauges close to the project site that contain a recent period of record (POR). This tool is used to show historical data, such as the MSL monthly 5-yr and 19-yr moving averages at the gauge along with the USACE Low, Intermediate, and High SLC Prediction Curves. It is important to note that the SLC trends and curves shown in this report use NOAA gauge data that is projected to the end of 2018 since this was when SLC was analyzed and incorporated into the beginning stages of modeling. These values may be slightly different when this report is ultimately published.

2.2.1.2 Historic Sea Level Change Trends near San Juan, Puerto Rico

SAJ analyzed monthly MSL data from tide gauges around Puerto Rico and projected potential SLC scenarios out to the 100-yr planning horizon. Figure A - 53 shows NOAA tide gauges around the island with long-term MSL data, where the two longest records around the island belong to the San Juan, La Puntilla, San Juan Bay, PR NOAA Station 9755371 (discontinuous data since 1962) and the Magueyes Island, PR NOAA Station 9759110 (discontinuous data since 1955). The San Juan Bay NOAA Station 9755371 provided the MSL trend baseline for the San Juan study area, which lies approximately 3.0 miles west of the Condado shoreline (western-most portion of the San Juan study area) in the San Juan Bay. The MSL trend from 1962 to 2018 for that station is 2.04 mm/yr (0.0067 ft/yr) +/- 0.39 mm/yr (0.0013 ft/yr) at 95% confidence (Figure A - 54).

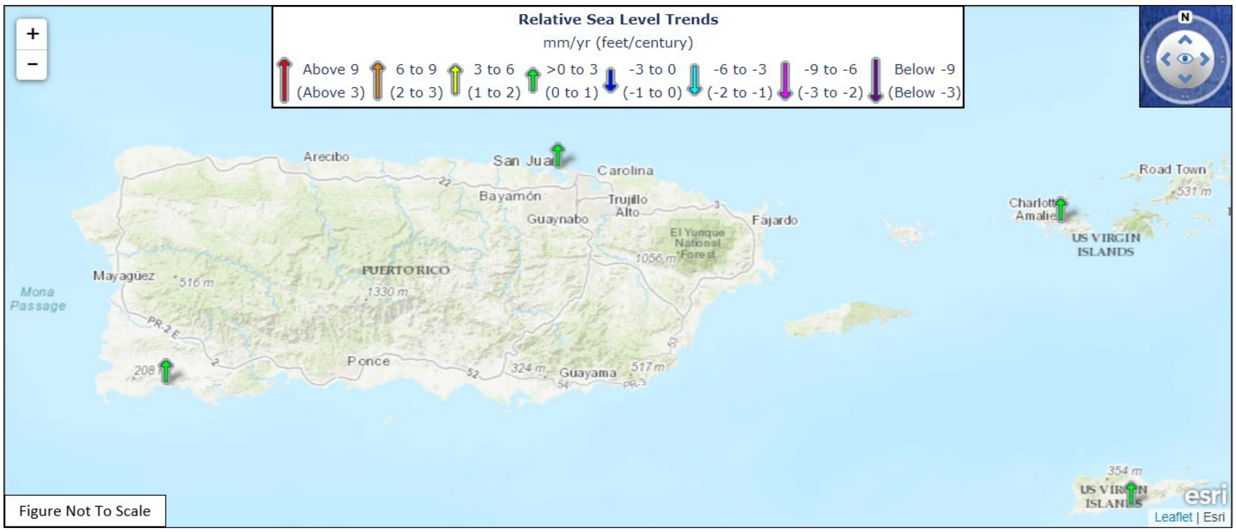

Figure A - 53. Relative SLC Trends Around Puerto Rico (NOAA, 2020b)

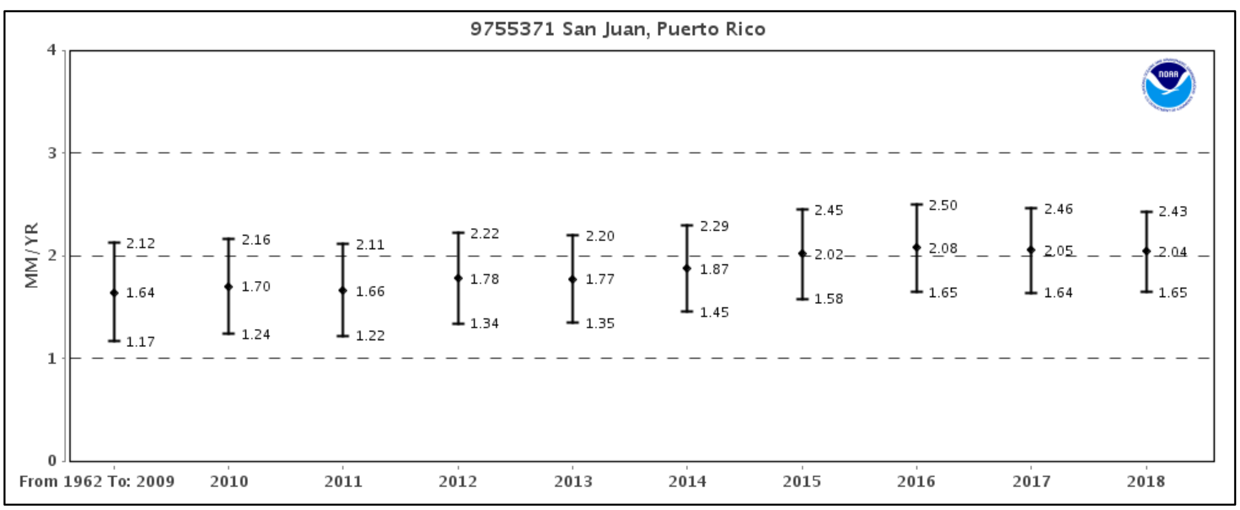

Figure A - 54. SLC Trends at NOAA's San Juan Station Over the Past Decade (NOAA, 2020b)

2.2.1.3 Sea Level Change Projections for San Juan, Puerto Rico

Based on USACE guidance and the historic local MSL trends in San Juan, SAJ developed three curves projected to the 2127 (100-yr) planning horizon. The USACE low SLR curve simply extrapolates the USACE linear trend, like extrapolating an historic SLC rate as shown in Figure A - 55. The regional USACE linear trend for San Juan (SLC Calculator) projected to 0.57 ft by 2077 and 0.90 ft by 2127 using NOAA's MSL trend stated previously. The USACE intermediate curve uses the NRC I b value and the SLR equation in Section 2.2.1 to obtain an intermediate SLR projection of 1.21 ft by 2077 and 2.52 ft by 2127. The USACE high curve uses the NRC III b value and the previous equation to obtain a high SLR estimation of 3.25 ft by 2077 and 7.66 ft by 2127. These data, along with 5- and 19-yr moving averages, are easily plotted with the USACE Sea Level Tracker tool. Table A - 11 and Figure A - 56 display this information, where moving averages for San Juan are currently tracking the intermediate SLC curve. These data lead the decision to formulate CSRM measures around the intermediate curve; however, SAJ will assess economic and physical performances of proposed measures versus the low and high USACE SLC curves following confirmation of a tentatively selected plan (TSP) in San Juan. Adaptation strategies may be developed to mitigate the risk and increased vulnerability based on each TSP alternative's sensitivity to SLC. It is important to note that NOAA (2013a) computed VLM for the San Juan area that yielded very small tectonic vertical shifts from 1962 to 2006 (0.000066 ft/yr or 0.079 inches in 100 yrs). Thus, VLM was not considered here.

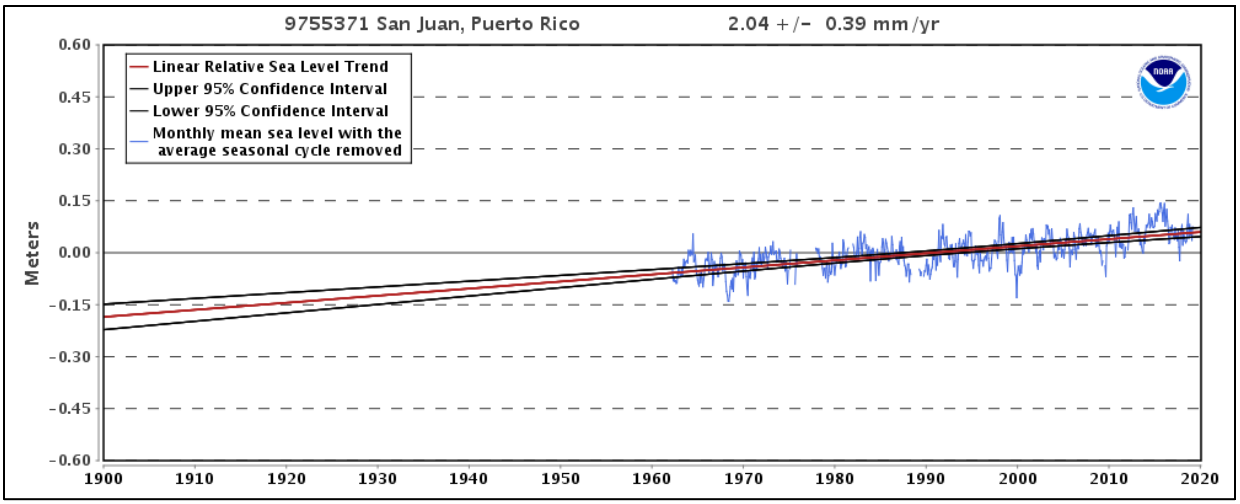

Figure A - 55. SLC Trend at NOAA's San Juan Station

Table A - 11. SLC Projections in San Juan

Yr	Low (Baseline) ft-PRVD02	Intermediate (NRC I) ft-PRVD02	High (NRC III) ft-PRVD02
2020	0.19	0.26	0.48
2028	0.24	0.36	0.72
2077	0.57	1.21	3.25
2127	0.90	2.52	7.66

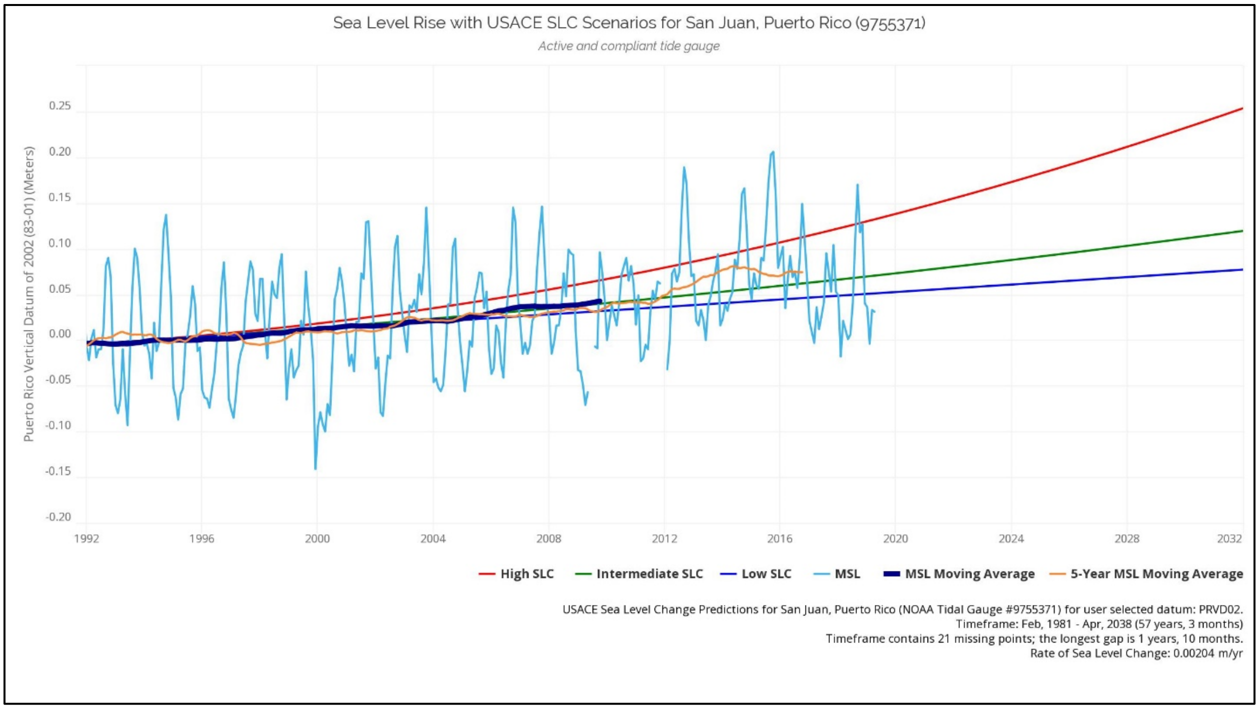

Figure A - 56. SLC Projections with Monthly, 5-yr, and 19-yr MSL Moving Averages in San Juan

2.2.1.4 Relative Sea Level Change Impact on San Juan Studies

The USACE Sea Level Tracker can plot EWLs and design or terrain thresholds over SLC projections, which is an easy but important step to ensuring that a plan or design can endure a changing climate over a century. Figure A - 57 displays the relative SLC projections from 2020 (present day) to 2127, the NOAA 1% Annual Exceedance Probability (AEP) above the intermediate curve, and average first-floor elevations (FFE) for Ocean Park (6.7 ft-PRVD02) and Condado (18.7 ft-PRVD02). Figure A - 58 shows datums and EWL return period values against Ocean Park and Condado average FFEs. Based on the average FFEs, Ocean Park has a relatively low probability of coastal inundation caused solely by the effects of SLC over the next 100 yrs, and Condado has an extremely low probability of coastal inundation caused solely by the effects of SLC over the next 100 yrs. Ocean Park and Condado are the only two areas considered in this section since they are the only two focus areas that currently contain footprints in the TSP (further discussed in Section 4.6).

Optimizing design parameters for potential CSRM measures such as breakwater or revetment crest elevations will be performed later in the study while considering recent guidance such as ECB 2020-6 (USACE, 2020). Future optimizing analyses could result in proposing project modifications or adaptation strategies (i.e. plan to construct management measures that are designed with the high SLC curve instead of the intermediate SLC curve) to minimize the risk of project failure if sea level rise rates accelerate in the San Juan study area.

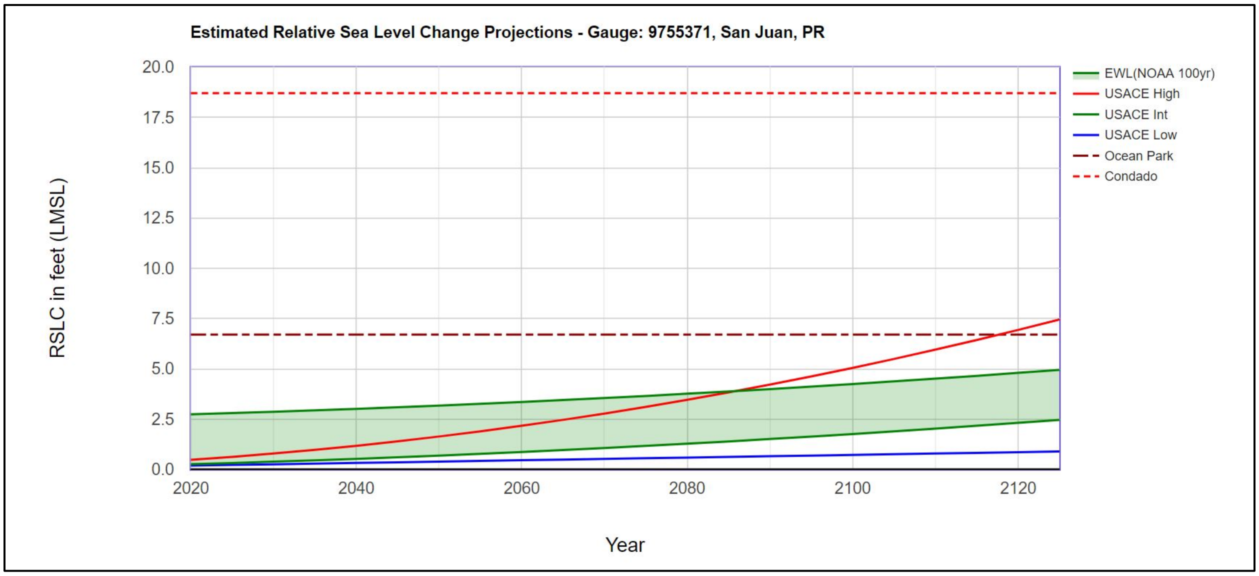

Figure A - 57. SLC vs Average FFEs for Ocean Park (6.7 ft-PRVD02) and Condado (18.7 ft-PRVD02)

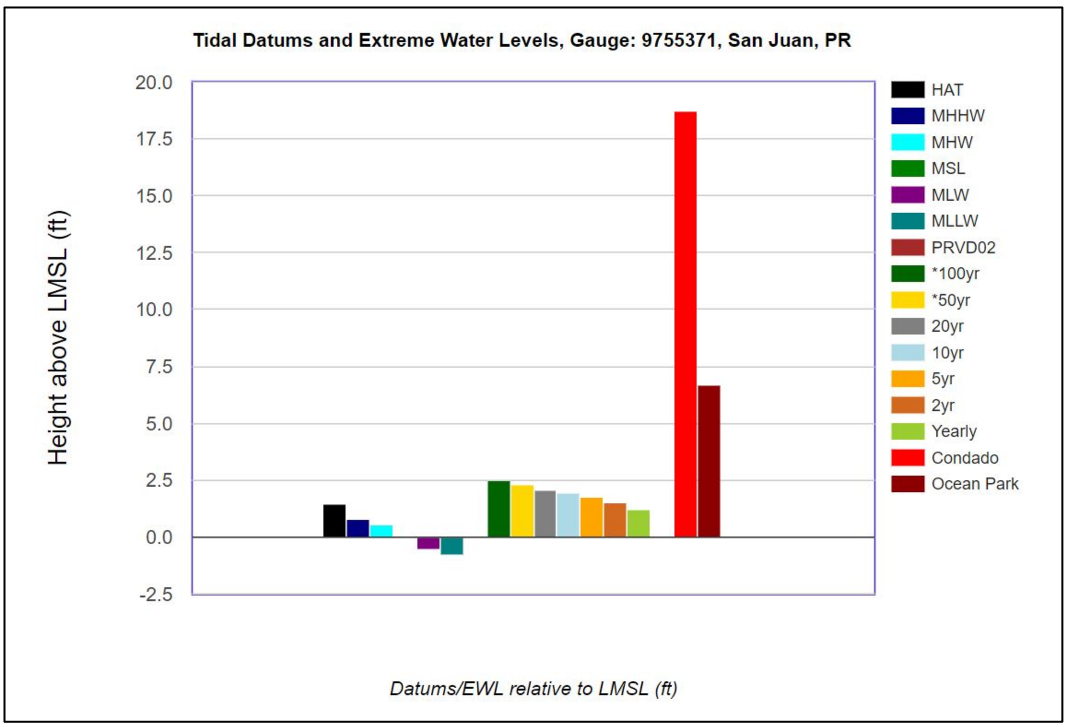

Figure A - 58. Tidal Datums and EWL's for the San Juan Area

2.2.1.1 Historic Sea Level Change Trends near Rincón, Puerto Rico

Like the San Juan study area, SAJ analyzed monthly MSL data from tide gauges around Puerto Rico and projected potential SLC scenarios out to the 100-yr planning horizon. As mentioned previously, Figure A - 53 shows NOAA tide gauges around the island with long-term MSL data, where the Magueyes Island, PR NOAA Station 9759110 (discontinuous data since 1955) was used in SLC considerations for the Rincón study area. The Magueyes Island station lies approximately 8.0 miles south-southeast of the Córcega shoreline (southern-most portion of the San Juan study area), and the MSL trend from 1955 to 2018 for that station is 1.82 mm/yr (0.0060 ft/yr) +/- 0.31 mm/yr (0.0010 ft/yr) at 95% confidence (Figure A - 59 and Figure A - 60).

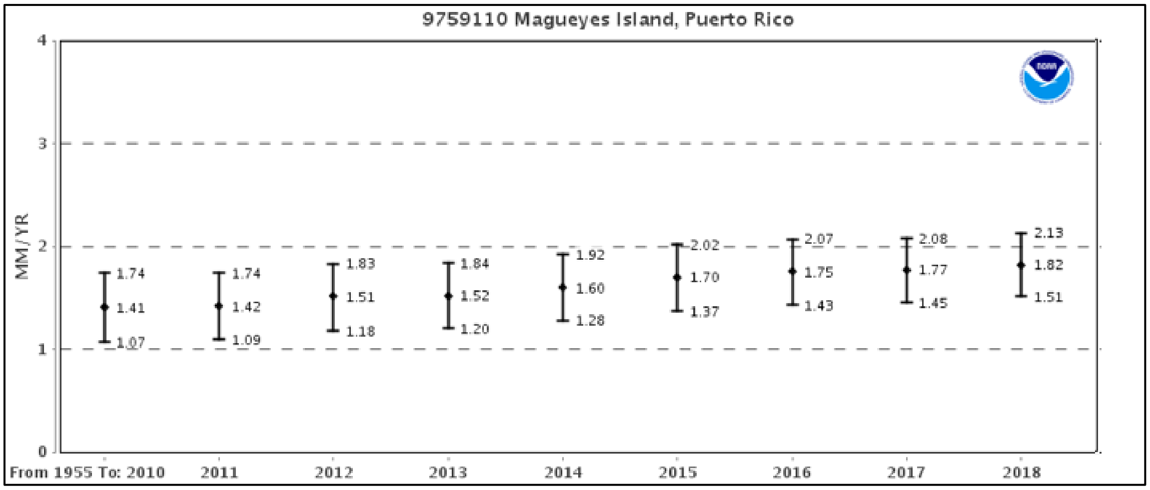

Figure A - 59. SLC Trends at NOAA's Magueyes Island Station Over the Past Decade (NOAA, 2020b)

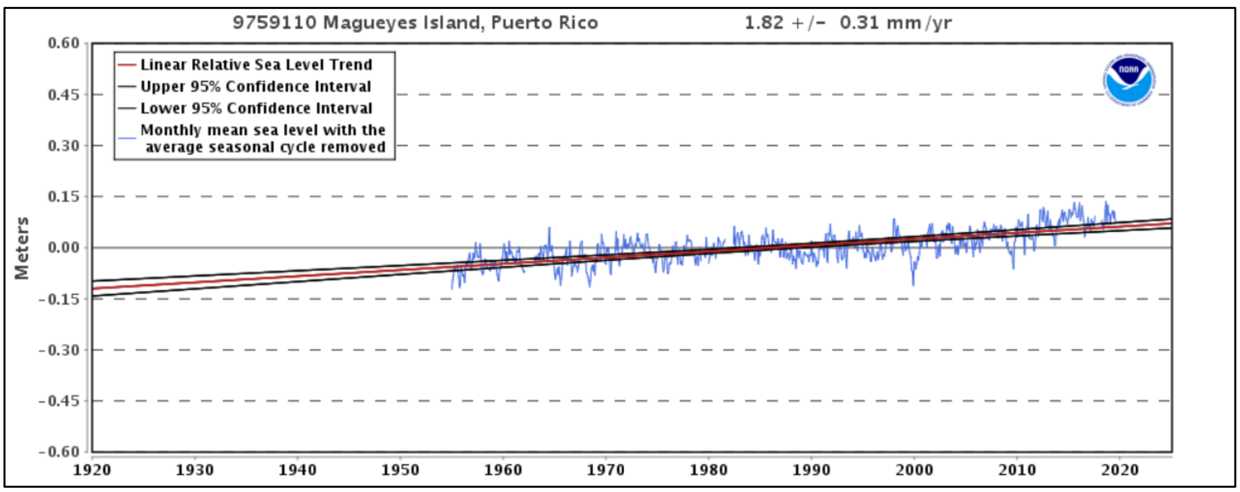

Figure A - 60. SLC Trend at NOAA's Magueyes Island Station

2.2.1.2 Sea Level Change Projections for Rincón, Puerto Rico

Again, like the San Juan study area, SAJ developed three curves projected to the 2123 (100-yr) planning horizon for the Rincón study area. Table A - 12 shows that the regional USACE linear trend for the Rincón area projects to 0.51 ft by 2077 and 0.81 ft by 2127, the USACE intermediate projects to 1.15 ft by 2077 and 2.43 ft by 2127, and the USACE high curve projects to 3.19 ft by 2077 and 7.56 ft by 2127. Figure A - 61 displays this information graphically, where moving averages for the Rincón area are somewhat divided. The current MSL elevation and 19-yr moving average (light and dark blue lines) are near or under the intermediate SLC curve, but the 5-yr moving average suggests more recent water level data is tracking between the intermediate and high SLC curves around the farthest recorded datapoint (2016-2017). The SAJ team decided to plan formulate around the intermediate curve like the San Juan approach, but future sensitivity studies in Rincón using the high curve may show that adapting a project to an accelerated rise in sea level (i.e. high-curve projections) may be applicable in this area. It is important to note that NOAA (2013a) computed VLM for the San Juan area that yielded very small tectonic vertical shifts from 1962 to 2006 (0.0016 ft/yr or 1.93 inches in 100 yrs). Thus, VLM was not considered here.

Table A - 12. SLC Projections for the Magueyes Island Gauge (Applied to the Rincón Study Area)

Yr	Low (Baseline)	Intermediate (NRC I)	High (NRC III)
	ft-PRVD02	ft-PRVD02	ft-PRVD02
2020	0.17	0.24	0.46
2028	0.21	0.33	0.70
2077	0.51	1.15	3.19
2127	0.81	2.43	7.56

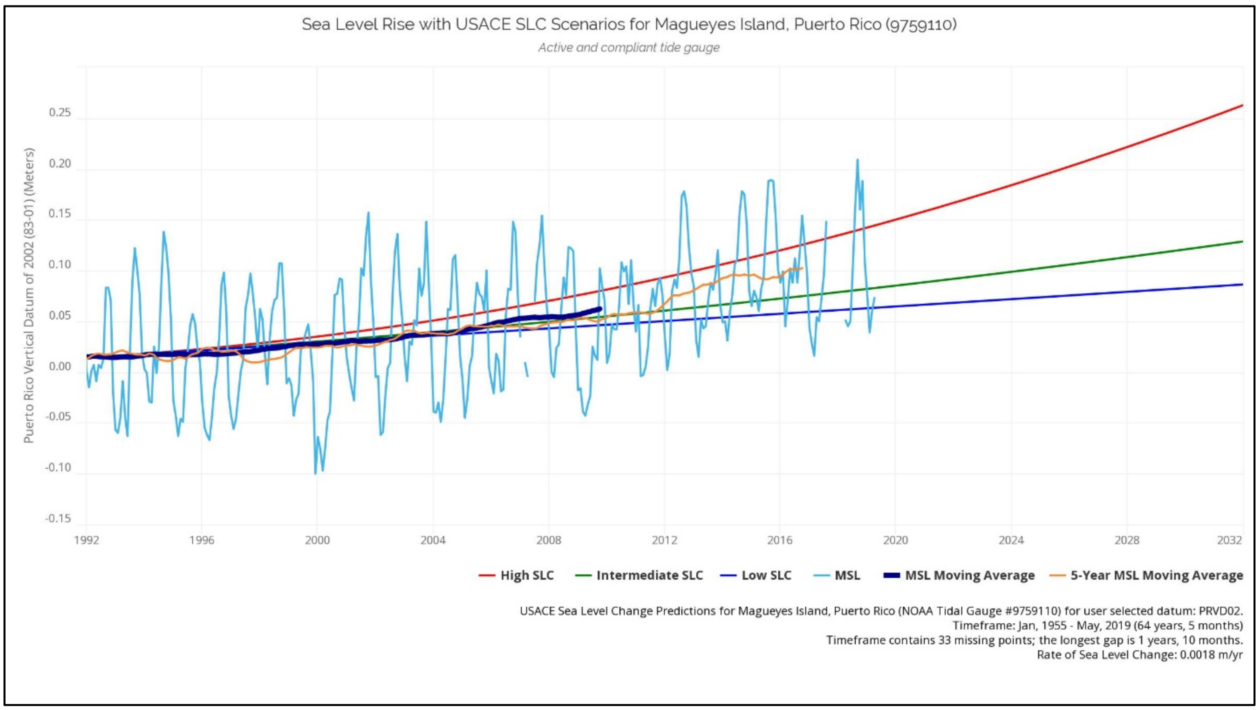

Figure A - 61. SLC Projections with Monthly, 5-yr, and 19-yr MSL Moving Averages at Magueyes Island

2.2.1.3 Relative Sea Level Change Impact on Rincón Studies

The USACE Sea Level Tracker plot with SLC curves, the NOAA 1% AEP, EWLs, and average FFEs (9.4 ft-PRVD02) for the Rincón area is shown in Figure A - 62. Figure A - 63 shows the tidal datums and EWLs vs average Rincón FFEs. Both plots show that, based on the average FFEs, Rincón has a relatively low probability of coastal inundation caused solely by the effects of SLC over the next 100 yrs. However, optimizing design parameters for potential CSRM measures in Rincón will still be performed later in the study while considering recent guidance such as ECB 2020-6 (USACE, 2020). Future optimizing analyses could result in proposing project modifications or adaptation strategies to prevent inundation due to higher water levels.

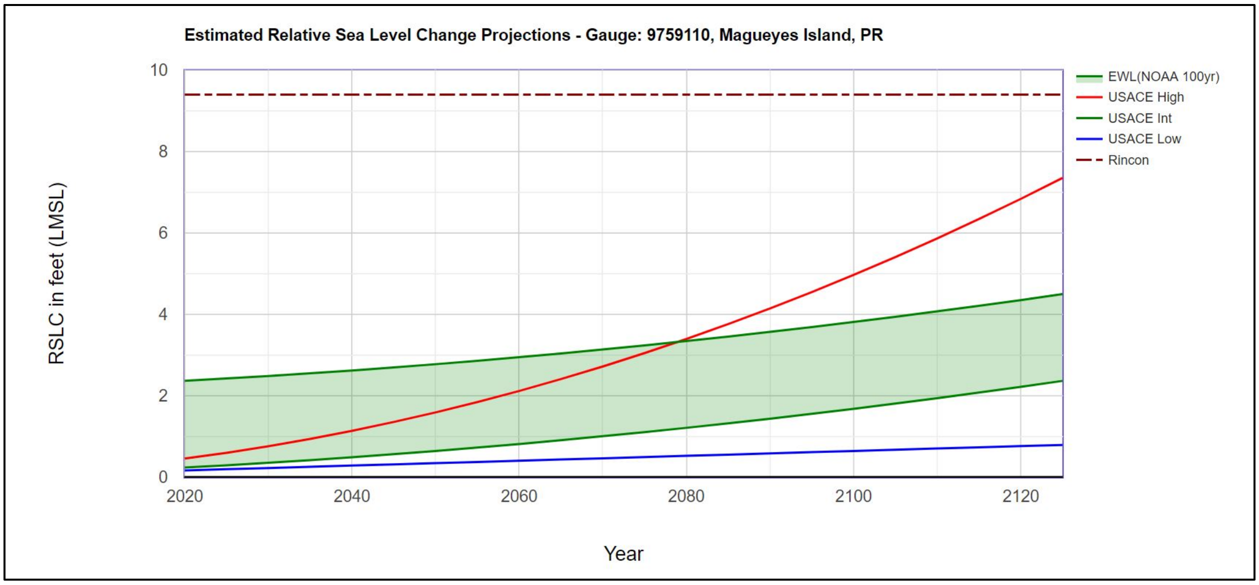

Figure A - 62. SLC Curves vs Average FFEs for Rincón (9.4 ft-PRVD02)

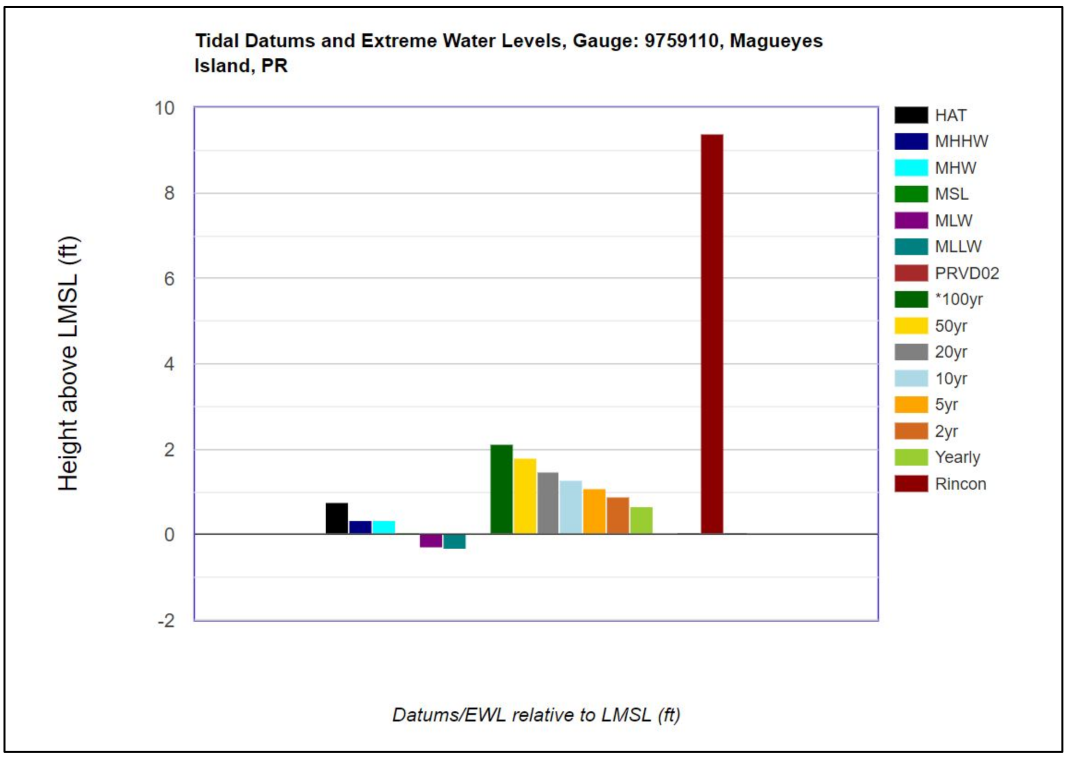

Figure A - 63. Tidal Datums and EWL's for the Rincón Area

2.3 Rainfall Effects

The primary purpose of a CSRM study is to mitigate or minimize erosion problems and potential storm vulnerability of ocean-fronted coastal structures in a study's location. However, it is important to recognize that other water sources could result in compound flooding and/or residual damages along a coastline. One source potential inundation includes rainfall-driven inland flooding due to inadequately sized or underperforming stormwater management features (i.e. pumps and gravity discharge structures).

For example, stormwater pump failure occurred during Hurricane Maria when the Baldorioty pumps did not remove storm water from major highway PR 3, which resulted in storm water backing up into the Ocean Park area (personal communications). This urban stormwater management is the responsibility of the NFS, but potential effects that impact the existing stormwater management system should be considered. For most of the project area, rainfall discharges into the Condado and San Jose Lagoons, where existing stormwater outfalls were noted in Condado and Ocean Park. If these outfalls are expected to be impacted by the Tentatively Selected Plan (TSP), then retrofitting or replacing these outfalls will be coordinated with the NFS. It is not expected that proposed project alternatives including sand nourishment, rock revetment, or offshore breakwaters would cause adverse impacts to the existing stormwater runoff patterns. Notably, a more in-depth, qualitative assessment of rainfall effects in this project's study area will be completed between draft and final reporting.

2.4 Back-Bay Flooding

As stated in Section 2.3, this study primarily focuses on minimizing erosion problems and potential storm vulnerability of ocean-fronted coastal structures in this study's locations (the coastlines of San Juan and Rincón). However, it is still important to consider flood waters entering the project area from the bay side, which could result in compound flooding when combined with inundation from the ocean side of the project area. The San Juan focus areas that are most vulnerable to inundation coming from bays include Condado, Ocean Park, and Isla Verde (the eastern portion of Carolina Beach that is nearest the Torrecilla Lagoon was screened out of this study's scope before engineering assessment and modeling was completed, but this location was included in the preliminary efforts of the San Juan Metro CSRM Feasibility Study). The Rincon focus area does not have a bay landward of the study coastline, precluding Rincon from the back-bay flooding discussion.

Assessing flood water flow paths can indicate if back-bay flooding may impact a project area, which generally tend to flow from higher elevations to pool in lower elevations. Condado's average upland elevation and average first floor elevation in the project area immediately north of the Condado lagoon is roughly 12 ft-PRVD02 and 18.7ft-PRVD02; thus, back-bay flooding is not considered to impact Condado's coastal structures. However, the low-lying areas just north of the San Jose lagoon may allow bay water to flow to the south side of the Ocean Park and Isla Verde Project areas. Preliminary hydrodynamic modeling for the San Juan Metro CSRM Feasibility Study showed that the Caño Martín Peña (CMP) Deepening Project (a study in parallel of this effort) is extremely important to back-bay water levels in the San Jose Lagoon (reference the CMP Deepening Project and San Juan Metro CSRM Feasibility Study reports for more information on the effects of adjacent shorelines due to channel dredging). Figure A - 64 shows the effects on flow and associated bay surge levels through the CMP and in the San Jose Lagoon with and without the CMP dredging project. The associated 100-yr maximum surge levels within the lagoon when the CMP is dredged is under 3-ft PRVD02, which is less than the average elevation around PR3 (roughly 3 ft-PRVD02). Bay water would need to breech PR3 and propagate roughly 1,500 ft from the lagoon to impact the closest point in the Ocean Park study area (average first-floor elevations in this area are 6.7 ft-PRVD02). Further, bay water would need to exceed the average upland elevation of the Isla Verde coastal structures closest to the San Jose Lagoon (9-ft PRVD02) to induce compound flooding in this area.

It is important to note that the San Juan Metro CSRM Feasibility Study completely analyzed back-bay flooding with the Generation 2 Coastal Risk Model (G2CRM) in the San Juan area. Thus, bay-side structure inundation damages were assessed for each of the aforementioned lagoons, including a complete TSP to mitigate bay flooding from the Condado Lagoon.

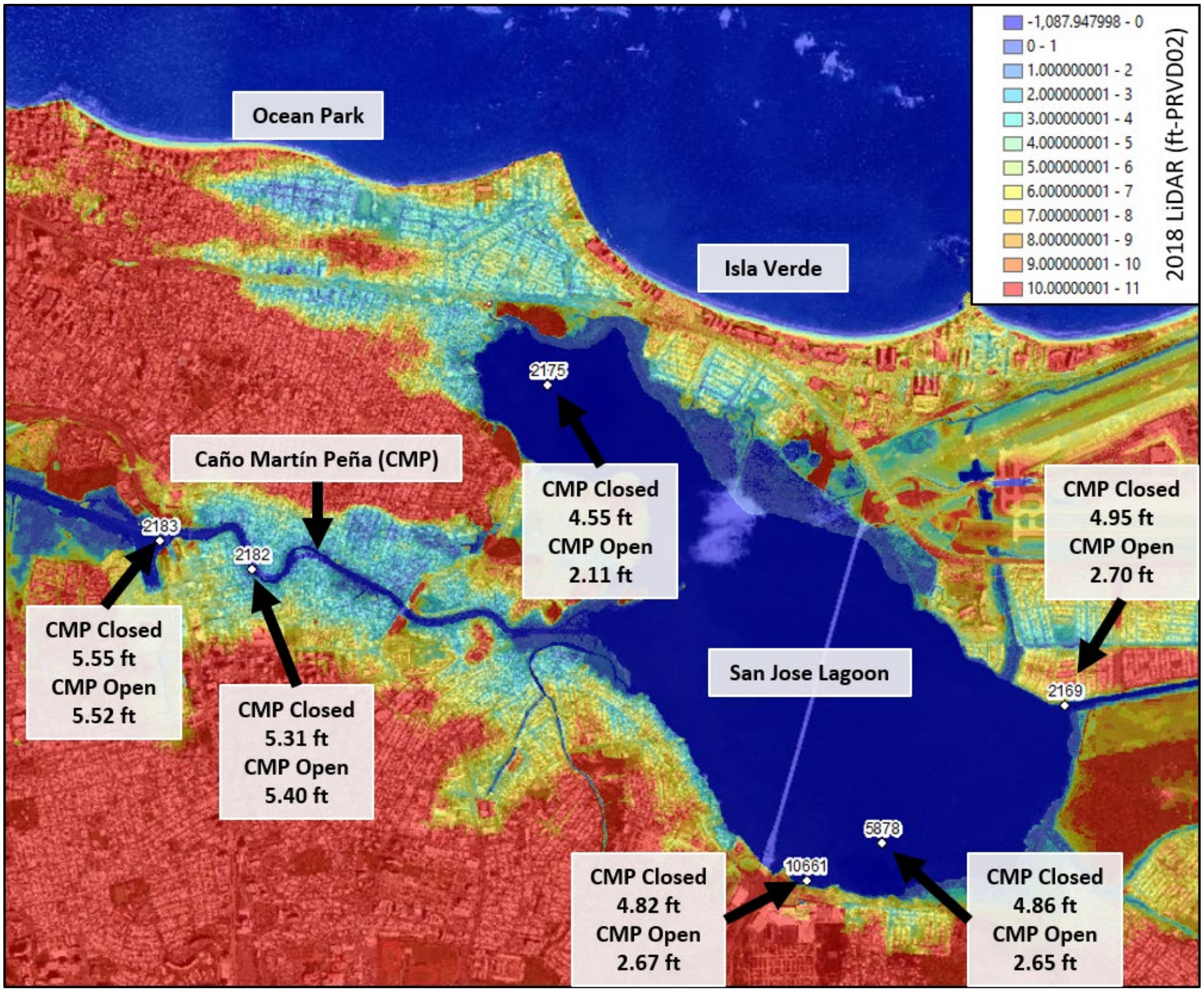

Figure A - 64. 100-yr Storm Surge Levels with and without the CMP Project

3.0 BEACH-*FX* PROJECT EVOLUTION MODEL

Federal participation in CSRM projects is based on a favorable economic justification in which the benefits of the project outweigh the costs. Determining the Benefit to Cost Ratio (BCR) requires both engineering (project performance and evolution) and planning (alternative analysis and economic justification) analyses. The interdependence of these functions has led to the development of the life-cycle simulation model Beach-*fx*. Beach-*fx* combines the evaluation of physical performance and economic benefits and costs of shore protection projects (Gravens et. al., 2007), particularly beach nourishment, to form the basis for determining the justification for Federal participation. This section describes the engineering aspects of the Beach-*fx* model.

3.1 Model Overview

Beach-*fx* is an event-driven life-cycle model. USACE guidance (USACE, 2017) requires that flood risk management (FRM) studies include risk and uncertainty. The Beach-*fx* model satisfies this requirement by fully incorporating risk and uncertainty throughout the modeling process (input, methodologies, and output). Over the project life cycle, typically 50 yrs, the model estimates shoreline response to a series of storm events with defined annual exceedance probabilities (AEPs). These plausible storms, the driving events, are randomly generated using a Monte Carlo simulation. Shoreline evolution in Beach-*fx* includes not only erosion due to the storms, but also allows for storm recovery, post-storm emergency dune and/or shore construction, and planned nourishment events throughout the life of the project. Risk based damages to structures are estimated based on the shoreline response in combination with pre-determined storm damage functions for all structure types within the project area. Uncertainty is incorporated not only within the input data (storm occurrence and intensity, structural parameters, structure and contents valuations, and damage functions), but also in the applied methodologies (probabilistic seasonal storm generation and multiple iteration, life cycle analysis). Results from multiple iterations of the life cycle can be averaged or presented as a range of possible values.

Within Beach-*fx*, the study area is represented by divisions of the shoreline referred to as “Reaches”. Because this term may also be used to describe segments of the shoreline to which project alternatives are applied, Beach-*fx* reaches will be referred to in this appendix as “model reaches”. Model reaches are contiguous, morphologically homogenous areas that contain groupings of structures (residences, businesses, walkovers, roads, etc.), all of which are represented by Damage Elements (DEs). DEs are grouped within divisions referred to as Lots. Figure A - 65 and Figure A - 66 show graphic depictions of the model setup. For further details about the specifics of Lot extents and DE grouping see the Economics Appendix.

Each model reach is associated with a representative beach profile that describes the cross-shore profile of the reach. While an effort is made to designate model reaches to include a single DNR monument from which historical survey data can be used to establish a representative profile for that reach, the positioning of the monument within each reach and the length of each reach are variable. Multiple model reaches may share the same representative beach profile and groupings of model reaches may represent a single design reach. Table A - 13 and Table A - 14 provides representative profiles and model reach identifiers.

Implementation of the Beach-*fx* model relies on a combination of meteorology, coastal engineering, and economic analyses and is comprised of four basic elements:

- Meteorological forcing;

- Coastal morphology;
- Economic evaluation; and
- Management measures.

The subsequent discussion in this section addresses the basic aspects of implementing the Beach-*fx* model. For a more detailed description of theory, assumptions, data input/output, and model implementation, refer to Gravens et al. (2007), Males et al. (2007), and USACE (2009).

Table A - 13. San Juan Model Nomenclature

Study Area	Model Segment	Planning Reach	Engineering Reach(es)*
San Juan	Condado (CO)	Condado A (CO-A)	R9 - R6
		Condado B (CO-B)	R5 - R2
		Condado C (CO-C)	R1
	Ocean Park (OP)	Ocean Park A (OP-A)	R16 - R15
		Ocean Park B (OP-B)	R14 - R4
		Ocean Park C (OP-C)	R3 - R1
	Isla Verde (IV)	Isla Verde A (IV-A)	R15 - R12
		Isla Verde B (IV-B)	R11 - R2
		Isla Verde C (IV-C)	R1

*Profiles are cross-shore lines taken at the center of each Engineering Reach (i.e. P1)

Figure A - 65. San Juan Model Areas

Table A - 14. Rincón Model Nomenclature

Study Area	Model Segment	Planning Reach	Engineering Reach(es)*
Rincon	Rincon (RC)	Rincon A (RC-A)	R1 - R10
		Rincon B (RC-B)	R11 - R22

*Profiles are cross-shore lines taken at the center of each Engineering Reach (i.e. P1)

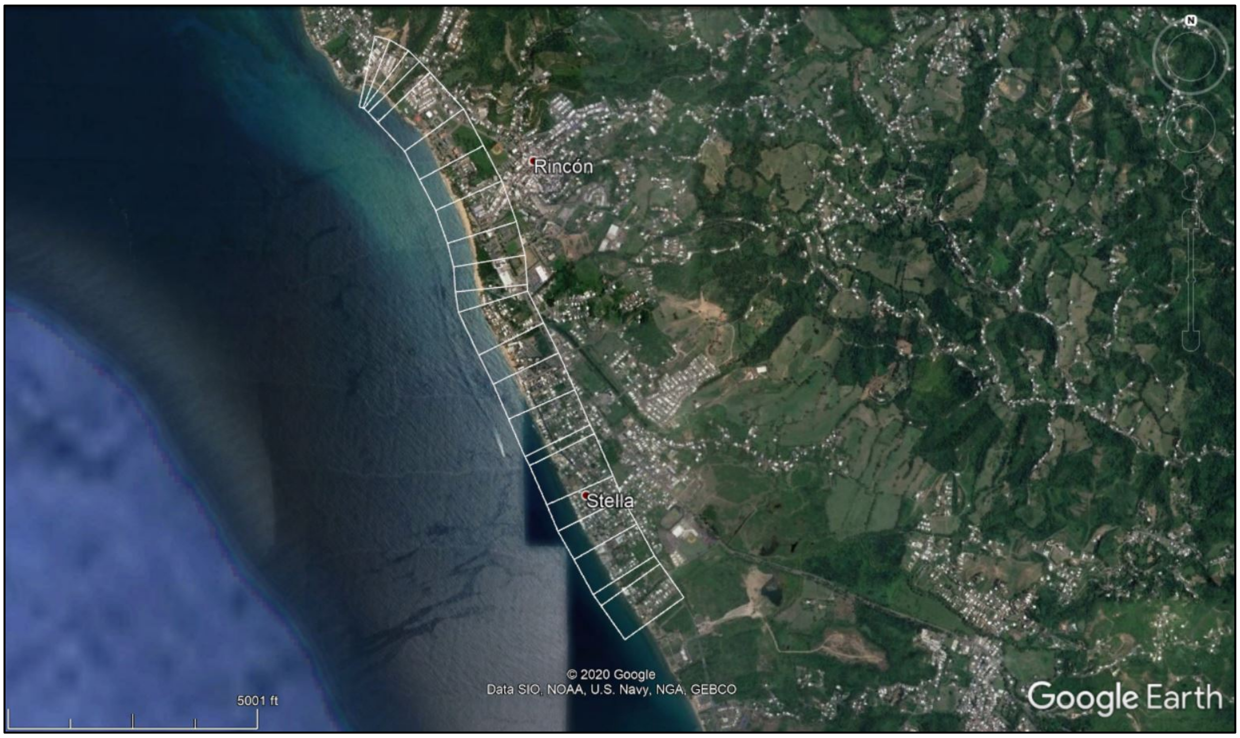

Figure A - 66. Rincón Model Areas

3.2 Meteorological Forcing

OWI GROW-FINE Caribbean - 2 (GFC-2) reanalysis data were used to develop a storm suite for the region. These data consist of 374 historical tropical events over the period 1930 - 2017 and 39 yrs (1979 – 2017) of continuous wind and wave hindcasts. ETs were extracted from the continuous hindcast data. The modeling system consists of the 2-Dimensional hydrodynamic model ADCIRC (ADvanced CIRCulation) and the OWI high-resolution 3rd generation spectral wave model known as OWI3G. This dataset has been validated (OWI 2018) and previously used in the development of storm suites.

3.2.1 Meteorological Forcing in San Juan

3.2.1.1 Tropical Cyclone Selection

OWI GFC-2 output point 93294, located just north of the project area (Lat 18.5°N, Lon 66.0°W) was used for the San Juan storm suite (Figure A - 67). This output point was in deep water (267.5 m) and linear wave theory was used to translate wave parameters to a depth of 40 ft. Several time series of variables were output at this location including: Date, Water Level, Significant Wave Height and Wave Period which were needed for input into the cross-shore change model.

The storm selection process followed the general direction of Gravens and Sanderson (2018). In the Technical Note (TN), data from the North Atlantic Comprehensive Coastal Study (NACCS) were used. The NACCS data were developed using a high-fidelity numerical hydrodynamic and wind-wave modeling system like that used in the OWI study. The main difference is that the NACCS study also examined the water level return period, so associated probability of occurrence for different water levels was available. In the absence of these data for the OWI dataset, instead of 'binning' the storms based on return period, they were binned based on storm surge elevation as discussed below.

A total of 374 storms were separated based on the time/date of occurrence and output interval at the save point. Of the 374 storms, 320 storms were defined and "de-tided" using the U-Tide (Codiga, 2011) MATLAB software package and the NOAA San Juan, La Puntilla, San Juan Bay PR (9755371) station predicted tide levels. To develop the storm suite the peak significant wave height of all storms was plotted in a histogram, but unlike Rincón, the San Juan threshold was set to 3 ft instead of 2 ft. All storms which produced a peak wave height less than 3 ft were discarded based on the initial distribution. This initial screening left 294 storm events for evaluation with peak wave heights between approximately 3.0 and a depth limited value of 30.6 ft. The storms were then binned based on maximum wave height into 1 ft increments. The distribution of storms within the bins is shown in Table A - 15 and a histogram is shown in Figure A - 68.

Within each bin the plots of wave height versus time were examined to determine representative storms for the storm suite selection. The peak wave height of all storms within a bin were lined up for easy comparison of the duration of elevated wave heights. For those bins which only contained a small number of storms, all storms were selected. For those which contained many storms, representative long, short, and average duration wave events were selected. This process resulted in a total of 53 storms being identified for the storm suite with the distribution also shown in Table A - 15. Each storm was then modulated to reflect three statistically defined tide ranges (high, medium, and low amplitude) at four surge-tide phases. The statistically defined tide range reflect the upper quartile, middle half and lower quartile of the tidal ranges. The three tidal ranges and four phase shifts result in 12 plausible total water elevation time series for a single representative storm.

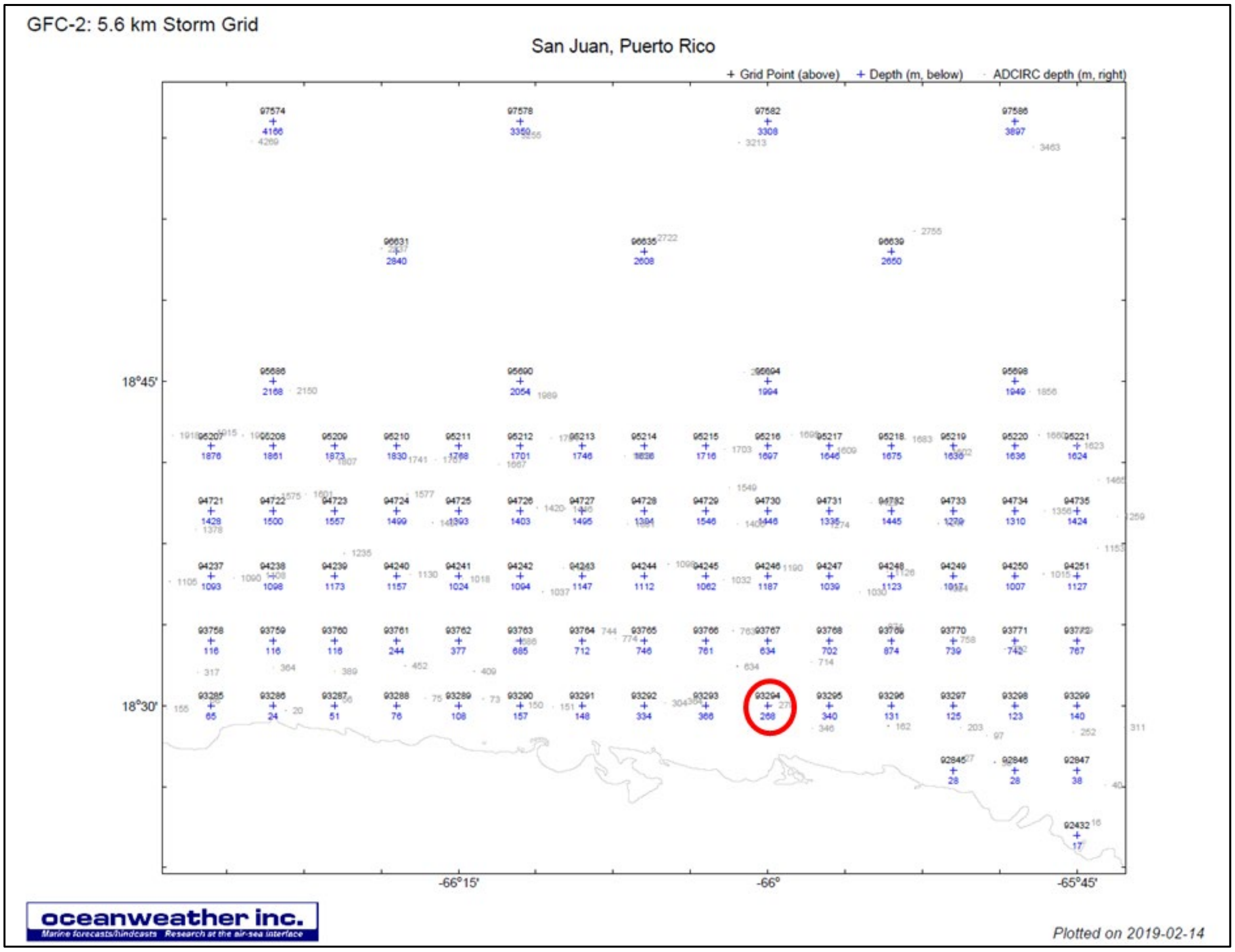

Figure A - 67. OWI GFC-2 Grid Points near San Juan, Puerto Rico

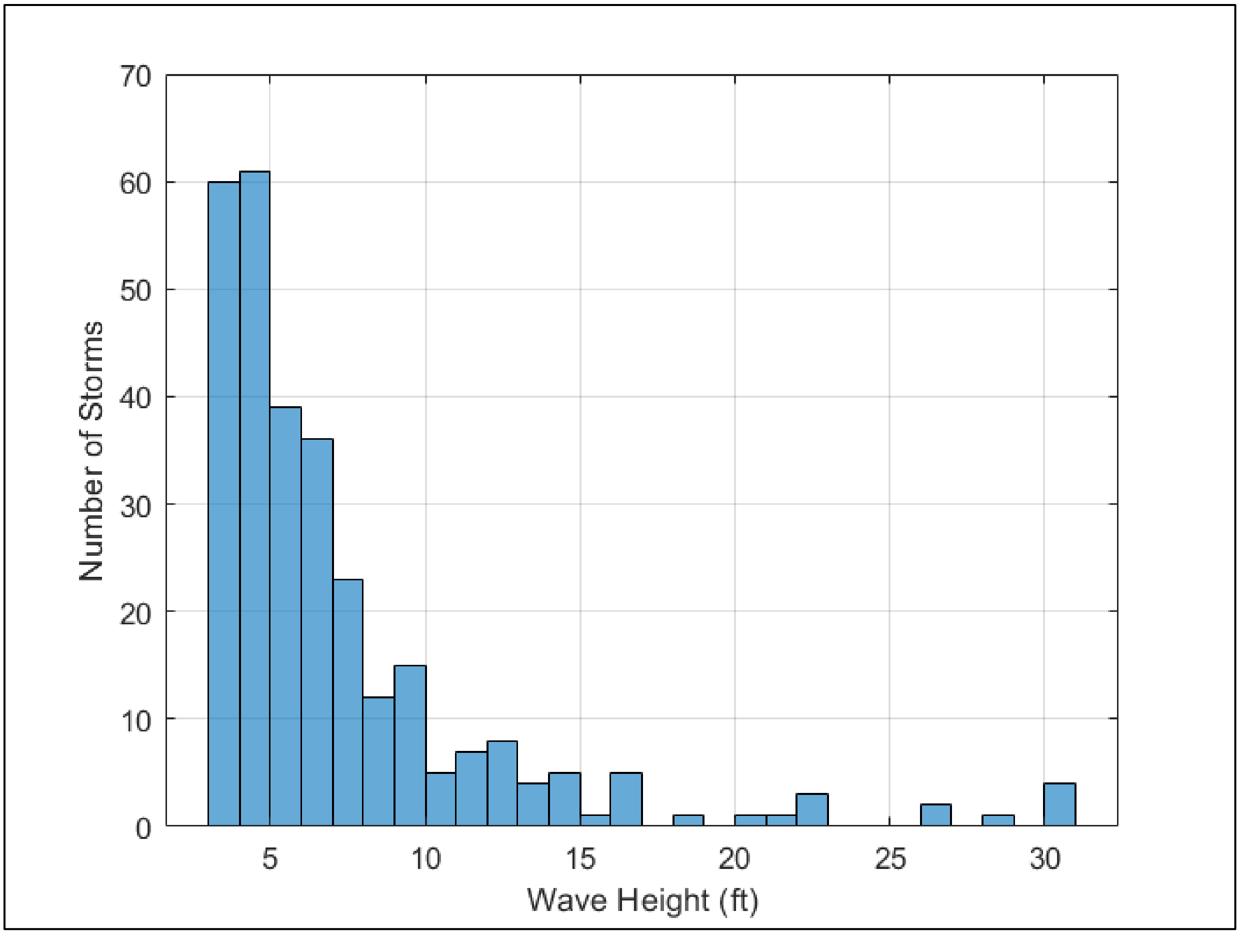

Figure A - 68. Distribution of Peak Wave Heights for OWI GFC-2 Grid Point 93294

Table A - 15. Distribution of TCs by Bin

Wave Height (ft)	Number of Storms in Record	Number of Storms Chosen for Suite
3.0 – 4.0	60	3
4.0 – 5.0	61	3
5.0 – 6.0	39	3
6.0 – 7.0	36	3
7.0 – 8.0	23	3
8.0 – 9.0	12	3
9.0 – 10.0	15	3
10.0 – 11.0	5	3
11.0 – 12.0	7	3
12.0 – 13.0	8	3
13.0 – 14.0	4	3
14.0 – 15.0	5	3
15.0 – 16.0	1	1
16.0 – 17.0	5	3
17.0 – 18.0	0	0
18.0 – 19.0	1	1
19.0 – 20.0	0	0
20.0 – 21.0	1	1
21.0 – 22.0	1	1
22.0 – 23.0	3	3
23.0 – 24.0	0	0
24.0 – 25.0	0	0
25.0 – 26.0	0	0
26.0 – 27.0	2	2
27.0 – 28.0	0	0
28.0 – 29.0	1	1
29.0 – 30.0	0	0
30.0 – 31.0	4	4
Total	**294**	**53**

3.2.1.2 <u>Extratropical Cyclone Selection</u>

To identify ET storms within the continuous hindcast dataset, a threshold wave height of 3 ft was used and events with wave height exceedances over three feet which occurred outside of hurricane season were selected. At this location, waves exceeding three feet are very common with over 10,000 occurrences recorded in the hourly continuous data. To further refine this number, the prominence of the peaks in the record was analyzed. The prominence of a peak measures how much the peak stands out due to its intrinsic height and its location in the time series relative to other peaks. In this way a low isolated peak can be more prominent than one that is higher but is an otherwise unremarkable member of a tall range. This allows the entire population to be sampled and a representative number of distinct peaks identified. This resulted in the identification of 301 unique storms with wave heights varying between 5.5 and 17.1 ft. After putting the storms into 1 ft bins based on peak wave height, representative storms were selected for each bin (30 total; Table A - 16).

Table A - 16. Distribution of ETs by Bin at OWI GFC-2 Grid Point 93294

Wave Height (ft)	Number of Storms in Record	Number of Storms Chosen for Suite
5.0 – 6.0	1	1
6.0 – 7.0	21	3
7.0 – 8.0	53	2
8.0 – 9.0	68	2
9.0 – 10.0	52	2
10.0 – 11.0	37	3
11.0 – 12.0	44	3
12.0 – 13.0	7	3
13.0 – 14.0	6	3
14.0 – 15.0	4	2
15.0 – 16.0	4	2
16.0 – 17.0	2	2
17.0 – 18.0	2	2
Total	**301**	**30**

3.2.2 Meteorological Forcing in Rincón

3.2.2.1 Tropical Cyclone Selection

The USACE Coastal Hazard System (CHS) is a coastal storm hazards data repository and mining system offering easy access to high fidelity numerical modeling and observed storm responses in a statistical context. For Puerto Rico this data has recently been developed as part the South Atlantic Coastal Study and was used for development of the TC suite. For this study, a reduced storm suite (RSS) consisting of 25 synthetic TCs were selected from the original 300 storm suite. The number of storms to be selected leveraged knowledge gathered from other previous and ongoing efforts regarding the minimum number of storms required to adequately capture the storm surge hazard. The goal of storm selection was to find the optimal combination of storms given a predetermined number of TCs to be sampled, referred to as an RSS. In the process of selecting TCs, it was determined that an RSS of 25 TCs adequately captured the storm surge hazard for the range of probabilities covered by the initial TC (ITC) suite.

The storm selection process was performed using the design of experiments (DoE) approach described in detail in Jia et al. (2015) and, more recently, Taflanidis et al. (2017) and Zhang et al. (2018). The DoE compares still water level (SWL), further in the text referenced as water elevation, hazard curves derived from the RSS to “benchmark” hazard curves corresponding to the FSS at a given number of save points within the study area. The difference between the RSS hazard curves and FSS benchmark curves is minimized in an iterative process considering multiple subsets of 25 TCs.

In summary, the general steps in this DoE approach for selecting a subset of storms are:

- Identify a save point critical to a project or study area, where optimization will be performed.
- Develop hazard curves for the ITC.
- Select number of storms to be sampled.
- Develop hazard curves for the RSS.

- Choose the range of probabilities for which hazard curves will be compared. RSS versus ITC differences can be computed along the entire hazard curve, or by prioritizing a specific segment of the curves, e.g., 5 to 500 yrs.
- Compute differences between RSS and ITC hazard curves.
- An iterative sensitivity analysis is performed to determine the optimal combination of storms constituting the RSS.
- Once the optimal combination of storms is determined, an optional analysis can be performed to evaluate the benefits of increasing storm subset size; finalize storm selection.

For this study, a metamodel with recursive iterative implementation was used to select an optimal subsample of the CHS storms. The method is based on Gaussian process regression metamodeling (Taflanidis et al. 2017; Zhang et al. 2018). In this approach, an initial RSS is recursively obtained in the 300 storm ITC suite. A metamodel is produced for the chosen save point (488) shown in Figure A - 69 based on these 25 events with hurricane JPM parameters as inputs and ADCIRC storm surge as output. The metamodel is then used to predict the SWL hazard curves for the save point location. The metamodel of each 25-sample surrogate, for example, is trained and hazard curves are produced at the save point locations. The best 25-storm sample is determined by minimizing the error across the parameter space using a genetic algorithm where the error is between the reduced sample and the full 300 storm set. Many permutations of 25 events are sampled using a Monte Carlo sampling of the entire parameter space. This process is repeated until an optimal 25-event sample is defined that minimizes the error between the target (ITC) hazard curve and the sample (RSS).

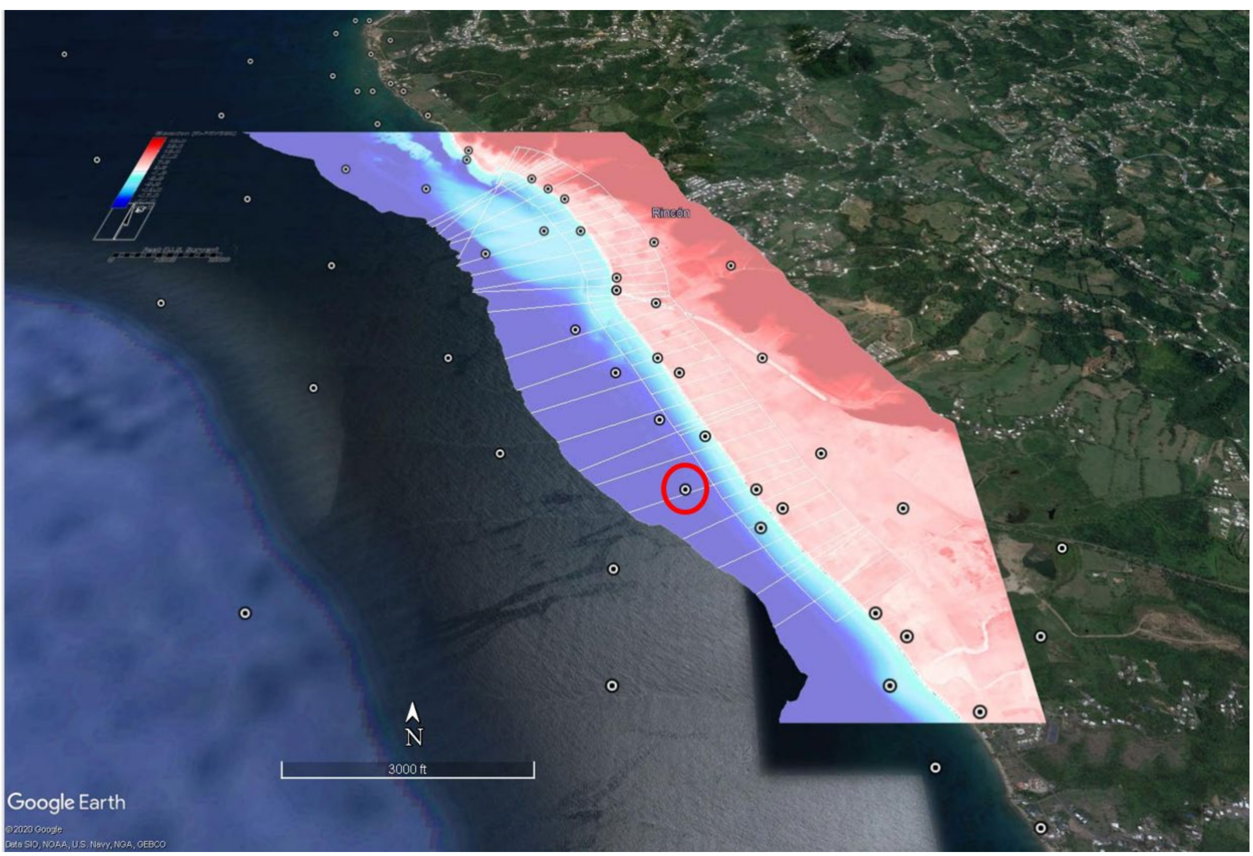

Figure A - 69. CHS Save Points near the Rincón Study Area (Station 488 Circled in Red)

Figure A - 70 shows the results of the optimization process for the RSS considering the probability of storm occurrence as a means of matching the reduced suite to the "benchmark" or full storm suite hazard curve (blue). The figure illustrates that a sample of 25 storms converges and ultimately results in a hazard-curve error very close to zero for the intended range of Annual Exceedance Probabilities (AEPs) of the full storm set (i.e., 1 to 10^{-5}). The tracks for the RSS storms are depicted in Figure A - 71.

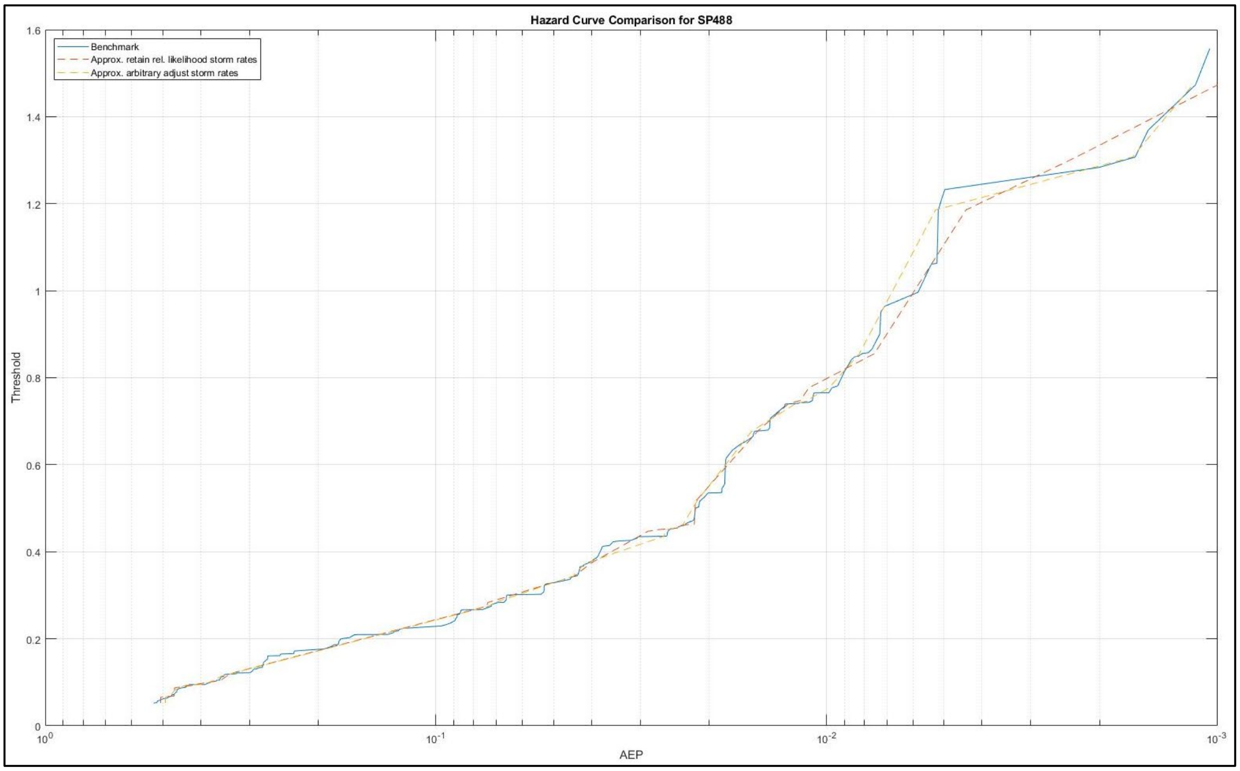

Figure A - 70. Storm Selection Optimization

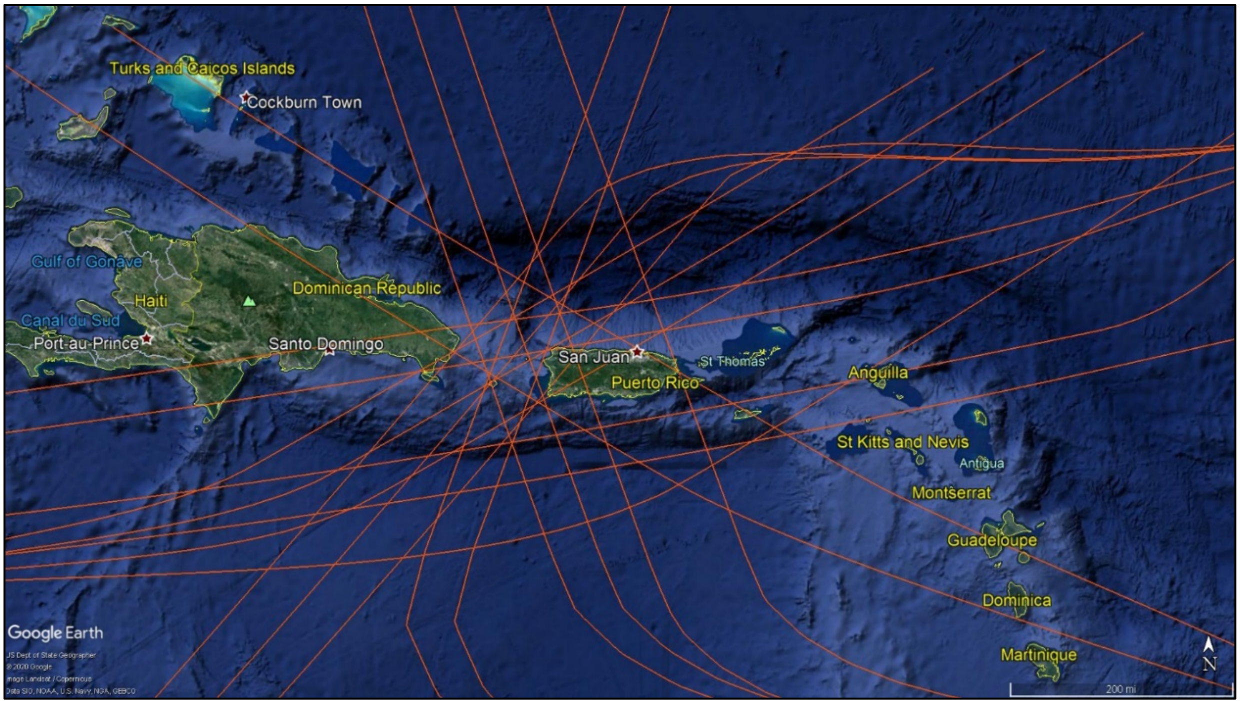

Figure A - 71. 25 Selected TC Tracks

The 25-storm tropical dataset at save point 488 was recorded in approximately 10.1 m water depth. It covers the approximately 0.2 to 0.002 AEP, which correspond to 0.38 m to 1.17 m still water levels and 1.77 m to 5.59 m wave heights. Histograms for the peak still water level and the peak wave height are shown in Figure A - 72 and Figure A - 73, respectively. Each storm was assigned an appropriate probability mass from CHS, then modulated to reflect three statistically defined tide ranges (high, medium, and low amplitude) at four surge-tide phases. The statistically defined tide range reflect the upper quartile, middle half, and lower quartile of the tidal ranges. The three tidal ranges and four phase shifts result in 12 plausible total water elevation time series for a single representative storm resulting in a total of 300 possible TC combinations.

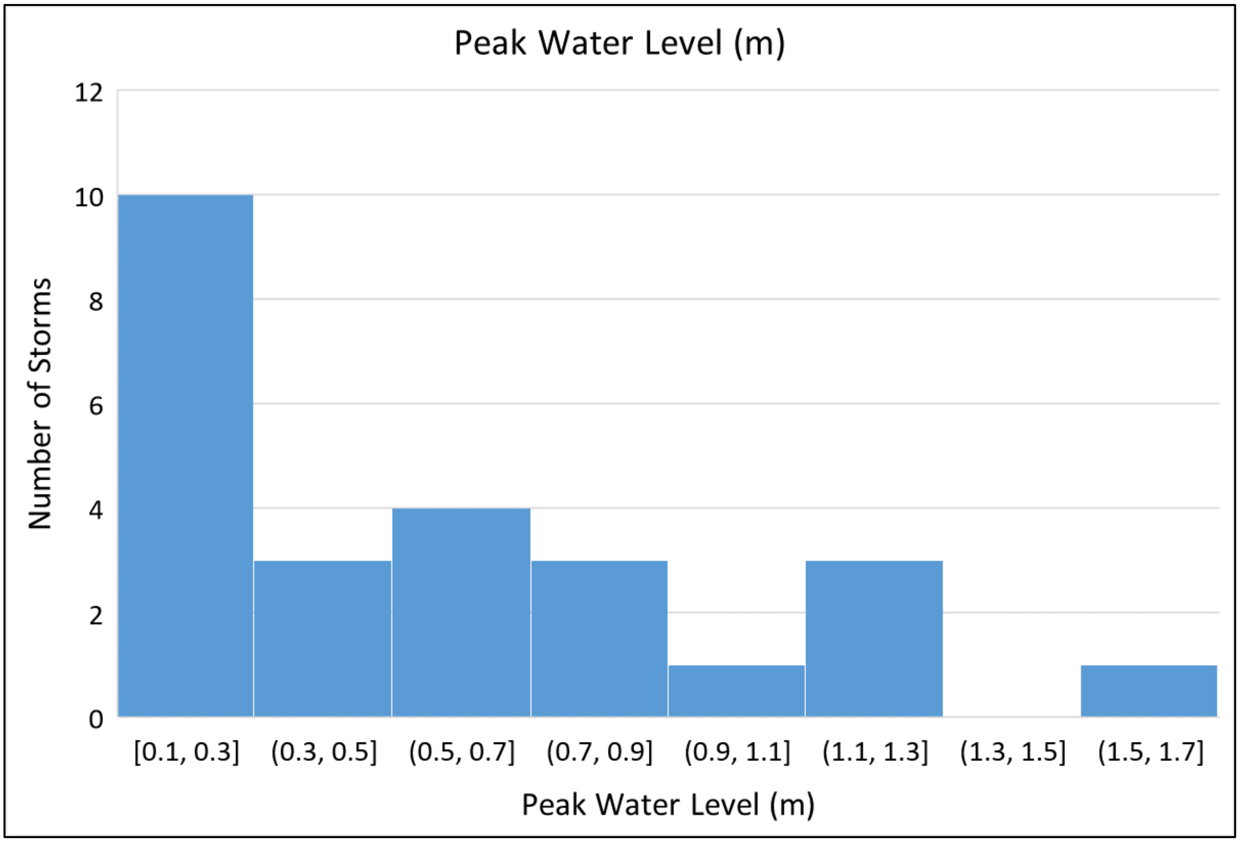

Figure A - 72. Selected CHS TC Peak Water Levels before Tides (m)

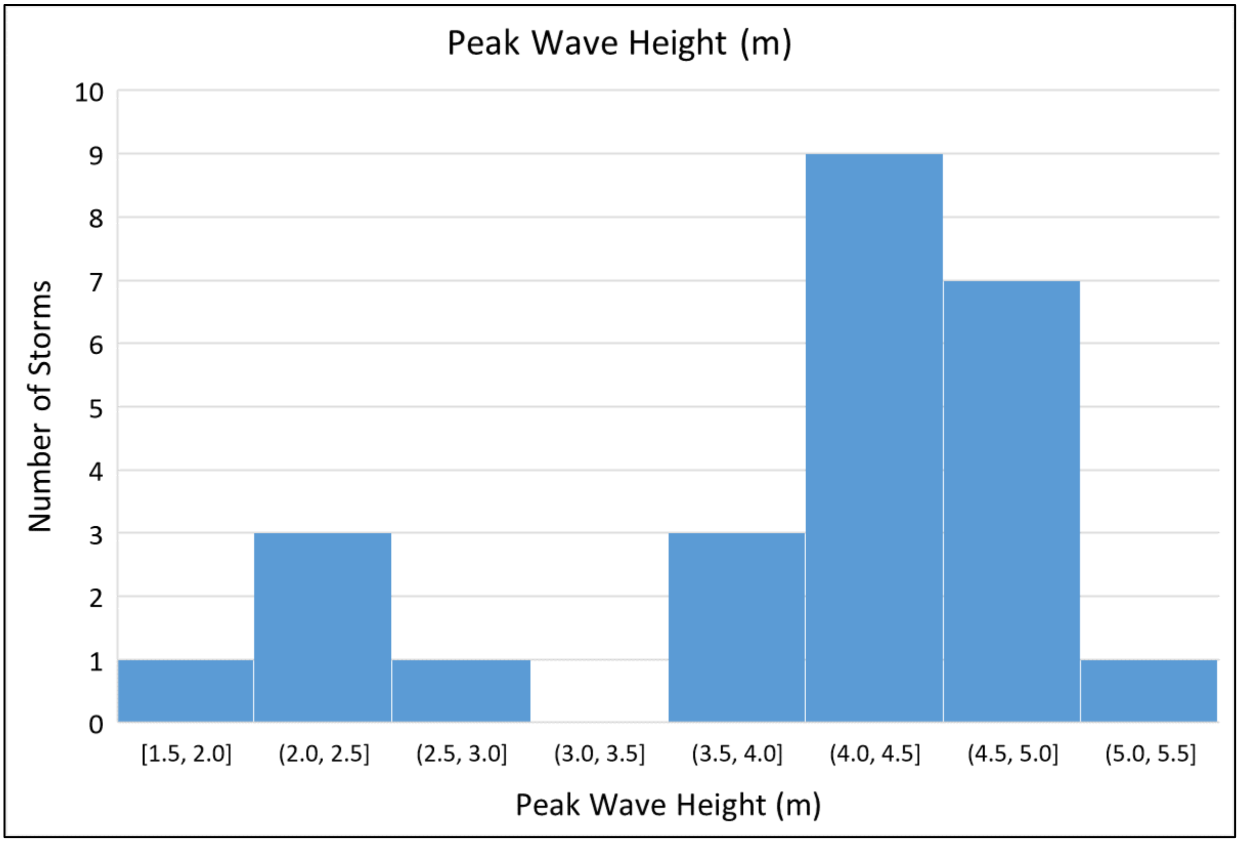

Figure A - 73. Selected CHS TC Peak Wave Heights (m)

3.2.2.2 Extratropical Cyclone Selection

CHS data are not available to develop the ET suite. For the ET storm suite, NDBC buoy 41115 was examined. The buoy is located just north of the project site in 32.9 m water depth. The NDBC timeseries was first transformed to the CHS save point water depth of 10.1 m. Then using the same minimum peak wave height of 1.5 m and 7-day window over the almost 9 yrs of observations, 96 different events were identified. These events range in peak wave height up to a height of 7.33 m which exceeds the 0.0001 AEP as calculated in the CHS at save point 488. This likely is a result of the largely non-linear transformation that occurs between buoy location and the project location as well as the exposure of the buoy. Using the closest CHS save point (14835) to the buoy, the 7.33 m wave height is closer to the 0.01 AEP as opposed to the 0.0001 AEP.

The peak wave heights from the buoy observations after transformation are shown in the histogram in Figure A - 74, where an event was chosen from each 0.5 m bin. Six total ETs were chosen to cover this spectrum (1 from OWI and 5 from NDBC). For the ETs, since the duration is typically longer than the tropical and near peak levels occur throughout the tidal cycle only one tide combination was modeled corresponding with the peak tide amplitude and maximum phase. Relative probabilities were assigned based on the statistical analysis of the NDBC data and their relative occurrence in the observations.

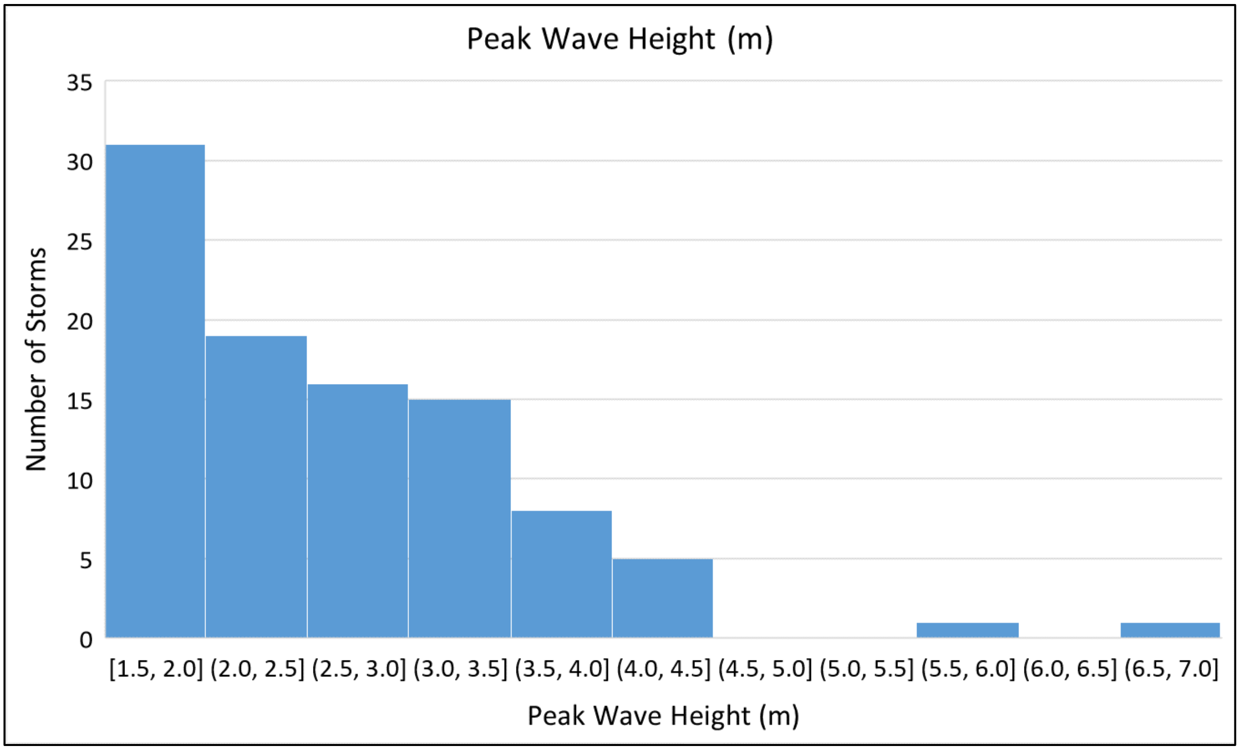

Figure A - 74. NDBC Peak Wave Heights (m)

3.2.2.3 Storm Seasons

Two storm seasons were defined a tropical season extending from June through November and an extratropical season for December through May. This allows Beach-fx to choose any of the TCs in the tropical season and any of the ETs in the extratropical season. This was chosen to accommodate the synthetic, date-less TCs from CHS.

The storm rate for the tropical season was estimated by examining historical TC tracks within a 200 nautical mile radius of the project site as shown in Figure 9. Discarding post-TC and post-ET events led to 228 storm events between 1851 and 2020 or a storm rate of 1.35 storms per yr.

For the ETs, there isn't a historical database to examine like there is for the TCs. To supplement for this fact, the NDBC record for buoy 41115 was again examined. Rather than attempting to transform the waves to a shallow depth using linear theory, the raw buoy observations were examined. A peaks-over-threshold (POT) analysis was done with a value of 2.53 m and a window of 7 days. The 2.53 m represents the 0.2 AEP wave height at the buoy location based on CHS save point 14835. The results of the POT analysis show 35 storms over the approximately 9-yr record or a storm rate of 4.04 storms per yr.

3.3 Coastal Morphology

The Beach-*fx* model estimates changes in coastal morphology through four primary mechanisms:

- Storm-Induced shoreline response from a cross-shore change model;
- Applied shoreline change rate;
- Project-induced shoreline change; and
- Post-storm berm recovery.

Combined, these mechanisms allow for the prediction of shoreline morphology for both with and without project conditions.

3.3.1 Storm-Induced Shoreline Response

Storm-Induced shoreline response is generally determined by applying a plausible storm suite that drives the Beach-*fx* model. The meteorological forcing is applied to simplified beach profiles that represent the shoreline features of the project site. The CSHORE (Cross-Shore Change) model was the tool of choice in this study to estimate cross-shore, storm-induced beach changes based on, but not limited to, the following: storm conditions, initial profiles, and shoreline characteristics such as beach slope and grain size (Johnson et al., 2012). CSHORE output consists of post-storm beach profiles, maximum wave height and wave period information, and total water elevation including wave setup. Pre- and post-storm profiles, wave data, and water levels were extracted from CSHORE and imported into the Beach-*fx* Shoreline Response Database (SRD). The SRD is a relational database that stores CSHORE results from all plausible storms so Beach-*fx* can look up a pre-defined range of anticipated beach profile configurations when theoretical storms impact an area in life-cycle simulations.

3.3.1.1 Idealized Representative Profiles

In order to develop the idealized beach profiles, it was necessary to first develop representative profiles for the project shoreline. The number of representative profiles developed for any given project depends on the natural variability of shoreline itself. Typically, historical profiles at each FDEP R-monument would be compared over time, aligned, and then averaged into a composite profile representative of the shoreline shape at that given R-monument location. Composite profiles would then be compared and separated into groupings according to the similarity between the following seven dimensions:

- Upland elevation;
- Dune slope;
- Dune height;
- Dune width;
- Berm height;
- Berm width; and
- Foreshore slope.

3.3.1.2 Future Without Project Profiles

The base yr for the present study is 2028, and the model start yr is 2019 (shoreline evolution data, SLC data, etc. were established up to 2019). In order to determine the condition of the project shoreline at the model start yr, historical pre-project surveys were studied. The most recent survey (prior to initiation of this study), was taken by the USACE in 2018 and was the closest representation of 2019 shoreline.

3.3.1.3 Cross-Shore Change Modeling

CSHORE simulates beach profile changes that result from varying storm waves and water levels. These beach profile changes include the formation and movement of major morphological features such as longshore bars, troughs, and berms. CSHORE is a two-dimensional model that considers only cross-shore sediment transport. The model assumes that simulated profile changes are produced only by cross-shore processes. Longshore wave, current, and sediment transport processes are not included.

CSHORE is an empirically based numerical model, which was formulated using both field data and the results of large-scale physical model tests. Input data required by CSHORE describes the storm being simulated and the beach of interest. Basic requirements include time histories of wave height, wave period, water elevation, beach profile surveys, and median sediment grain size.

CSHORE simulations are based on six basic assumptions:

- Waves and water levels are the major causes of sand transport and profile change
- Cross-shore sand transport takes place primarily in the surf zone
- The amount of material eroded must equal the amount deposited (conservation of mass)
- Relatively uniform sediment grain size throughout the profile,
- The shoreline is straight and longshore effects are negligible
- Linear wave theory is applicable everywhere along the profile without shallow-water wave approximations

Once applied, CSHORE allows for variable cross shore grid spacing, wave refraction, randomization of input waves conditions, and water level setup due to wind. Output data consists of a final calculated profile at the end of the simulation, maximum wave heights, maximum total water elevations plus setup, maximum water depth, volume change, and a record of various coastal processes that may occur at any time-step during the simulation (accretion, erosion, over-wash, boundary-limited run-up, and/or inundation).

3.3.2 Shoreline Change Rates

Long-term shoreline changes (erosion or accretion) for an area is best defined by continuously repeated (i.e. yearly, every five yrs, every decade, etc.) topographic and bathymetric surveys collected in the same location. However, such data were not available for the PR Coastal Study areas. Due to the lack of repeated physical survey data, a combination of referenced work, USACE LiDAR, and Google Earth Imagery were used to define the long-term erosion in Rincón and San Juan.

3.3.2.1 <u>San Juan Shoreline Changes</u>

Data for San Juan included Deltares' 2019 white paper and associated data, where shoreline detection methods such as satellite imagery stitching and comparison were used to develop a comprehensive database of shoreline erosion and accretion rates from 1984-2019. Other information used to compile long-term erosion rates by transect in San Juan include Google Earth imagery, USACE 2016 and 2018 LiDAR, and 1930's aerial photographs. Long-term shoreline response (erosion or accretion) in San Juan is generally minor compared to Rincón (no change at headlands over the past 90 yrs and minimal shoreline retreat in much of the pocket beach centers). Table A - 17 details the long-term erosion rates used in San Juan modeling efforts for this study, and Figure A - 75 shows the San Juan shoreline in the 1930's vs 2020.

Table A - 17. Erosion Rates by Reach in San Juan, Puerto Rico

Half Reach (Profile)	Condado (ft/yr)	Ocean Park (ft/yr)	Isla Verde (ft/yr)
1	-0.30	0.00	-0.43
2	-0.43	-1.15	-0.31
3	-0.41	-2.53	-0.09
4	-0.60	-1.89	-0.39
5	-0.40	-1.30	-0.69
6	0.00	-1.43	-0.37
7	0.00	-0.73	-0.04
8	0.00	-0.73	0.00
9	0.00	-0.85	0.00
10	-	-1.38	0.00
11	-	-1.40	-0.18
12	-	-1.34	-0.09
13	-	-0.05	0.00
14	-	-2.25	0.00
15	-	-2.44	0.00
16	-	-0.24	-

Figure A - 75. Aerial Imagery in San Juan as an Example of the Relatively Stable Shoreline

3.3.2.2 Rincón Shoreline Changes

Thieler, et al. (2007) provided the primary long-term erosion rates for the Rincón project area from 1936-2006, and Google earth imagery provided more recent shoreline information from 1993-2019. USACE LiDAR from 2016 and 2018 also provided pre-post Maria shoreline positions to assess the shoreline erosion impacts in the area from this storm and other notable events during that time frame. The overall long-term erosion rates that were used in the Rincón modeling effort is shown as the average in Figure A - 76, where positive values denote accretion and negative values denote erosion.

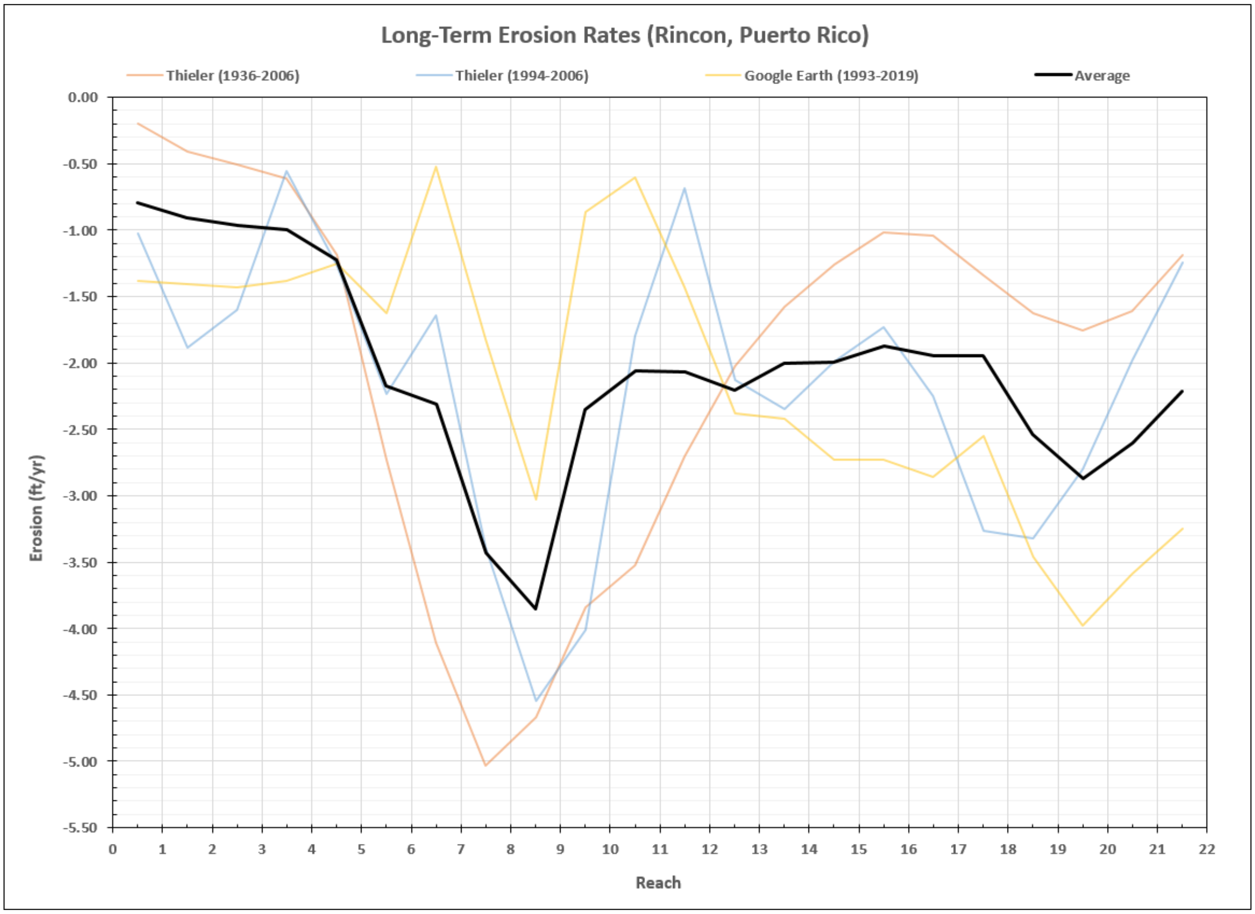

Figure A - 76. Long-Term Erosion in Rincón, Puerto Rico by Study Area Modeling Reach

3.3.3 Post-Storm Berm Recovery

Post storm recovery of the eroded berm width after passage of a major storm is a recognized process. Although present coastal engineering practice has not yet developed a predictive method for estimating this process, it is an important element of post-storm beach morphology. Within Beach-*fx*, post-storm recovery of the berm is represented in a procedure in which the user specifies the percentage of the estimated berm width loss during the storm that will be recovered over a given interval. It is important to note that the percentage itself is not a “stand alone” parameter that is simply applied during the post storm morphology computations. The percentage of berm recovery is estimated prior to model calibration and becomes a tunable calibration parameter to ensure model convergence.

3.4 Economic Evaluation

The Beach-*fx* model analyzes the economics of coastal storm risk management projects based on the probabilistic nature of storm associated damages to structures in the project area. Damages are treated as a function of structure location and construction, the intensity and timing of the storms, and the degree of protection that is provided by the natural or constructed protection elements. Within the model, damages are attributed to three mechanisms:

- Erosion (through structural failure or undermining of the foundation)
- Flooding (through structure inundation levels)
- Waves (through the force of impact)

Although wind may also cause shoreline changes, coastal storm risk management projects are not designed to mitigate for impacts due to wind. Therefore, the Beach-*fx* model does not include this mechanism. Damages are calculated for each damage element following each storm that occurs during the model run. Erosion, water level, and maximum wave height profiles are determined for each individual storm from the lookup values in the previously stored SRD. These values are then used to calculate the damage driving parameters (erosion, inundation level, and wave height) for each damage element.

The relationship between the value of the damage driving parameter and the percent damage incurred from it is defined in a user-specified "damage function". Two damage functions are specified for each damage element, one to address the structure and the other to address the structure contents. Damages due to erosion, inundation, and wave attack are determined from the damage functions and then used to calculate a combined damage impact that reduces the value of the damage element. The total of all FWOP damages is the economic loss that can be mitigated by the coastal storm risk management project.

A thorough discussion of the economic methodology and processes of Beach-*fx* can be found in the Appendix B: Economics.

3.5 Management Measures

Shoreline management measures that are provided for in the Beach-fx model are nourishment, revetment, and offshore breakwaters. Full FWP analyses and associated modeling has not been completed on some of the proposed management measures. Once this has been completed, a more thorough discussion will be provided in this section.

3.5.1 Nourishment

Planned nourishments are handled by the Beach-*fx* model as periodic events based on nourishment templates, triggers, and nourishment cycles. Nourishment templates are specified at the model reach level and include all relevant information such as order of fill, dimensions, placement rates, unit costs, and borrow-to-placement ratios. Planned nourishments occur when user defined nourishment triggers are exceeded and a mobilization threshold volume is met. At a pre-set interval, all model reaches which have been identified for planned nourishment are examined. In reaches where one of the nourishment threshold triggers is exceeded, the required volume to restore the design template is computed. If the summation of individual model reach level volume requirements (to fill the given nourishment template) exceeds the mobilization threshold volume established by the user, then a nourishment is triggered, and all model reaches identified for planned nourishment are restored to the nourishment template. Emergency nourishments are generally limited beach fill projects conducted by local governments in response to storm damage. Puerto Rico has not ever nourished the San Juan or Rincón coastlines, so emergency nourishment was not included in the Beach-*fx* analysis.

Beach-*fx* planned nourishment templates have three nourishment distance triggers (1) berm width, (2) dune width, and (3) dune height. Each distance trigger is a fractional amount of the corresponding nourishment template dimension. When the template dimensions fall below the fraction specified by the trigger, a need for nourishment is indicated. For any project template, the berm width trigger can be set such that a minimum berm width (what has been traditionally referred to as a “design berm”) can be maintained, allowing the remainder of the template to act as sacrificial fill (traditional “advance fill”), or the berm trigger can be set to allow minimal erosion of the berm allowing the project interval and mobilization threshold volume to govern the nourishment cycle. This management measure has not yet been simulated, but specific parameters will be discussed once that occurs.

3.5.2 Revetment

This management measure is currently being simulated, so specific parameters will be discussed once management modeling is completed.

3.5.3 Offshore Breakwaters

Breakwater analyses have not yet been simulated, but specific parameters will be discussed once that occurs.

3.6 Tentatively Selected Plan Discussion

The TSP for the PRCS currently consists of rock revetment on the western side of Punta Las Marías, a breakwater field with nourishment in front of the sandy portion of beach in Ocean Park, rock revetment surrounding Punta Piedrita between Ocean Park and Condado, nourishment between Punta Piedrita and the inclined groin at La Concha in Condado, and rock revetment from Quebrada Los Ramos spanning south roughly 5,600 ft. However, FWP modeling and analyses are not yet complete; thus, these alternatives are not definite. A more thorough discussion of the final TSP will follow FWP activities.

4.0 PROJECT DESIGN

Full FWP analyses and modeling have not yet been completed. Once this has been completed, a more thorough discussion of the project design will be discussed in this section.

4.1 San Juan Project Design

4.1.1 San Juan's Ocean Park Project Design

The design for the TSP in the Ocean Park focus area consists of rock revetment at the headlands, or points, segmenting the Ocean Park pocket beach and a breakwater field seaward of the Ocean Park sandy areas (R4-R14) with a periodic 50-yr nourishment plan.

4.1.1.1 Ocean Park Revetments

The revetment design for both eastern- and western-most portions of Ocean Park is the same, and design parameters for revetment are as follows (Figure A - 77):

- Location: R1-R3 (Reach C) and R15-R16 (Reach A)
- Length: Approximately 1750 ft in Reach C and 1400 ft in Reach A
- Crest Elevation: 11 ft PRVD02
- Crest Width: 12 ft
- Side slopes: 3H:1V
- Stone size: 3-5 Ton, approx. 4 ft diameter stone
- Exposed Stone Type: Granite

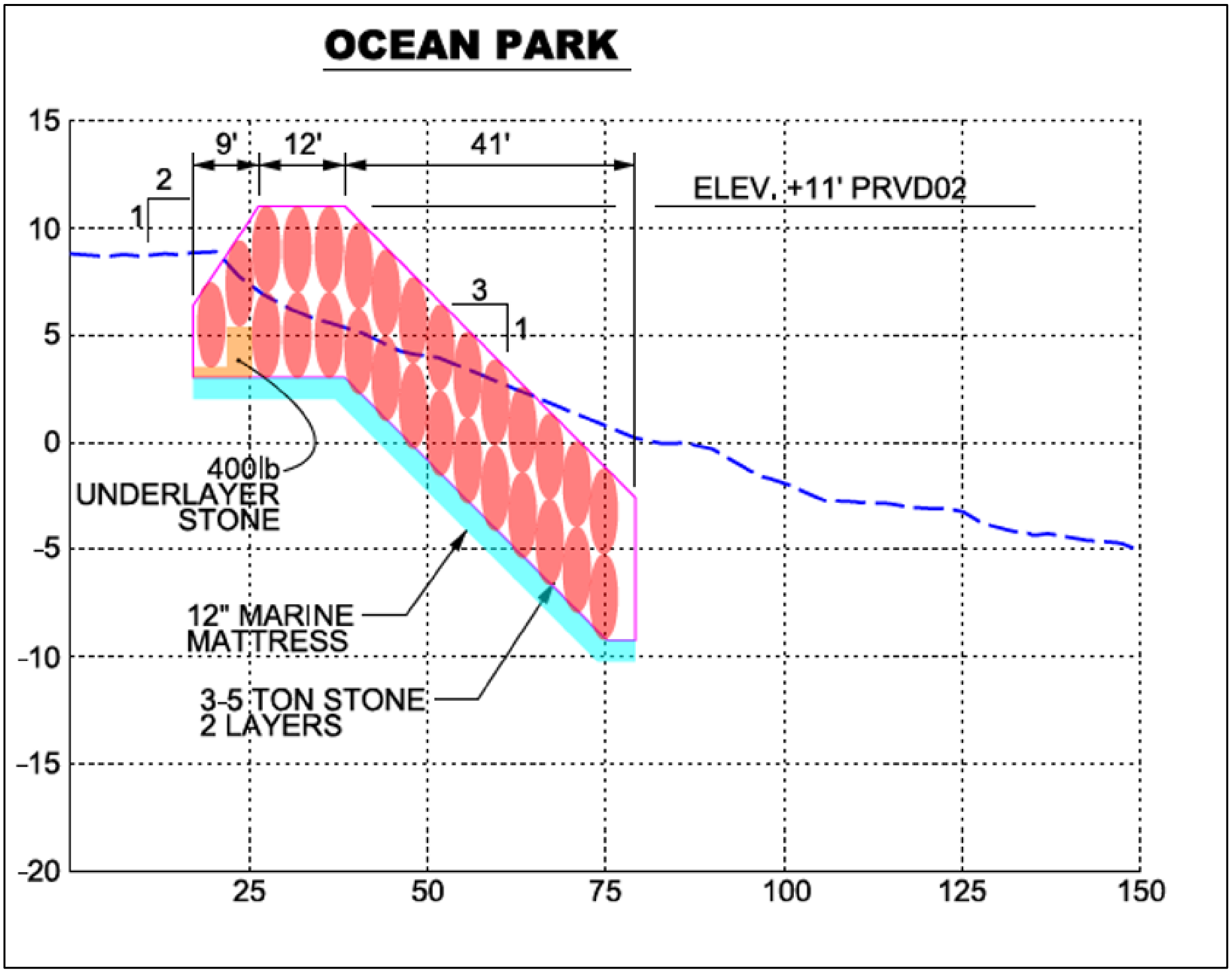

Figure A - 77. Ocean Park Revetment Design

4.1.1.2 <u>Ocean Park Breakwaters</u>

The current breakwater design in Ocean Park Planning Reach B consists of 8 breakwaters with crest elevations at MLW and crest dimensions of 600 ft long by 15 ft wide. Side slopes of 2H:1V and the depth at each breakwater will determine the overall height of the structure. From East to West, BWs are numbered 1-8 (Figure A - 78). BWs 1-5 (eastern location of OP) are located at depths in the 15-ft-PRVD02 range, which is sampled at Profile 8 below (cross-section shown in Figure A - 79). BW 6-8 are located at depths between 18 ft-PRVD02 to 22 ft-PRVD02 depths which is sampled at the profile 12 (cross-section shown in Figure A - 80).

- Location: R4-R14
- Number of breakwaters: 8
- Crest Length (each breakwater): 600 ft
- Cross-shore Distance: 500 ft from approx. 0 ft contour
- Gap Distance: 7 @ 250 ft long
- Crest Elevation: -0.77 ft PRVD02 (MLLW)
- Crest Width: 15 ft
- Side slopes: 2H:1V
- Stone size: 5-7 Ton, approx. 4.5 ft diameter stone
- Exposed stone type: Granite

Figure A - 78. Ocean Park Breakwater Design (Plan View)

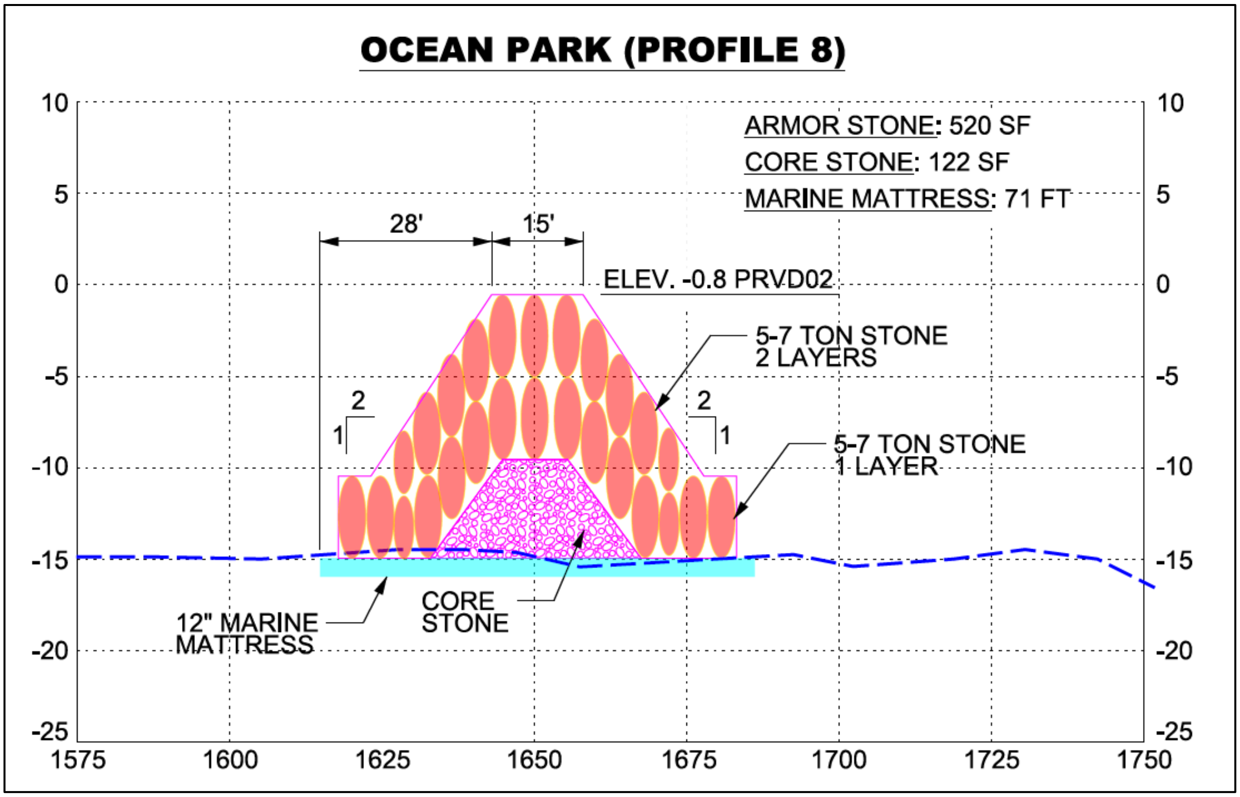

Figure A - 79. Cross-Section of Breakwaters in Eastern-Reach B

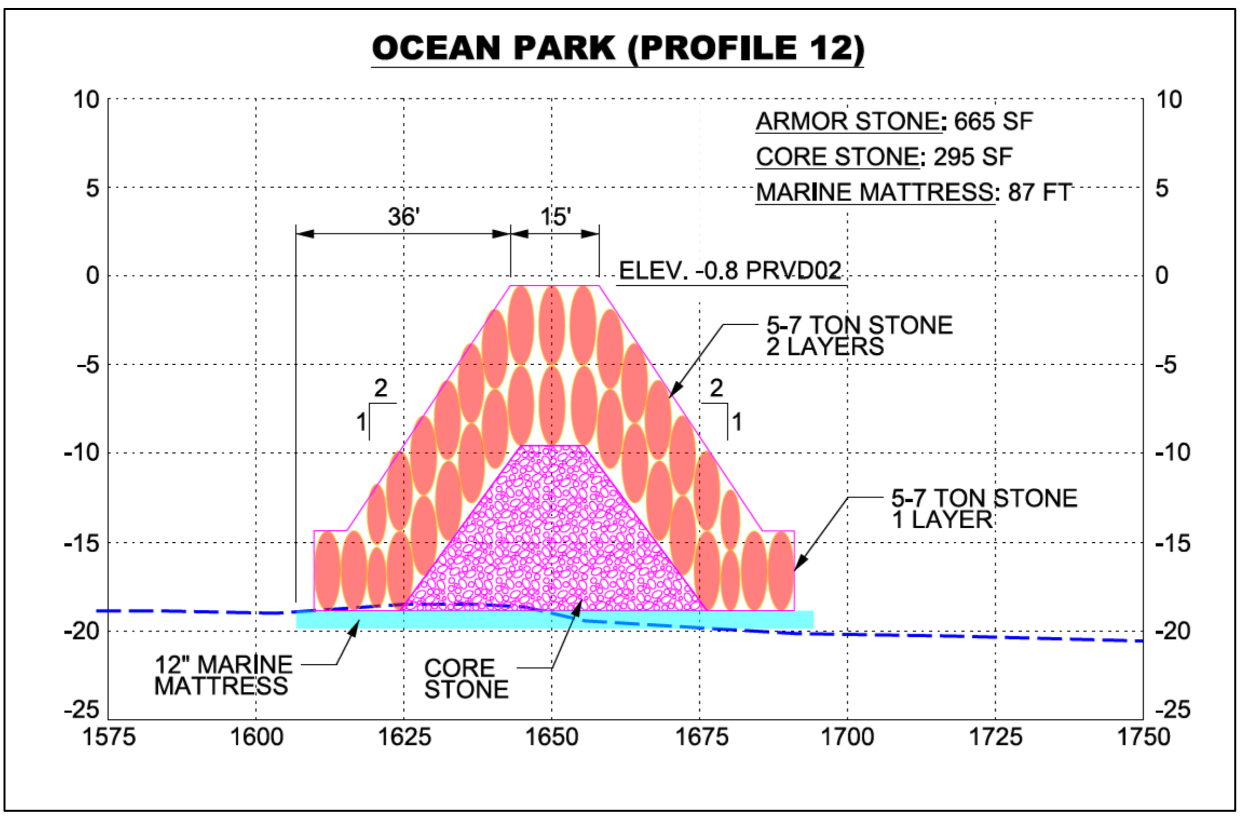

Figure A - 80. Cross-Section of Breakwaters in Western-Reach B

4.1.2 San Juan's Condado Project Design

The currently rocky shoreline in the eastern-most Condado shoreline will include a rock revetment with the following design parameters. It is important to note that FWP analyses are still underway, so optimization of these parameters could lead to different values before SAJ releases this report to the public. Figure A - 81 shows the current design graphically.

- Location: R1
- Length: Approximately 1000 ft
- Crest Elevation: 14 ft PRVD02
- Crest Width: 12 ft
- Side slopes: 3H:1V
- Stone size: 3-5 Ton, approx. 4 ft diameter stone
- Exposed Stone Type: Granite

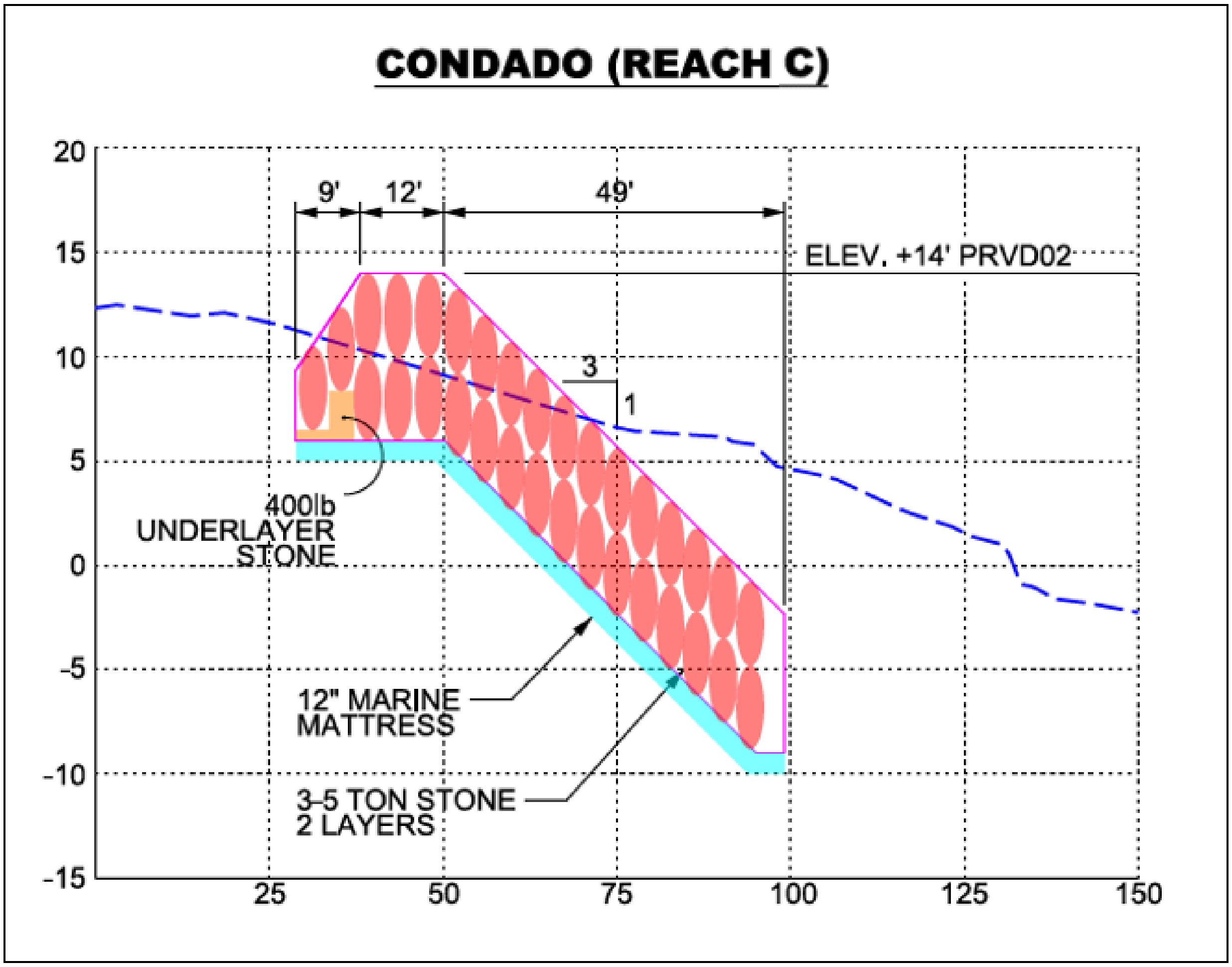

Figure A - 81. Condado's Reach C Revetment Design

The sandy stretch of coast from Engineering Reach 2 to Engineering Reach 5 in the center of Condado is considered Planning Reach B. This planning reach will likely include a 50-yr periodic nourishment. However, this FWP analysis is not yet complete, so this is still subject to change at this time.

4.2 Rincón

The currently proposed revetment in Rincón will include the following design parameters (shown graphically in Figure A - 82), but small-scale nourishment and breakwater options are still being considered at this time.

- Location: R14-R19
- Length: Approximately 3280 ft
- Crest Elevation: 11 ft PRVD02
- Crest Width: 10 ft
- Side slopes: 3H:1V
- Stone size: 2-3 Ton, approx. 3 ft diameter stone
- Exposed stone type: Granite

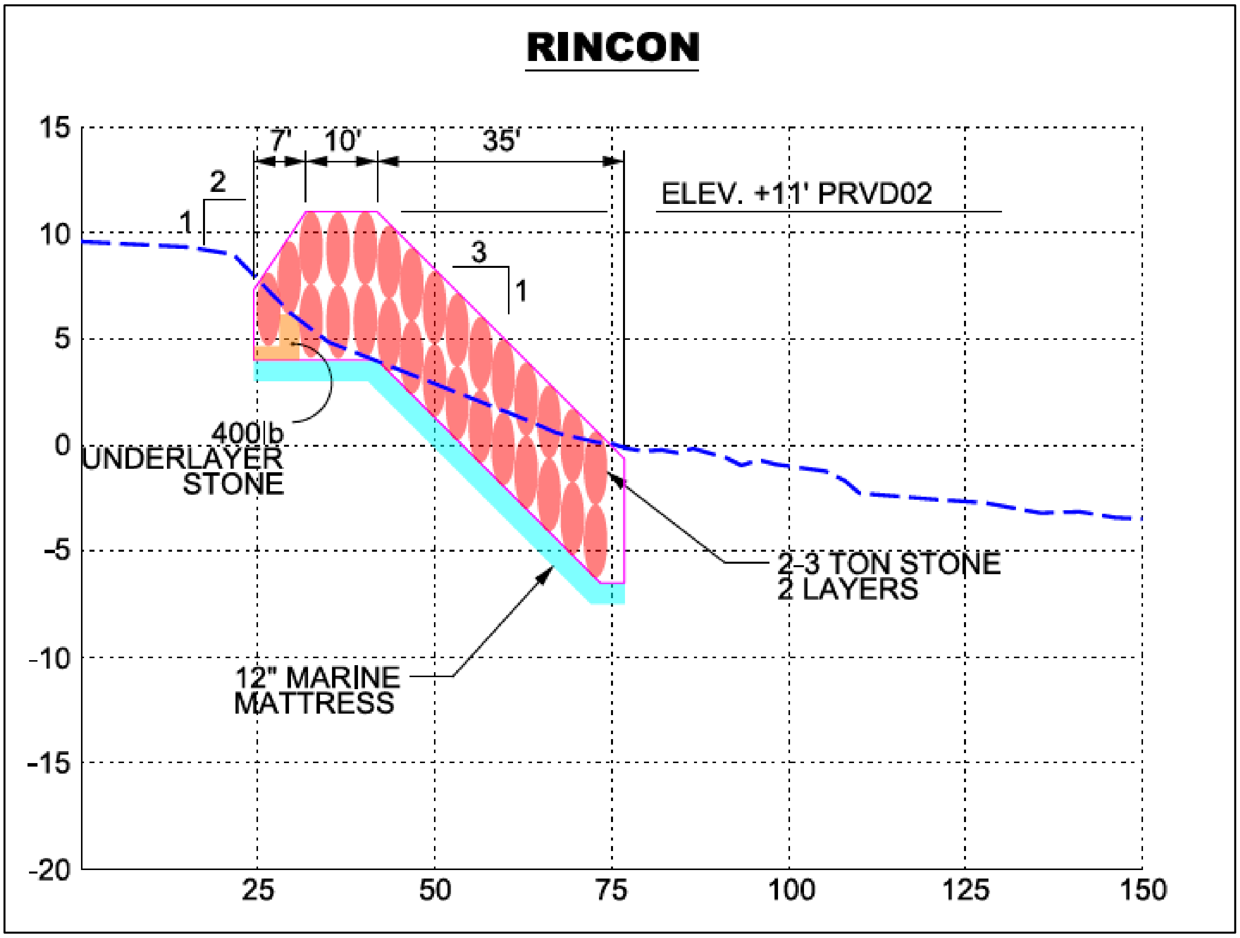

Figure A - 82. Rincón Revetment Design

5.0 SUMMARY AND ADAPTATION STRATEGY DISCUSSION

This section will include a summary of this report and a discussion around adapting projects for accelerated SLC rates over the life of the proposed CSRM measures once all analyses are complete.

6.0 REFERENCES

Bredesen, M. H., 2015. The Simulation & Evaluation of Surge Hazard Using a Response Surface Method in the New York Bight. UNF Graduate Theses and Dissertations. 568

Codiga, D. L., 2011. Unified Tidal Analysis and Prediction Using the UTide Matlab Functions. Technical Report 2011-01. Graduate School of Oceanography, University of Rhode Island, Narragansett, RI. 59pp. ftp://www.po.gso.uri.edu/pub/downloads/codiga/pubs/2011Codiga-UTide-Report.pdf

Dean, R. G., Dalrymple, R. A., 2002. Coastal Processes with engineering applications. Cambridge, United Kingdom. Cambridge University Press. 1st Ed., pp. 79 – 336.

Deltares, 2019. Historical Shoreline Positions Worldwide Derived from space. Period: 1984-2019.

FEMA, 2007. Atlantic Ocean and Gulf of Mexico Coastal Guidelines Update, Final Draft. Federal Emergency Management Agency. FEMA Region IV, FEMA Headquarters. Atlanta, GA. February 2007.

FEMA, 2009. Flood Insurance Study – Commonwealth of Puerto Rico and Municipalities. FEMA Region IV, FEMA Headquarters. Atlanta, GA. November 18, 2009.

Gravens, M. B., Males, R. M, and Moser, D. A., 2007. Beach-*fx*: Monte Carlo Life-Cycle Simulation Model for Estimating Shore Protection Project Evolution and Cost Benefit Analyses. Shore and Beach, Vol. 75(1): 12-19.

Gravens, M. B. and Sanderson, D. R., 2018. Identification and Selection of Representative Storm Events from a Probabilistic Storm Data Base. ERDC/CHL CHETN-VIII-9, January 2018.

Hesser, T., Cialone, A., Collins, C., Cox, A., Jensen, R., in preparation. Wave Information Study 35+ Year US Wave Hindcast

Hubertz, J. A., 1992a. User's Guide to the Wave Information Studies (WIS) Wave Model. Version 2.0. WIS Report 27, US Army Engineer Waterways Experiment Station. Vicksburg, MS.

Hubertz, J. A., 1992b. Uses for Marine Mattresses in Coastal Engineering. ERDC/CHL, US Army Corps of Engineers, Vicksburg, MS.

Jia, G., A. A. Taflanidis, N. C. Nadal-Caraballo, J. A. Melby, A. B. Kennedy, and J. M. Smith, 2016. Surrogate Modeling for Peak or Time-Dependent Storm Surge Prediction Over an Extended Coastal Region using an Existing Database of Synthetic Storms. Natural Hazards 81:909-938.

Males, R. M., Gravens, M. B, Moser, D. A., and Rogers, C. M., 2007. Beach-*fx*: Life-Cycle Risk Analysis of Shore Protection Projects. Proceedings of the 30th International Conference on Coastal Engineering, J. M. Smith (ed.). Singapore, Japan: World Scientific Publishing Company, Inc.

NOAA, 2012a. Global Sea Level Rise Scenarios for the US National Climate Assessment. NOAA Tech Memo OAR CPO-1. 37 pp, US Department of Commerce, National Oceanic and Atmospheric Administration, Center for Operational Oceanographic Products and Services: Silver Spring, MD.

NOAA, 2012b. National Oceanic and Atmospheric Administration's National Geodetic Survey – Vertical Datums. Silver Spring, MD. Retrieved from https://www.nrc.gov/docs/ML1422/ML14223A019.pdf on 13 May 2020.

NOAA, 2013a. Estimating Vertical Land Motion from Long-Term Tide Gauge Records. National Oceanic and Atmospheric Administration. Technical Report NOS CO-OPS 065. Silver Spring, MD.

NOAA, 2013b. Extreme Water Levels of the United States 1893-2010. US Department of Commerce, National Oceanic and Atmospheric Administration, Center for Operational Oceanographic Products and Services: Silver Spring, MD.

NOAA, 2019. Coast Pilot 5 - 47th Edition, 2019 covers the Gulf of Mexico from Key West, FL to the Rio Grande, including Puerto Rico and the Virgin Islands. US Department of Commerce, National Oceanic and Atmospheric Administration, Center for Operational Oceanographic Products and Services: Silver Spring, MD.

NOAA, 2020a. Puerto Rico Fast Facts. National Oceanic and Atmospheric Administration: Office for Coastal Management. Silver Spring, MD. https://coast.noaa.gov/states/puerto-rico.html. Accessed 21 July 2020.

NOAA, 2020b. National Oceanic and Atmospheric Administration: Tides and Currents, Sea Level Trends. Silver Spring, MD. https://tidesandcurrents.noaa.gov/sltrends/sltrends.html. Accessed 21 July 2020.

New York City Panel on Climate Change, 2013. Climate Risk Information 2013: Observations, Climate Change Projections, and Maps. New York City Mayor's Office of Sustainability: New York, NY.

OWI, 2018. Global Reanalysis of Ocean Waves Fine Caribbean – 2 (GFC-2), Project Description, October 2018. Oceanweather Inc., Stamford, CT.

Taflanidis, A. A., J. Zhang, N. C. Nadal-Caraballo, and J. A. Melby, 2017. Advances in Surrogate Modeling for Hurricane Risk Management Assessment: Storm Selection and Climate Change Impacts. 12th International Conference on Structural Safety and Reliability, TU-Verlag, 552-561.

Tarbuck, E. J. and Lutgens, F. K., 2006. Earth science. Upper Saddle River, New Jersey: Pearson Education, Inc. 11th Ed., pp. 402 – 535.

Thieler, et al., 2007. Historical Shoreline Changes at Rincón Puerto Rico, 1936-2006. US Geological Survey Open-File Report, 2007-1017, 32 pg. Available at http://pubs.usgs.gov/of/2007/1017/.

USGS, 2014. St. Petersburg coastal and marine science center. Coastal change hazards: Hurricanes and extreme storms. Retrieved from http://coastal.er.usgs.gov/hurricanes/ extreme-storms/hurricanes.php

USACE, 1984a. Shore Protection Manual: Volume I. Coastal Engineering Research Center, Department of the Army. Washington DC.

USACE, 1984b. Shore Protection Manual: Volume II. Coastal Engineering Research Center, Department of the Army. Washington DC.

USACE, 1995. EM 1110-2-1614: Engineering and Design: Design of Coastal Revetments, Seawalls, and Bulkheads. Washington DC.

USACE, 1997. ER 1110-2-1407: Engineering and Design: Hydraulic Design for Coastal Shore Protection Projects. Washington DC.

USACE, 2006. ER 1105-2-101: Risk Analysis for Flood Damage Reduction Studies. Washington DC.

USACE, 2009. ERDC/CHL SR-0906: Beach-*fx* User's Manual: Version 1.0. Washington DC.

USACE, 2011. EC 1165-2-212: Sea Level Change Considerations for Civil Works Programs. Department of the Army. Washington DC.

USACE, 2017. ER 1105-2-101: Risk Analysis for Flood Damage Reduction Studies. Washington DC.

USACE, 2018. Sea Level Tracker User Guide. Version 1.0. US Army Corps of Engineers. Washington DC.

USACE, 2019a. EP 1100-2-1: Procedures to Evaluate Sea Level Change: Impacts, Responses, and Adaptation. Engineering Pamphlet No. 1100-2-1. US Army Corps of Engineers. Washington DC.

USACE, 2019b. ER 1110-2-8162: Sea-level Change Considerations in Civil Works Programs. Washington DC.

USACE, 2020. ECB 2020-6: Implementation of Resilience Principles in the Engineering & Construction Community of Practice. Engineering Construction Bulletin No. 2020-6. US Army Corps of Engineers. Washington DC.

Zhang, J., A. A. Taflanidis, N. C. Nadal-Caraballo, J. A. Melby, F. and Diop, 2018. Advances in Surrogate Modeling for Storm Surge Prediction: Storm Selection and Addressing Characteristics Related to Climate Change. Natural Hazards 94:1225-1253.